AD NUMBER

AD877164

LIMITATION CHANGES

TO:

Approved for public release; distribution is unlimited.

FROM:

Distribution authorized to U.S. Gov't. agencies and their contractors; Critical Technology; SEP 1970. Other requests shall be referred to Air Force Materials Laboratory, Attn; MAYE, Wright-Patterson AFB, Ohio 45433. This document contains export-controlled technical data.

AUTHORITY

AFML ltr, 21 May 1973

70

SB

MEASUREMENT OF COMPLEX PERMITTIVITY AND PERMEABILITY

A. S. and E. M. Thomas

A. S. THOMAS, INC.

TECHNICAL REPORT AFML-TR-70-87

September 1970

AIR FORCE MATERIALS LABORATORY
AIR FORCE SYSTEMS COMMAND
WRIGHT-PATTERSON AIR FORCE BASE, OHIO 45433

108

NOTICE

When Government drawings, specifications, or other data are used for any purpose other than in connection with a definitely related Government procurement operation, the United States Government thereby incurs no responsibility nor any obligation whatsoever; and the fact that the Government may have formulated, furnished, or in any way supplied the said drawings, specifications, or other data, is not to be regarded by implication or otherwise as in any manner licensing the holder or any other person or corporation, or conveying any rights or permission to manufacture, use, or sell any patented invention that may in any way be related thereto.

This document is subject to special export controls and each transmittal to foreign government or foreign nationals may be made only with prior approval of AFML (MAYE), WPAFB, Ohio 45433.

The distribution of this report is limited because the report contains technology identifiable with items on the strategic embargo list excluded from export or re-export under U.S. Export Control Act of 1949 as implemented by AFR 400-19.

This document may not be reproduced or published in any form in whole or in part without prior approval of the Government. Since this is a technical management report, the information herein is tentative and subject to changes, corrections and modifications.

Copies of this report should not be returned unless return is required by security considerations, contractual obligations, or notice on a specific document.

MEASUREMENT OF COMPLEX PERMITTIVITY AND PERMEABILITY

A. S. and E. M. Thomas

FOREWORD

This report was prepared by A. S. Thomas, Inc., 355 Providence Highway, Westwood, Massachusetts, under Air Force Contract F33615-69-C-1065, Project No. 5546 "Radar and IR Camouflage," Task No. 554603, "Physics of Radar Absorber Materials." The work was administered under the Air Force Materials Laboratory, Air Force Systems Command, Wright-Patterson Air Force Base, Ohio. R. M. Van Vliet and W. G. D. Frederick, MAYE, were project engineers for the laboratory.

The exploratory research was conducted at A. S. Thomas, Inc. under the direction of A. S. Thomas. The following scientific personnel participated in the performance of the work reported herein: E. M. Thomas, L. B. Raisty, E. V. Oates, W. J. Podgorni, and B. C. Pare.

The final report was submitted on 20 March, 1970.

This report has been reviewed and approved.

David J. Iden
Lt. Colonel, USAF
Chief, Electromagnetics Materials Branch
Materials Physics Division
Air Force Materials Laboratory

ABSTRACT

This program was conducted to derive a better technique for the measurement of the permeability and permittivity of lossy ferrites at microwave frequencies at temperatures up to 1000°F. Although the classical method of waveguide measurement techniques was used, a careful analysis of the sources of errors was undertaken and a computer aided analysis technique developed to establish the validity of the measurements.

The design of the sample holders and special tools for insertion of material is detailed.

The problem areas inherent in this type of measurement are not compounded by high temperatures, and good results can be obtained, provided great care is taken and sufficient homogeneous ferrite samples are available.

Three different ferrites were measured at microwave frequencies and temperatures up to 1000°F.

TABLE OF CONTENTS

LIST OF ILLUSTRATIONS

LIST OF TABLES

I. INTRODUCTION

It is well known to anyone familiar with the literature in connection with lossy ferrite materials and the numerous measurements reported in the literature in connection with radar absorbing materials, that all investigators have experienced serious problems in determining the complex permittivity (ε) and the complex permeability (μ) of these materials.

The work under this contract is directed to the measurements of ε and μ at high temperatures, which requires:

1. The use of a suitable sample holder with coefficient of thermal expansion comparable to the ceramic ferrite.

2. The determination of the temperature at the sample at which the measurement is being taken, and,

3. The design of special tools for inserting the samples at the shorting plate and moving the sample $\lambda/4$ away from the shorting plate.

The classical approach for measuring ε and μ is to:

1. Place a sample of thickness d at the short circuit in either a coaxial or waveguide sample holder and, by means of a slotted line connected to the sample holder, to obtain the position of a minimum of the voltage standing wave, NPS, and either the voltage standing wave ratio, VSWR, or the distance (ΔX_S) between the points of twice minimum power on the voltage standing wave.

2. Place the sample $\lambda/4$ away from the short circuit and obtain the position of a minimum of the voltage standing wave, NPO, and either the voltage standing wave ratio, or the distance (ΔX_O) between the points of twice minimum power on the voltage standing wave.

By means of solving a pair of transcentental equations containing the measured parameters NPS, NPO, ΔX_S, ΔX_O, the ε and μ of any material may be *uniquely* determined at a given frequency. However, the results

are not necessarily *valid*. For example, if the complex normalized ϵ and μ are defined as $\epsilon=\epsilon'-j\epsilon''$ and $\mu=\mu'-j\mu''$, then the following inequalities: $\epsilon'>1, \epsilon''>0$ and $\mu''>0$ must always hold for solid homogeneous materials such as sintered ferrite. However, now and then the ϵ', ϵ'' or μ'' are computed to be negative. Such results are unacceptable. Frequently random variations in the values of $\epsilon', \epsilon'', \mu'$ and μ'' as a function of frequency are obtained implying, erroneous results. These are due to:

1. Errors in the precise location of NPS and NPO and,

2. Errors in the determination of the VSWR or ΔX_s and ΔX_o.

Hence the problem of establishing the reliability of the complex ϵ and μ that is determined from the measurements of the null positions and VSWR in either coaxial line or waveguide is the same, whether the measurements are made at room or at elevated temperatures.

In order to determine the reliability of the measurements, samples of a single thickness d and double thickness 2d are measured and four determinations of ϵ and μ are obtained. By means of recomputing from the ϵ and μ obtained for each thickness the expected values of NPO, NPS, ΔX_s and ΔX_o for the other thickness, and by making suitable corrections for ΔX_s and ΔX_o the reliability of the measurements may be established. A computer program is being developed to evaluate the sources of errors in the measurements, and to accept or reject the result.

II. SAMPLE HOLDERS

The coaxial sample holder made of Kovar (a Westinghouse product), and described in detail in Technical Report AMFL-TR-69-18[1], proved to be very satisfactory, hence it was decided to make the waveguide sample holder of the same material.

Since Kovar is considered to be an exotic material, great difficulty was experienced in finding a source that would fabricate the waveguide sample holder to the required tolerances. Five techniques were considered - broaching, EDM (Electrical Discharge Machining), extrusion, and machining in parts and brazing. The first four proved to be exorbitant in price. The fifth required a careful search for a capable machining facility. A machine shop finally was found to undertake the job on a best effort basis. The drawings of the waveguide section are given in Figures 1 to 6. By maintaining careful liason with the machine shop, the final product was very satisfactory. However, the wall thickness had to be increased to 0.09 inches to maintain adequate tolerance. This unfortunately, as will be shown later, requires additional time for temperature stabilization from one increment of temperature to another. However, for the present purposes this is usable. If thinner walls are required for more production type work, the walls of the sample holder may be thinned from the outside by relatively expensive methods.

The fabrication procedure was a follows: rough machining, annealing, finish machining, annealing, grinding to required finish, furnace brazing, grinding to remove excess brazing material, annealing again and then polishing, and finally gold plating.

The machining, brazing and gold plating were carried out by three different contractors, each of whose operations required clear definition and close monitoring. Furnace brazing was chosen to avoid distortion.

The gold plating process involved a vacuum degassing operation, flashing with nickel, then gold plating the inside with special electrodes to ensure consistent thickness of the gold over the length of the sample holder. The

The text resumes on page 10

---

[1]Thomas, A. S. "High Temperature Measurements of Complex ε and μ." Technical Report AFML-TR-69-18, March 1969.

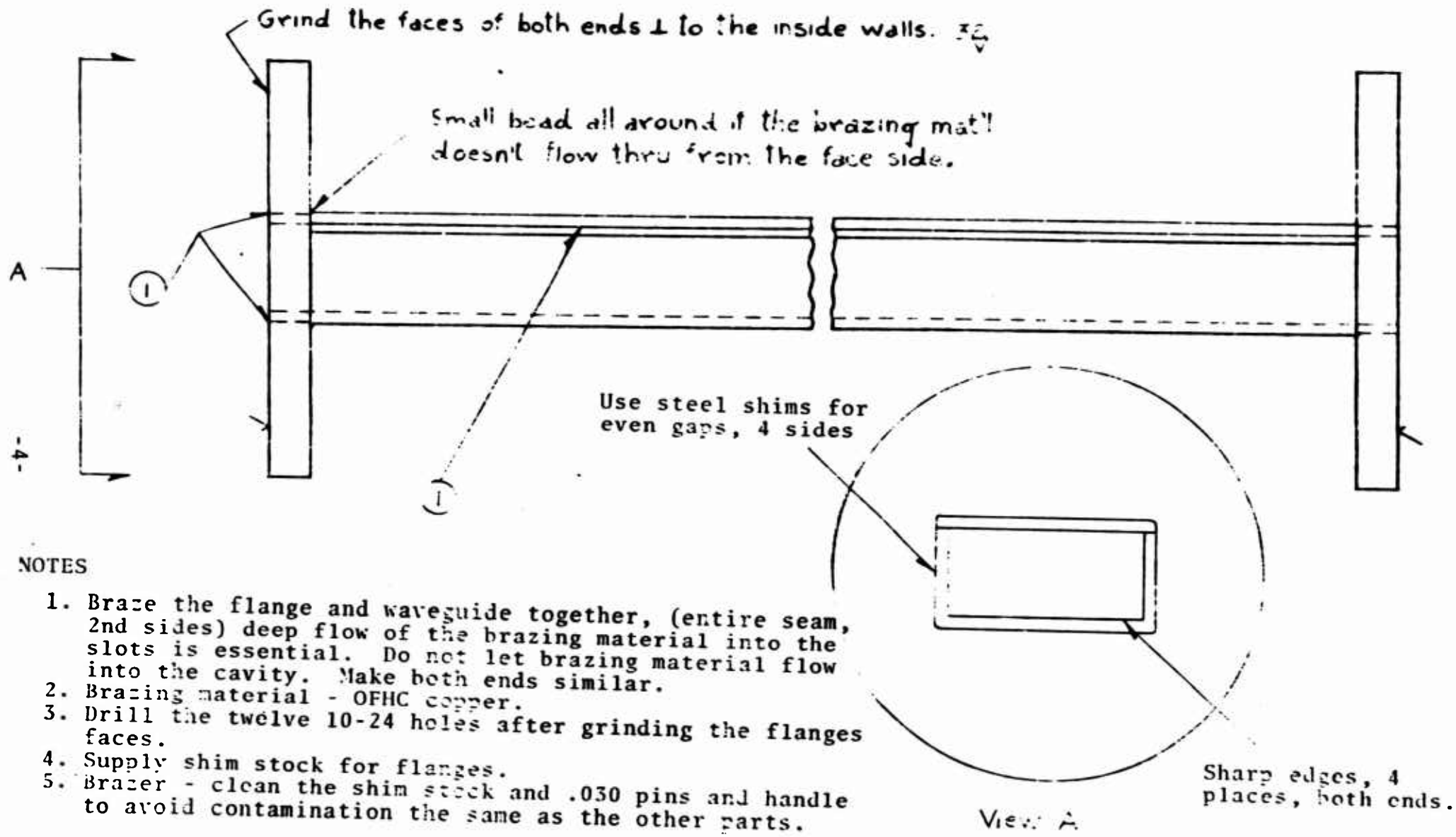

NOTES

1. Braze the flange and waveguide together, (entire seam, 2nd sides) deep flow of the brazing material into the slots is essential. Do not let brazing material flow into the cavity. Make both ends similar.
2. Brazing material - OFHC copper.
3. Drill the twelve 10-24 holes after grinding the flanges faces.
4. Supply shim stock for flanges.
5. Brazer - clean the shim stock and .030 pins and handle to avoid contamination the same as the other parts.

Figure 1. WAVE GUIDE ASSEMBLY

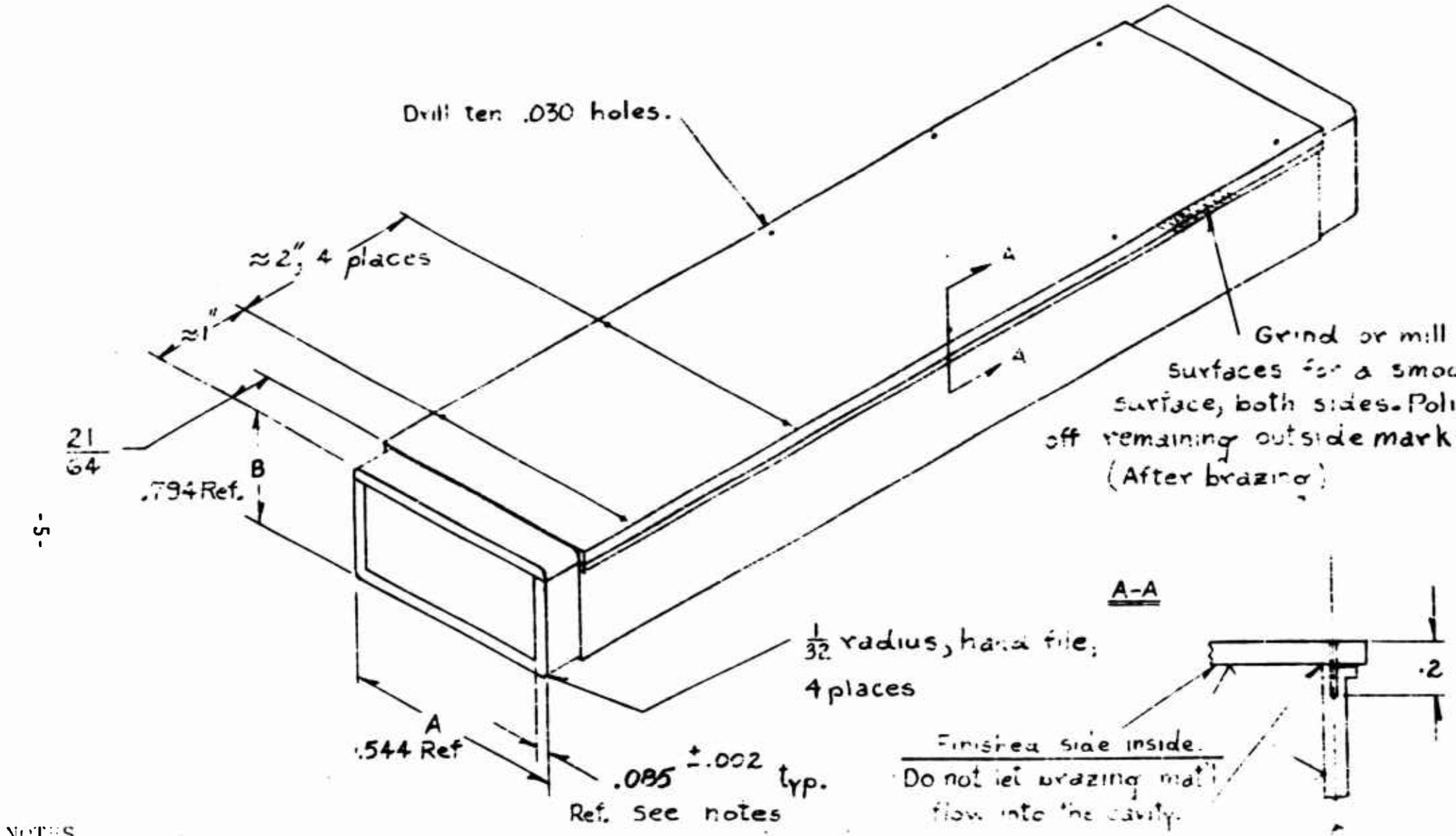

NOTES

1. Grind or mill 4 surfaces for an equal wall thickness, approx. .085, max. difference .004
2. Measure dimensions A and B for use in making the flanges.
3. Make both ends similar.
4. Supply ten .030 steel pins .18 long with ends rounded for below surface insertion.

Figure 2. WAVE GUIDE TUBE ASSEMBLY.

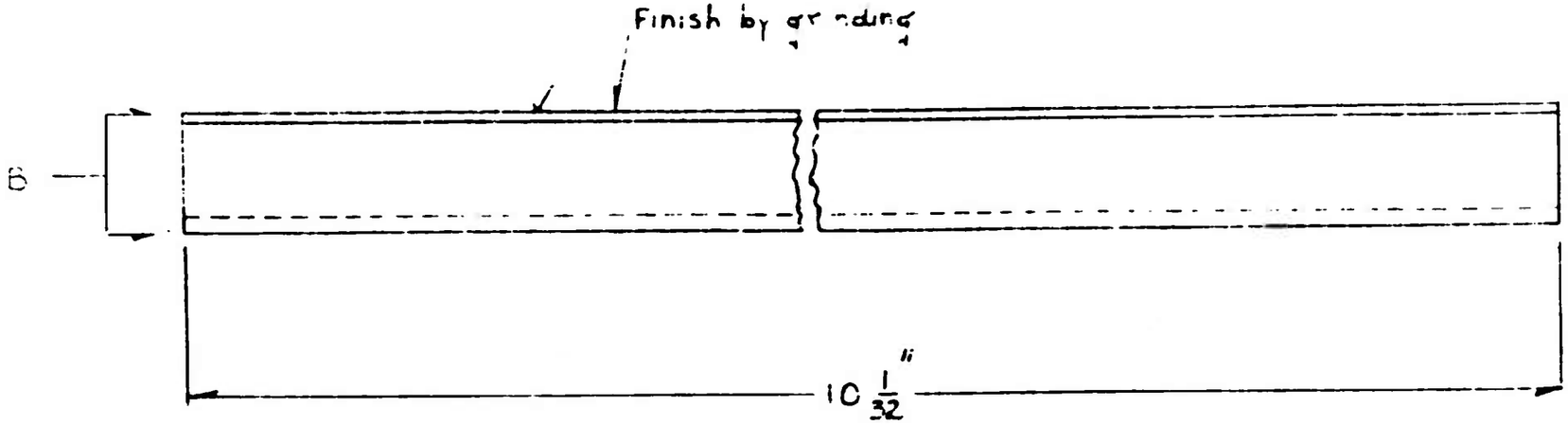

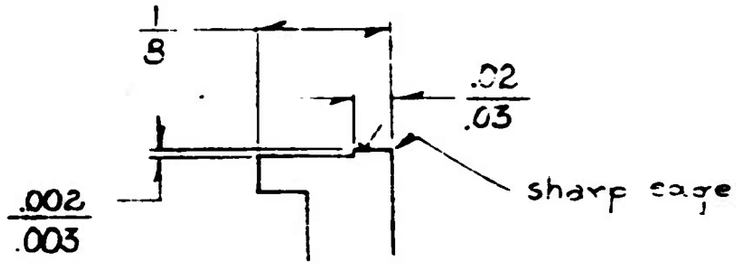

Detail A, typ. 4 places

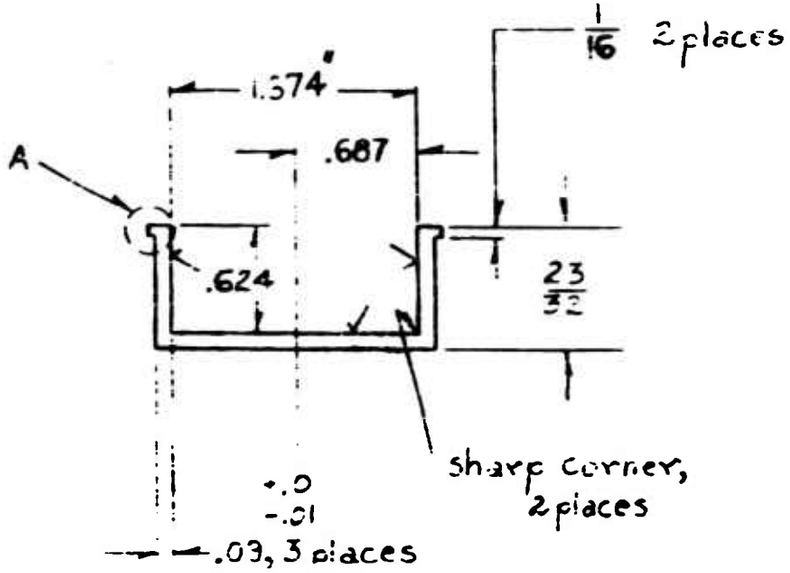

View B

NOTES

1. No. required - 1
2. Material - Westinghouse Kovar steel
3. Finish - where shown, free of machining marks, scratches, etc. The outer surfaces will be finished partly during this operation and partly later.
4. Tolerances .000 ±.004

Figure 3. WAVE GUIDE CHANNEL.

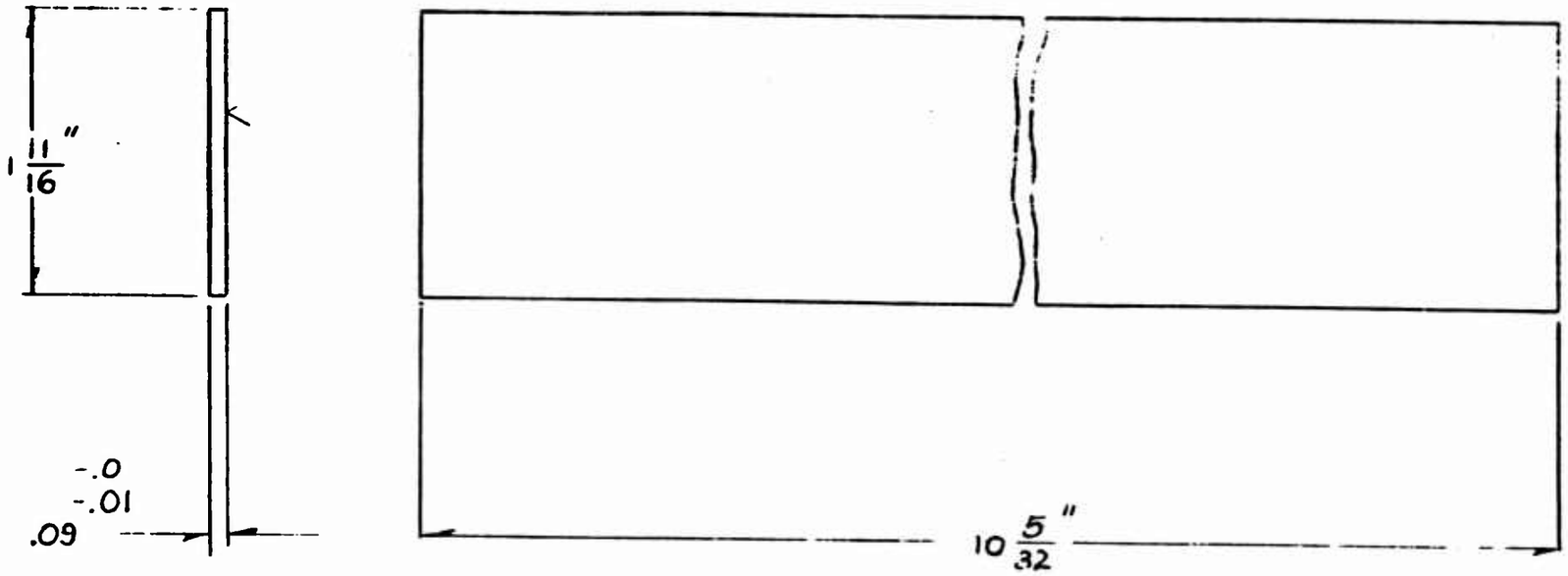

NOTES

1. Stress relieve before machining.
2. No. required - 1
3. Material - Kovar steel - make from 1/8 stock.
4. Grind 1 or both sides as necessary to make one side flat. 32

Figure 4. WAVE GUIDE COVER PLATE.

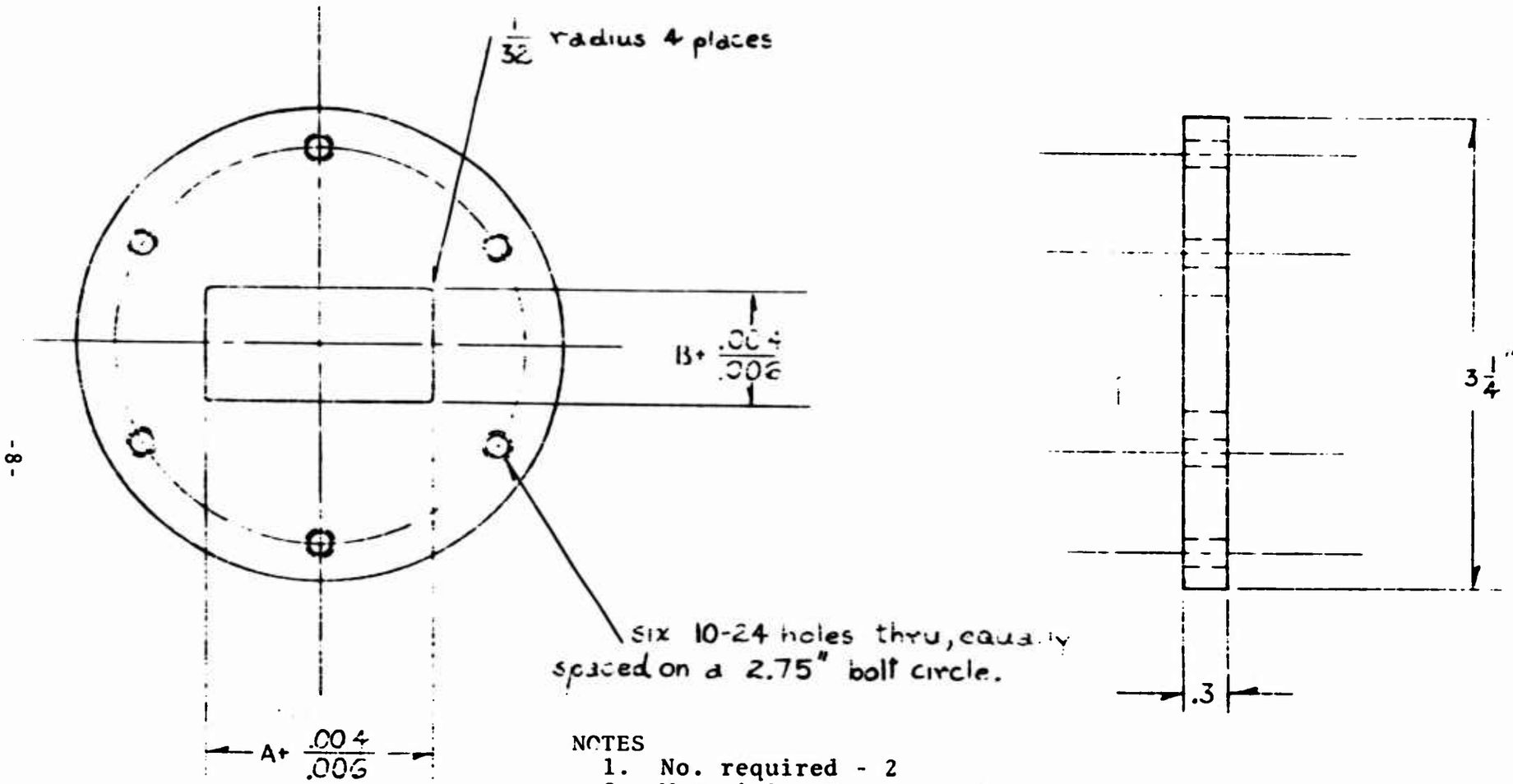

NOTES

1. No. required - 2
2. Material - Kovar steel
3. See dwg. 4 for dimensions A & B, add .004/.006 clearance for brazing material.
4. Drill the six 10-24 holes after the flanges have been brazed unto the waveguide and ground square.

Figure 5. WAVE GUIDE FLANGE.

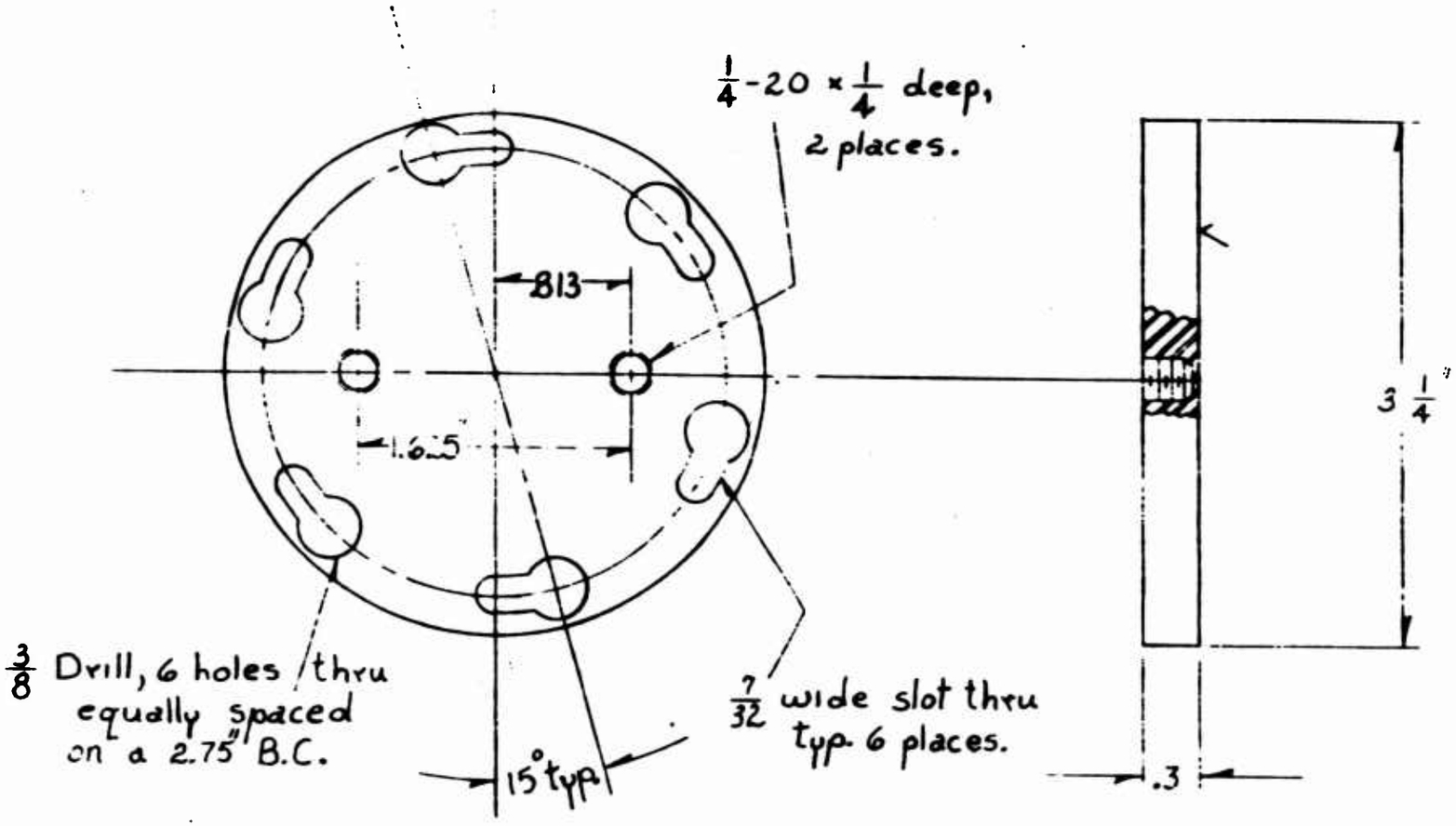

Material - Westinghouse Kovar steel
No. reauired-1

Figure 6. SHORTING PLATE.

same thickness of gold that was found satisfactory with the coaxial sample holder (0.6 mils) was used on the waveguide sample holder.

Special tools were devised for loading, moving and removing the samples from the waveguide, Figures 7 and 8. The vacuum extractor, Figure 7, ensures that the sample is normal to the waveguide walls, both on insertion as well as extraction. The $\lambda/4$ positioner, Figure 8, has a sufficiently large plunger face and an accurately aligned stop plate to guarantee that the sample does not tilt when moved $\lambda/4$ away from the short at any given frequency.

The ΔX, and therefore the VSWR were checked in the air-filled coaxial and waveguide sample holders. Since ΔX is related to VSWR for $\Delta X < .03\lambda$ as follows:

$$VSWR = \frac{\lambda}{\pi \Delta X}$$

where λ is the wavelength in coaxial line or waveguide,

the smaller the ΔX, the larger the VSWR.

The comparisons between the standard sample holders and the gold plated Kovar sample holders are given in Figures 9 and 10. The voltage standing wave minima, or "nulls", occur at distances of $\lambda/2$ from the shorting plate, so that null No. 1 is $\lambda/2$ away from the shorting plate, null No.2 is λ away from the shorting plate, etc. In Figure 9, the ΔX is given for nulls 8 to 11 at operating frequency of 3.17 GHz; null 8 is at a distance of 4λ away from the shorting plate, and is the first null that appears on the slotted line. Measurements of ΔX in the gold plated Kovar coaxial sample holder are compared with the measured values of X using the aluminum sample holder. It is readily seen from Figure 9 that, although ΔX increases with increased temperature, the ΔX at 1000°F measured in the gold plated sample holder remains below that of the aluminum sample holder at room temperature.

Figure 10 compares the ΔX with standard waveguide

Text resumes on page 15

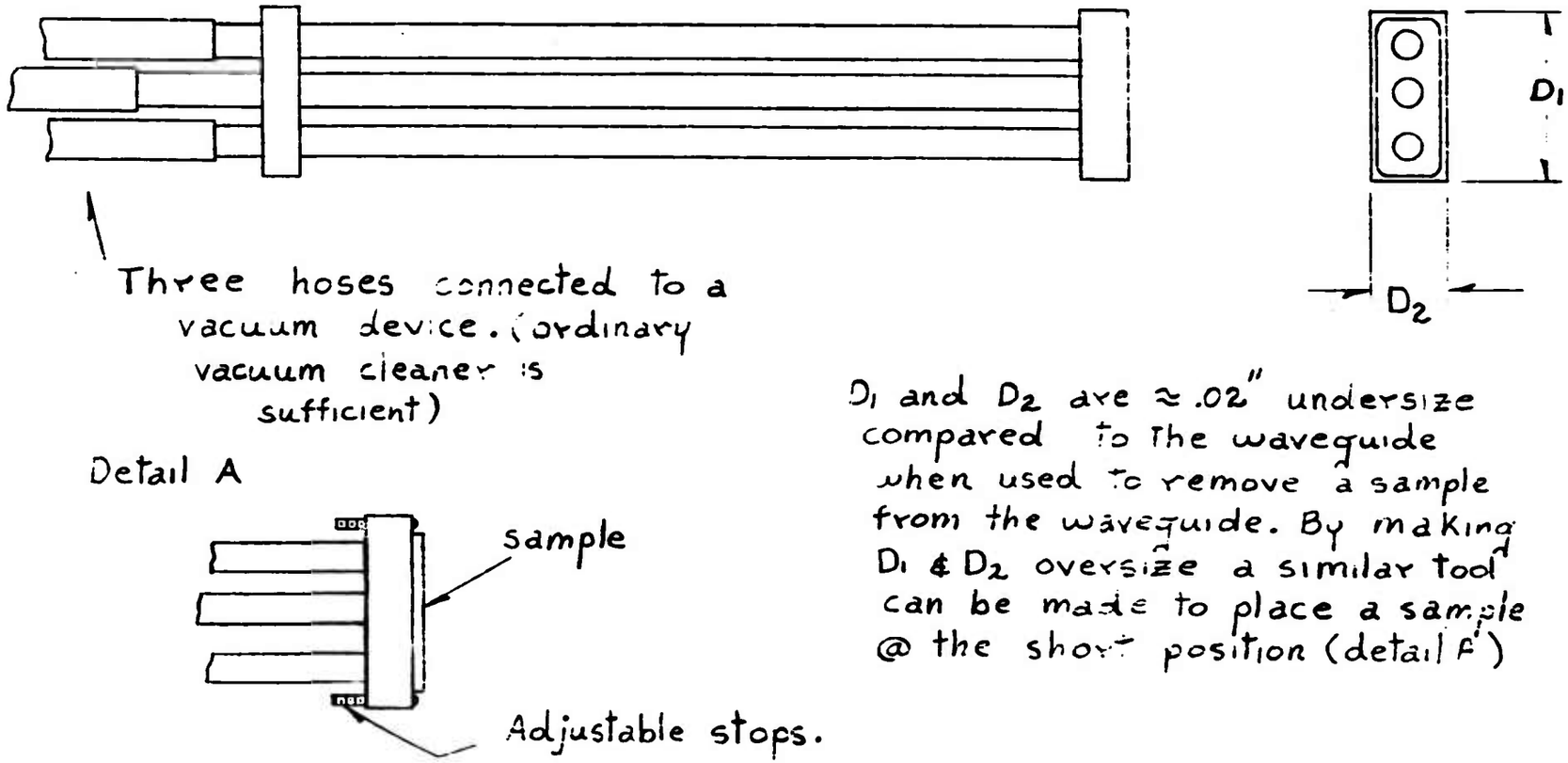

Figure 7. VACUUM SAMPLE EXTRACTOR.

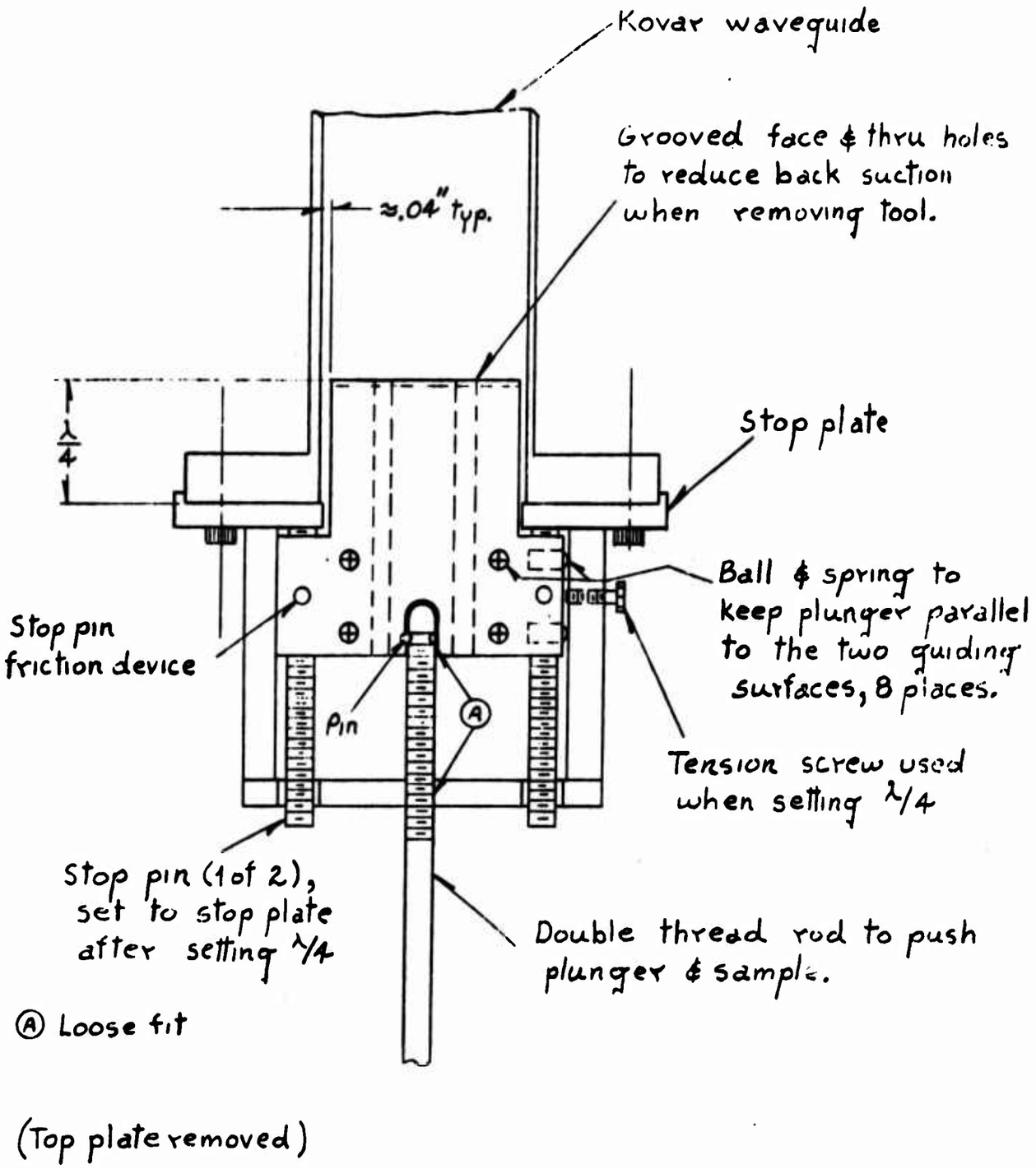

Figure 8. λ/4 POSITIONER (Waveguide).

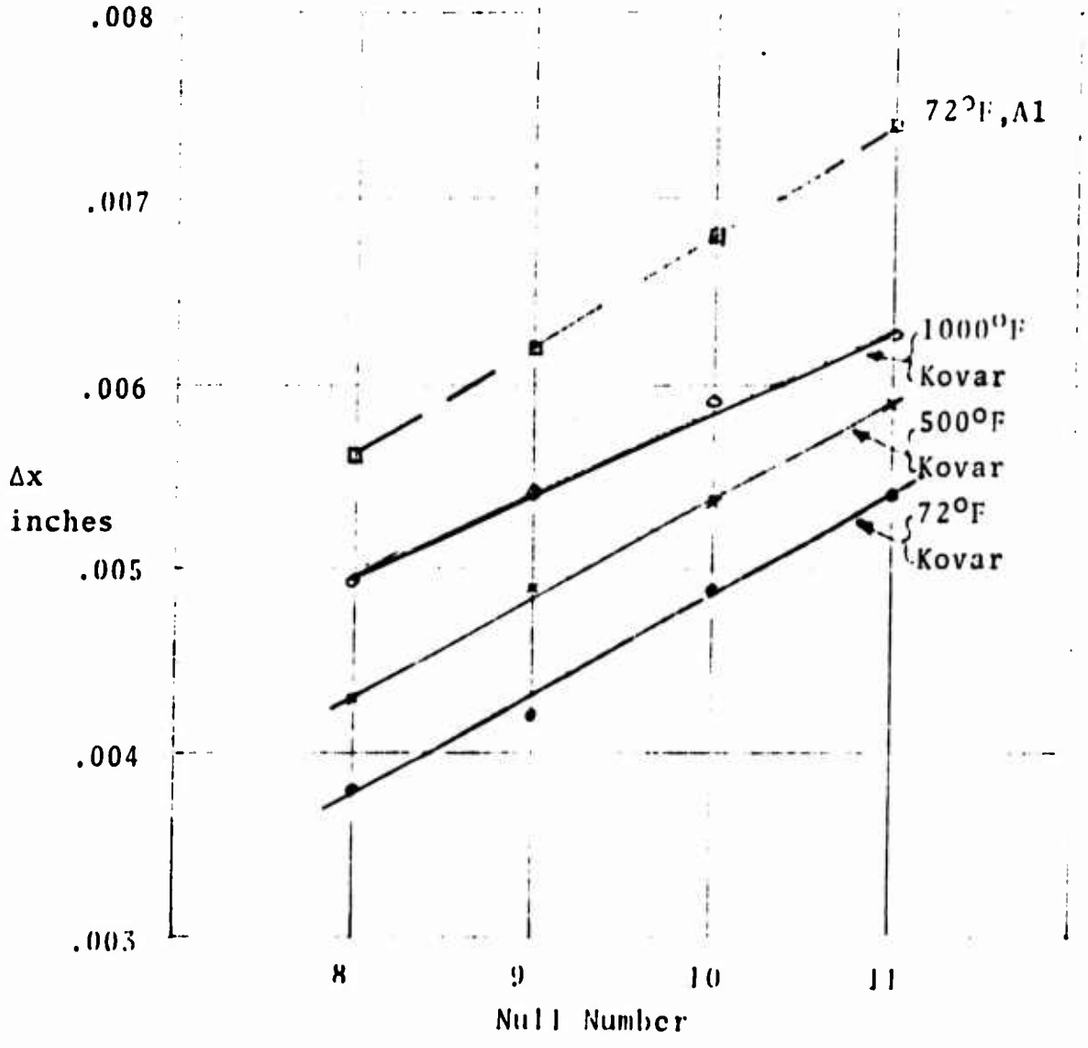

Figure 9. COMPARISON OF Δx IN AIR FOR KOVAR AND ALUMINUM COAXIAL LINE.

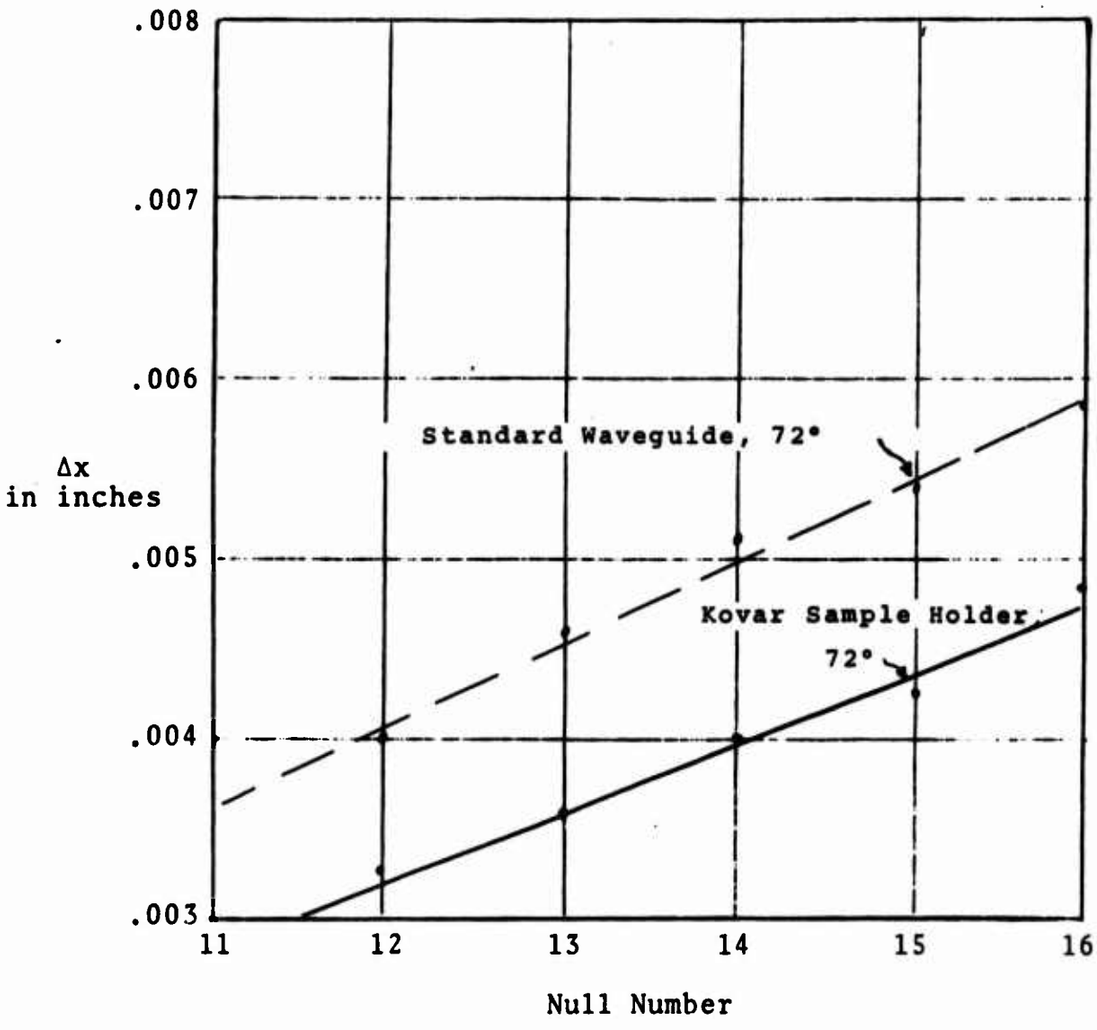

Figure 10. COMPARISON OF Δx IN AIR FOR KOVAR AND STANDARD WAVEGUIDE AT 72°F.

sample holder to that with the ten inch gold plated Kovar sample holder at 6.778 GHz. Here again the gold plated Kovar sample holder exhibited a lower ΔX and hence a higher VSWR than the standard waveguide.

Although the gold plated Kovar sample holders darkened with temperature cycling, the VSWR was not affected by this darkening.

Text continues on next page

III. TEMPERATURE STABILIZATION

It is of course essential to know the exact temperature of the sample at which a measurement is being made. Hence a careful study of the temperature stabilization within the sample has been undertaken. The furnace used has a temperature gradient. This was measured as a function of distance from one end of the furnace to the center of the furnace. The gradients or profiles for 250°, 500°, 750° and 1000° are given in Figures 11 to 14.

By placing thermocouples as shown in Figure 15, the per cent differences in temperature between the inside and outside of the sample holder were obtained. Figure 16 gives the temperature differences between the inside and outside temperatures of the sample holder and Figure 17 gives the differences in per cent as a function of time. It requires forty minutes for the temperature difference at 1000°F to fall below five per cent.

Figures 18 through 21 give the temperature versus time at the surface and inside the sample holder for temperature rises from 70°F. Figures 22 through 25 give the temperature as a function of time for 250°F changes in temperature from 250° to 1000°F.

The temperature inside the sample was studied with test setup as shown in Figure 26. One thermocouple is at the center conductor and another placed at the outside surface of the sample holder. Figures 27 through 32 give the temperature versus time for various temperature rises and the recovery time of the temperature inside and outside the sample. These figures show the initial temperature rise time to reach the test temperature, the subsequent temperature drop as the sample is inserted at the shorting plate or moved $\lambda/4$ away from the short and the recovery time of the temperature at the outer conductor and at the center conductor. As would be expected the recovery time at the center of the sample holder is much greater than at the surface.

Following is a brief summary of the results.

1. With the six inch sample holder at the center of the furnace, the temperature gradient is such that

Text resumes on page 39

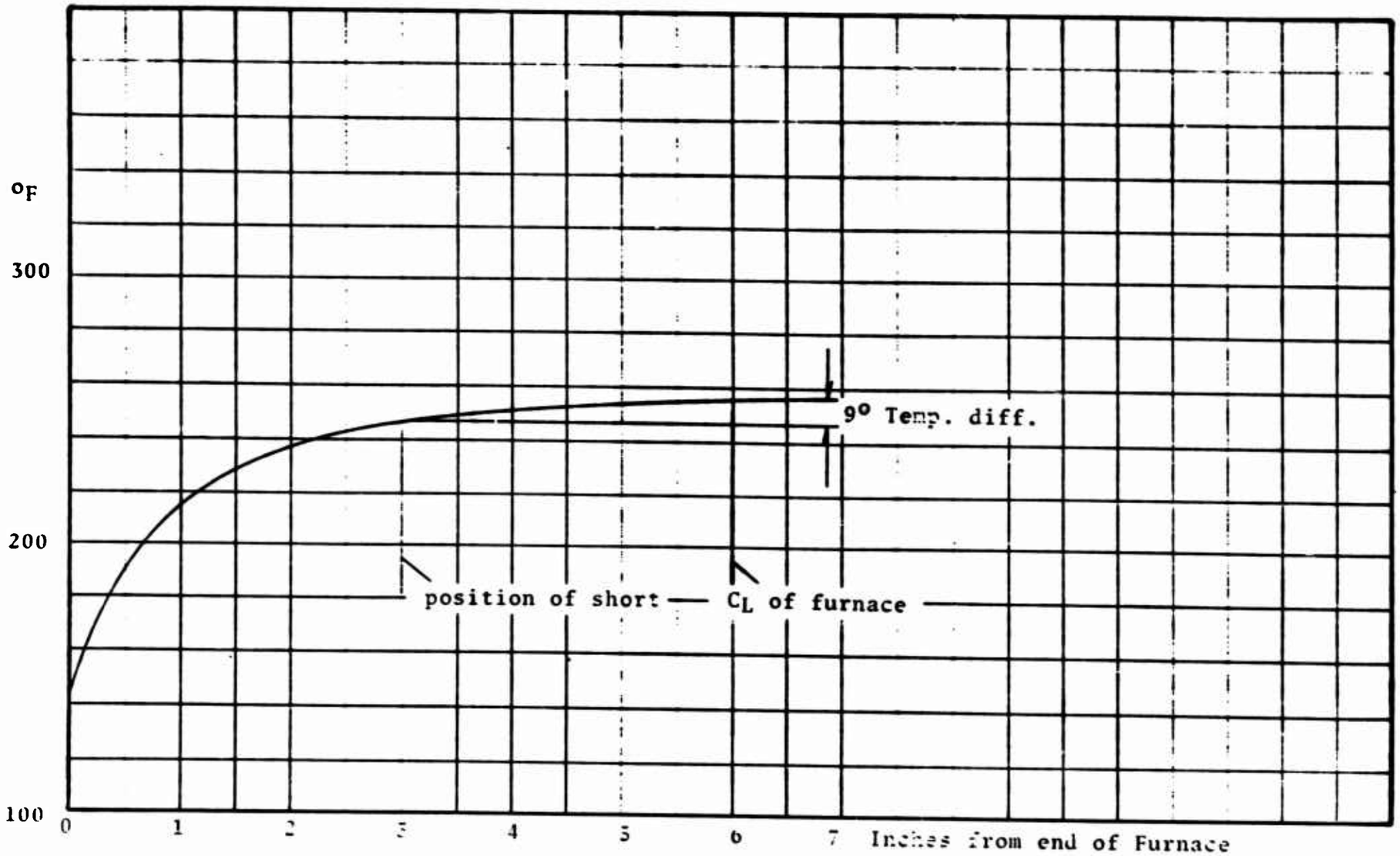

Figure 11. FURNACE TEMPERATURE PROFILE AT 250°F.

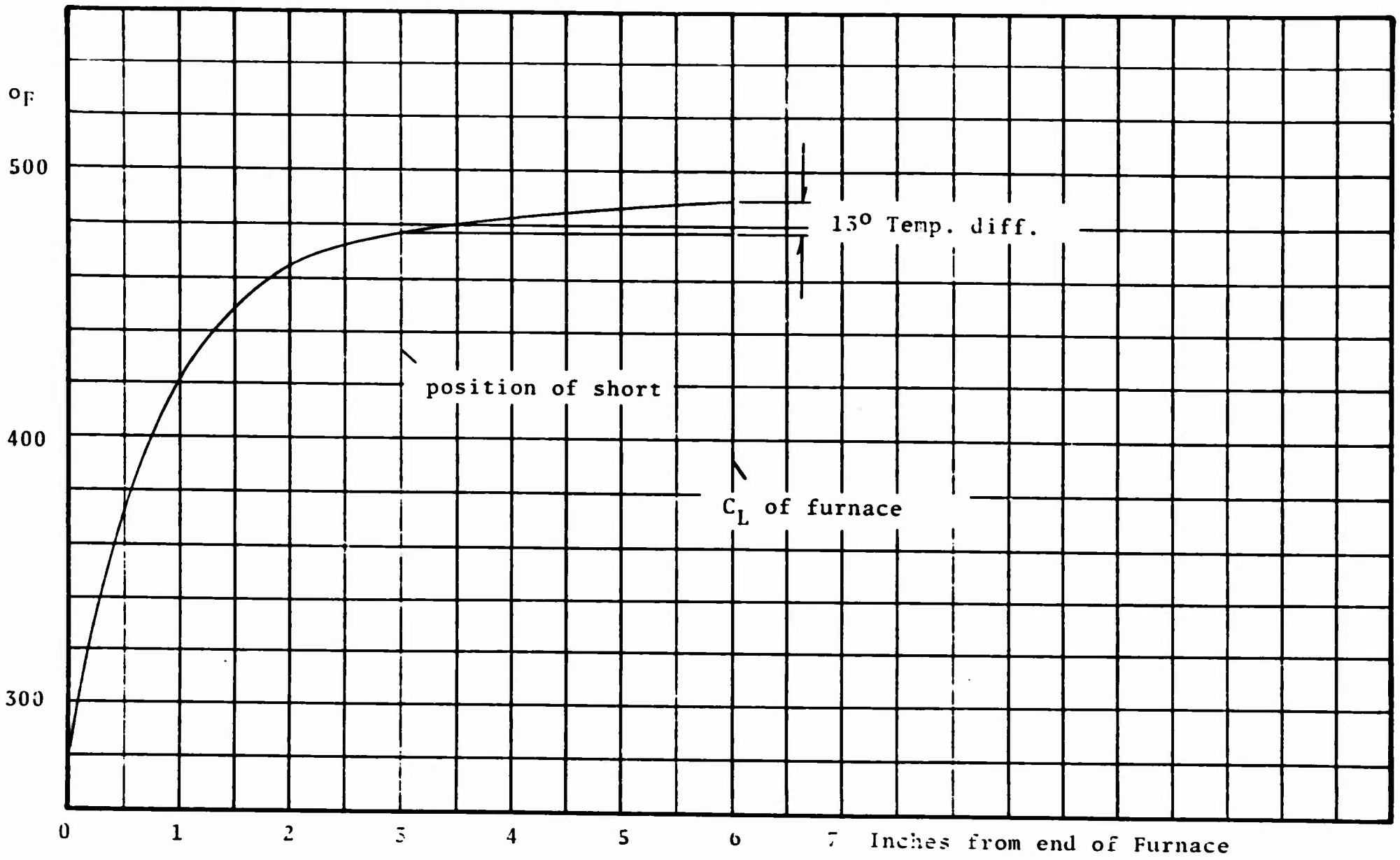

Figure 12. FURNACE TEMPERATURE PROFILE AT 500°F.

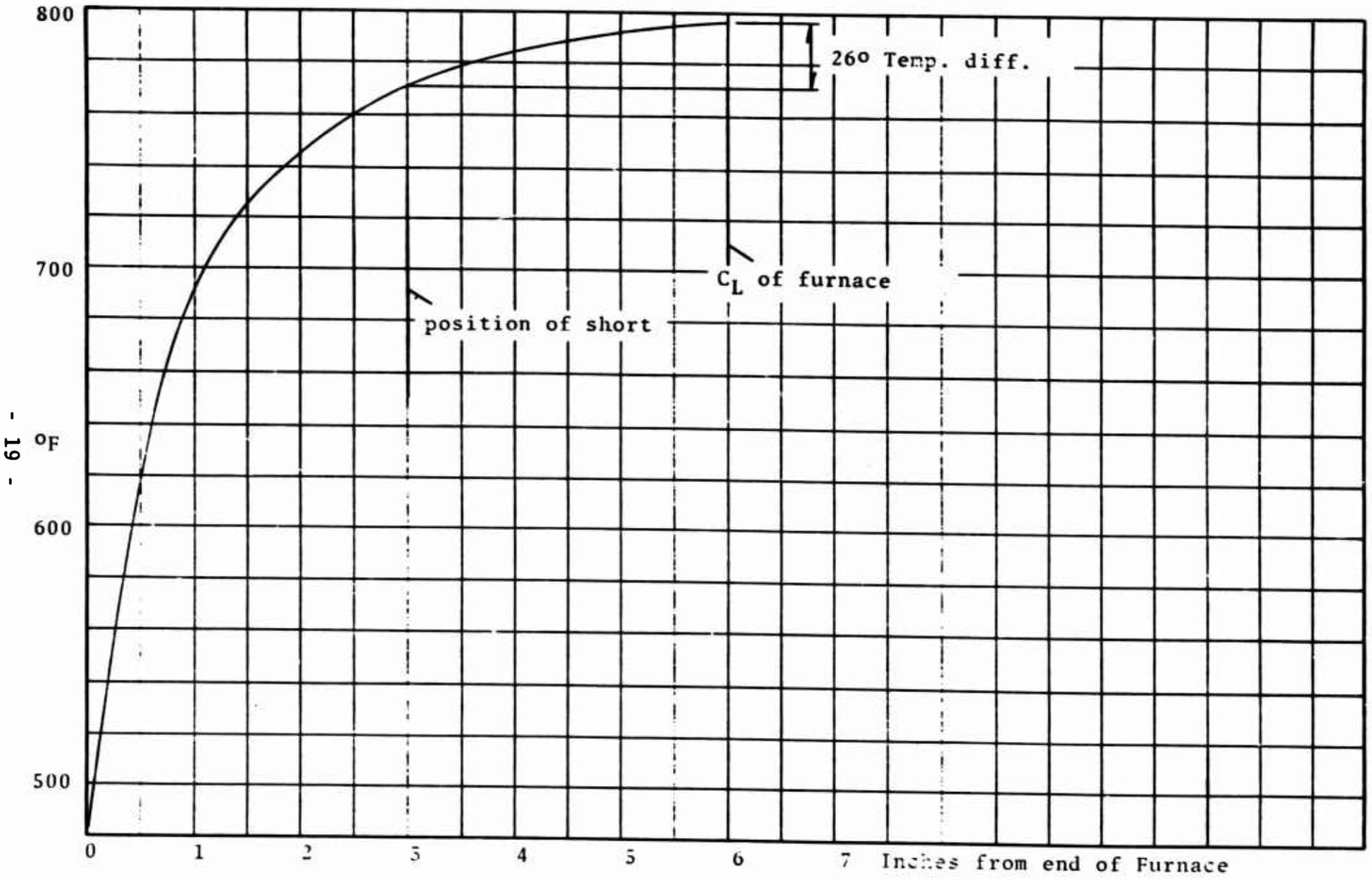

Figure 13. FURNACE TEMPERATURE PROFILE AT 750°F.

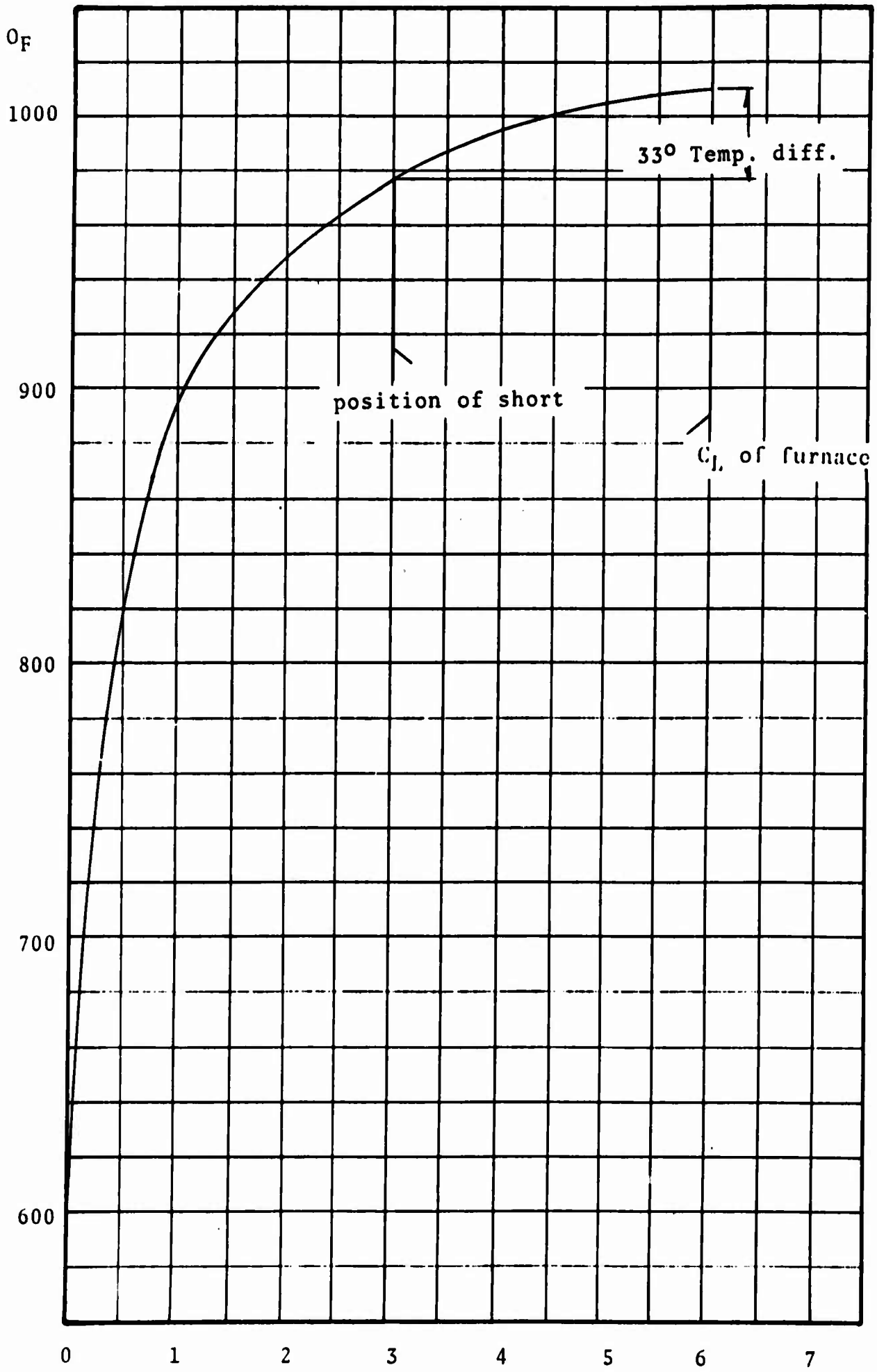

Figure 14. FURNACE TEMPERATURE PROFILE AT 1000°F.

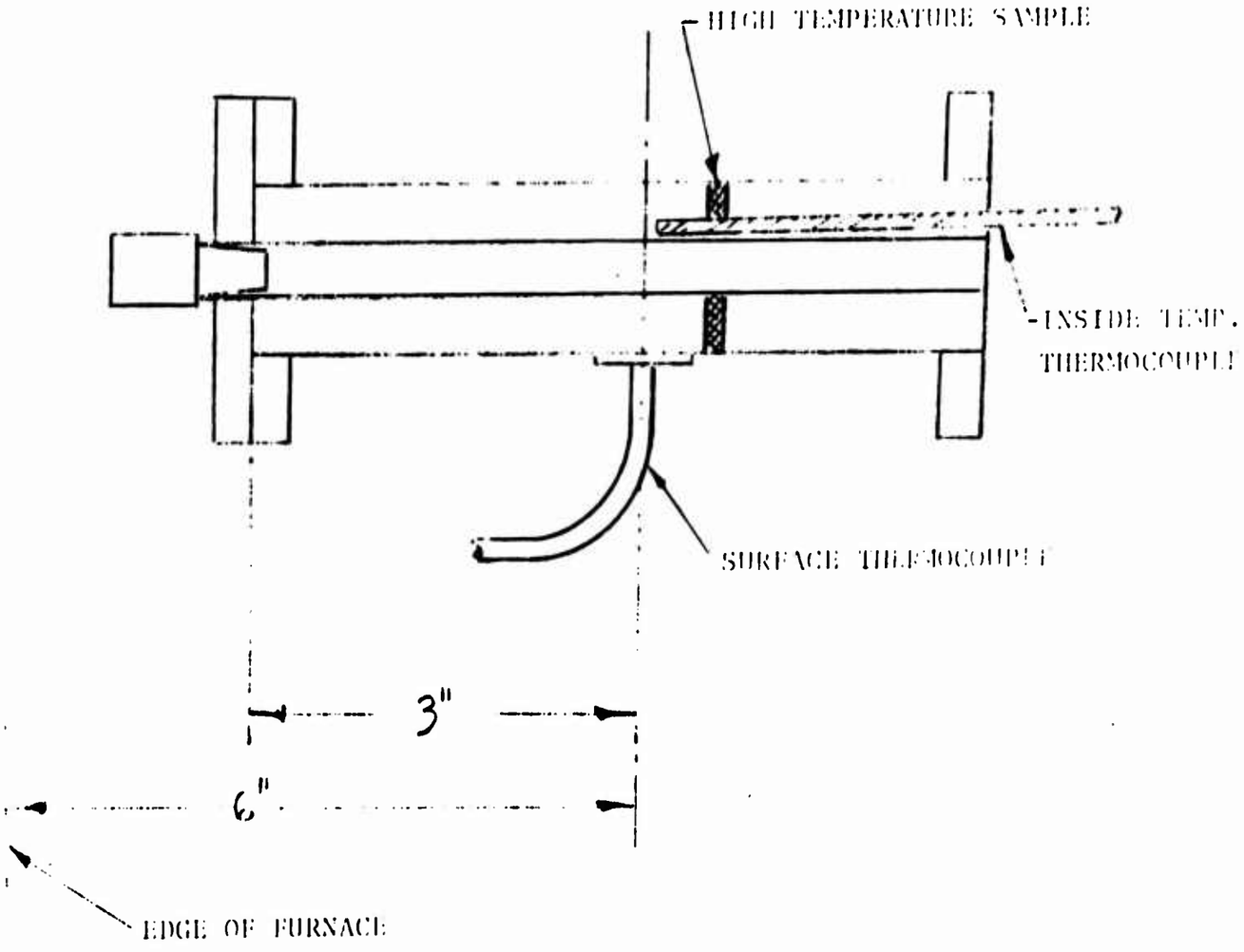

Figure 15. TEST SET-UP FOR MEASURING INSIDE Vs. OUTSIDE TEMPERATURES AS WELL AS AMBIENT TO TEST TEMPERATURES.

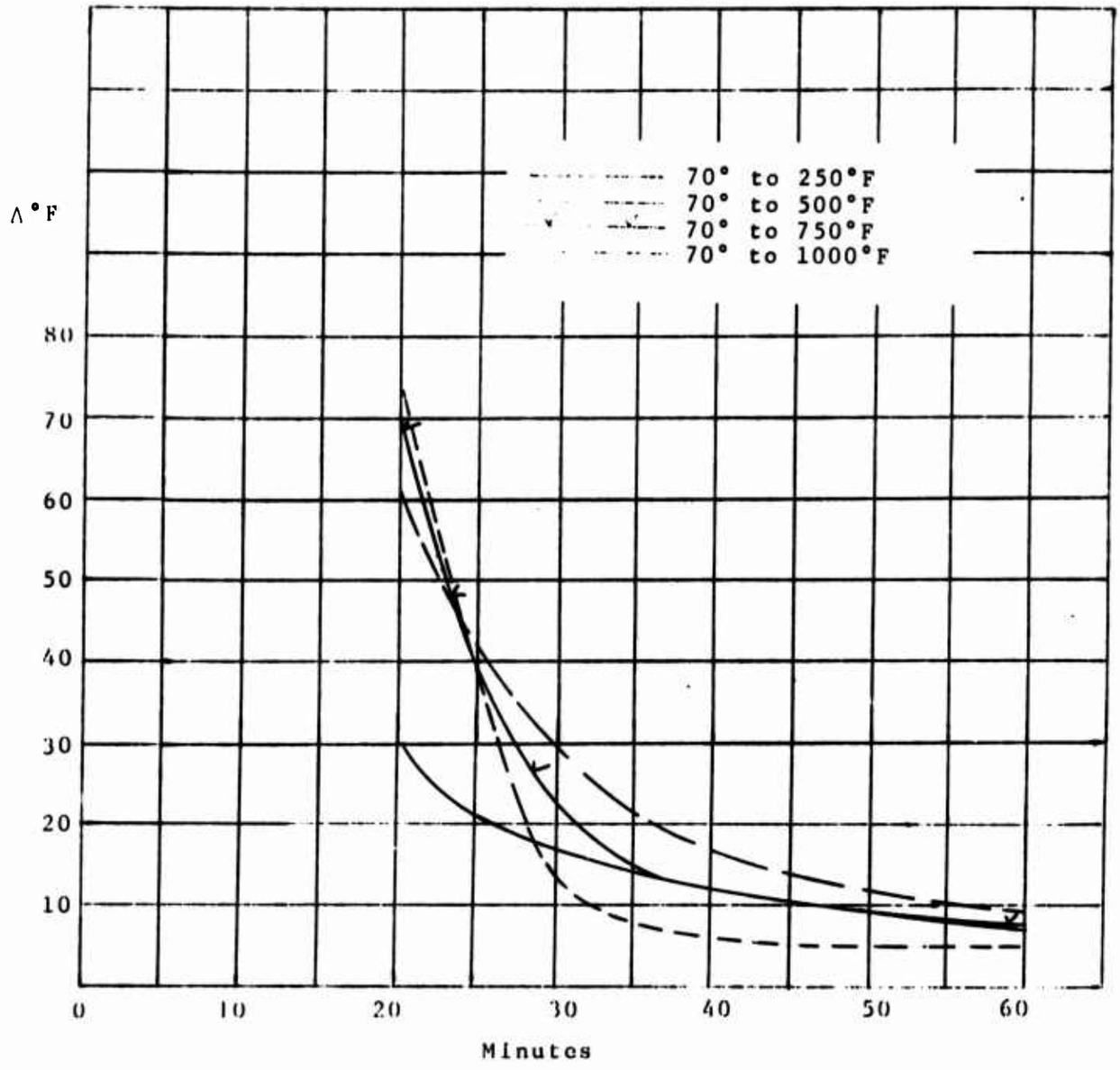

Figure 16. TEMPERATURE DIFFERENCES BETWEEN SURFACE AND INSIDE OF SAMPLE HOLDER Vs TIME.

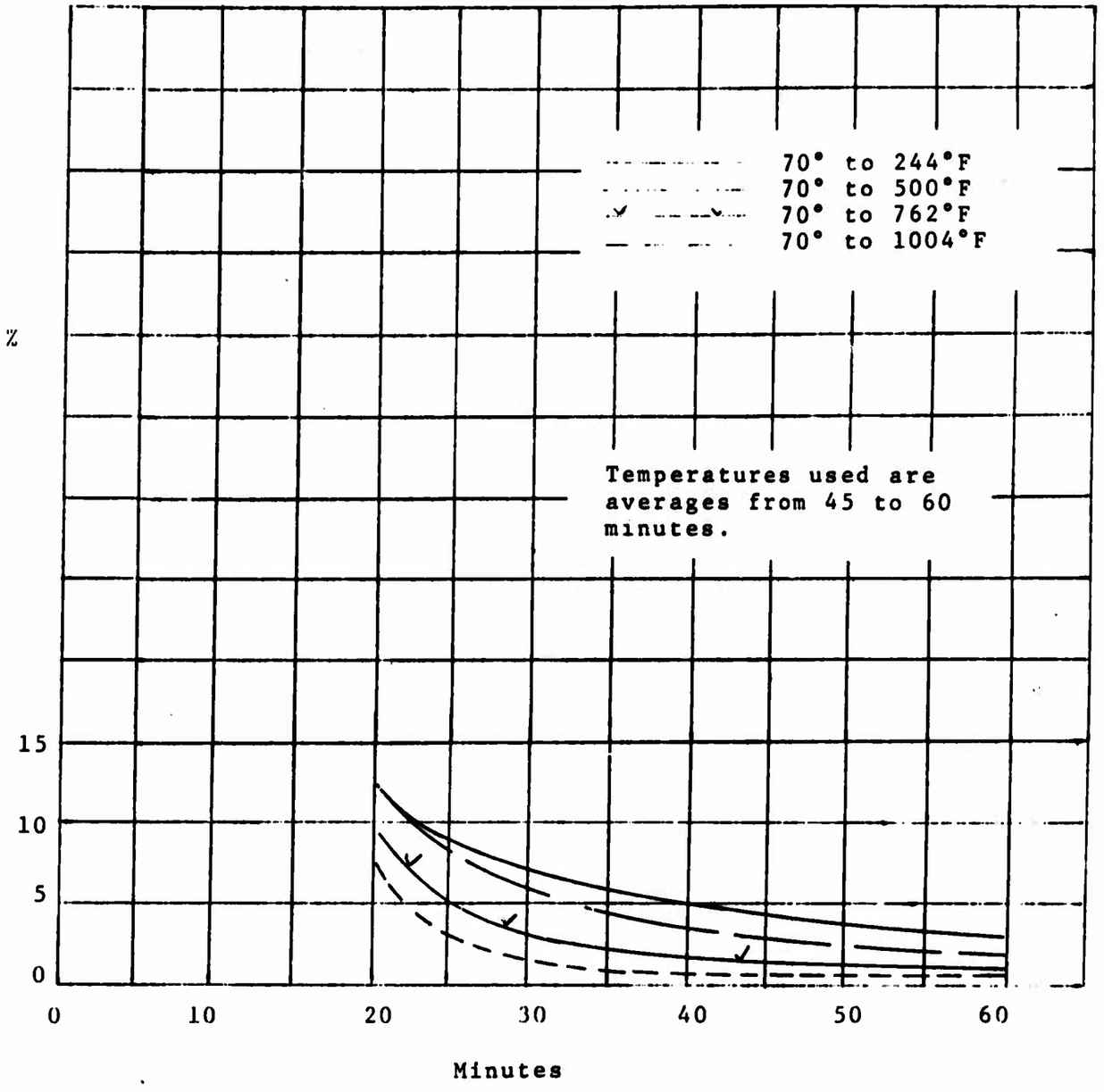

Figure 17, PERCENT TEMPERATURE DIFFERENCE BETWEEN INSIDE AND OUTSIDE TEMPERATURES Vs TIME.

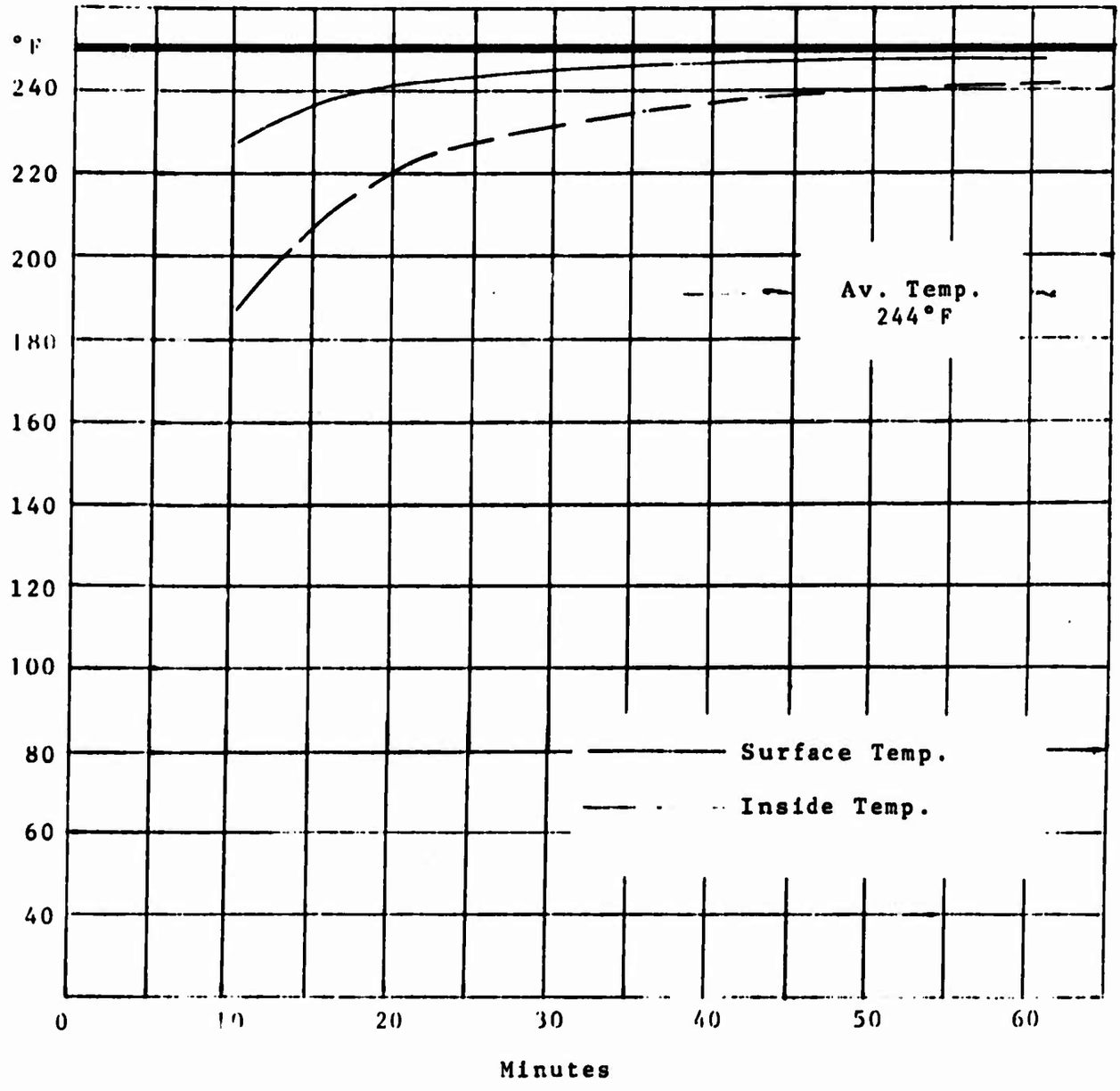

Figure 18. TIME/TEMPERATURE HISTORY 70°F to 250°F.

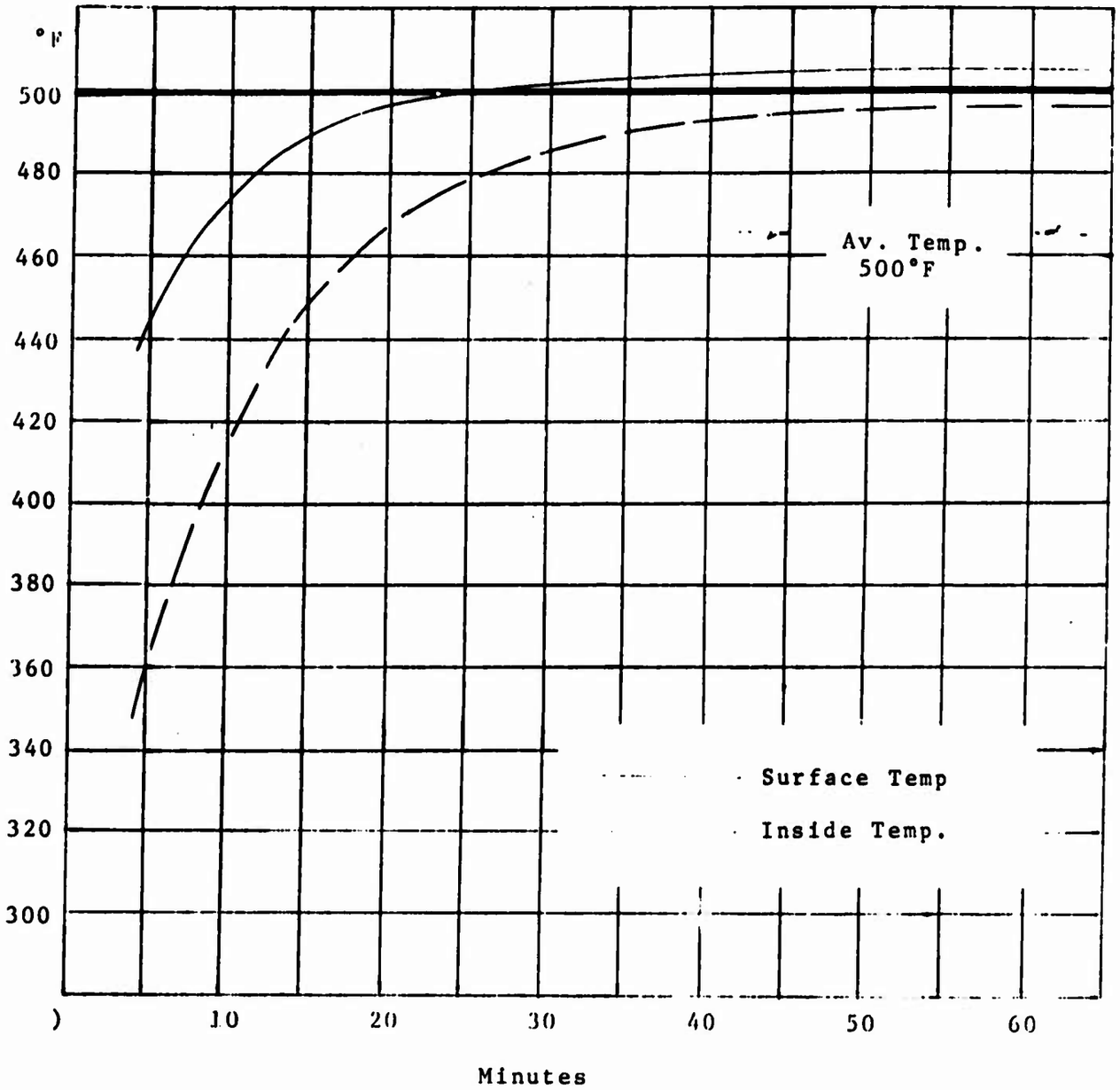

Figure 19. TIME/TEMPERATURE HISTORY 70°F to 500°F.

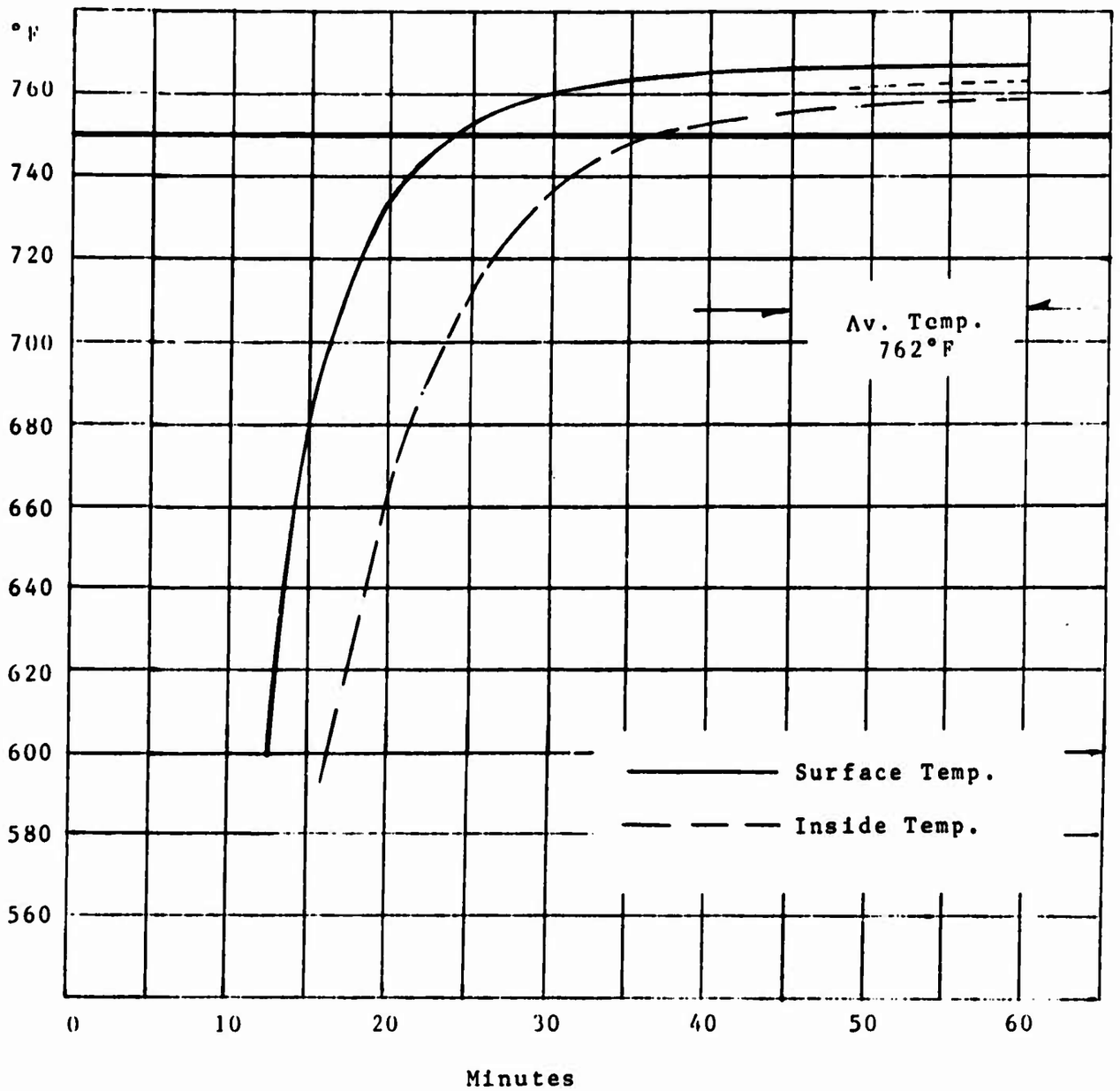

Figure 20. TIME/TEMPERATURE HISTORY 70°F to 750°F.

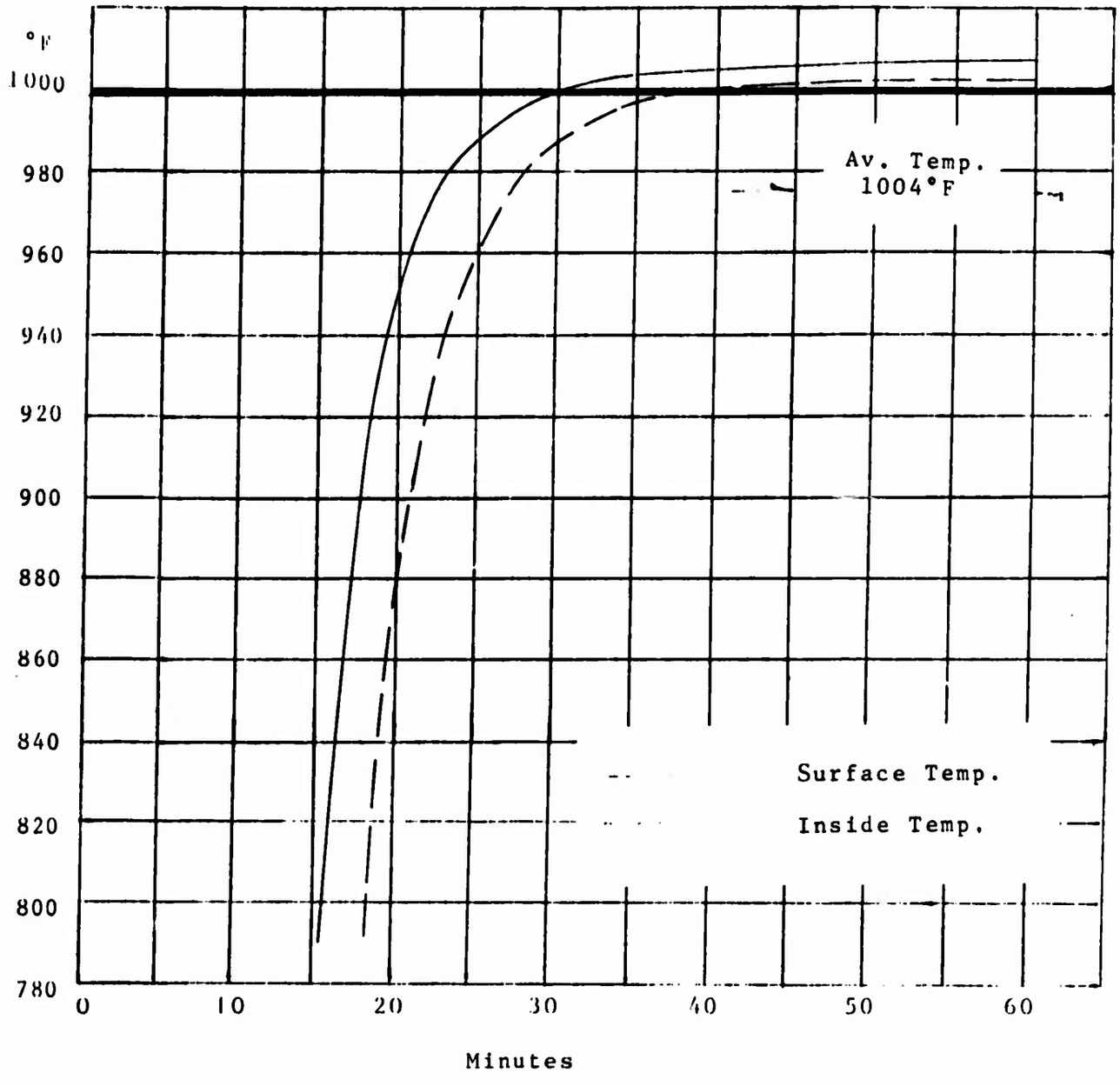

Figure 21. TIME/TEMPERATURE HISTORY 70°F TO 1000°F.

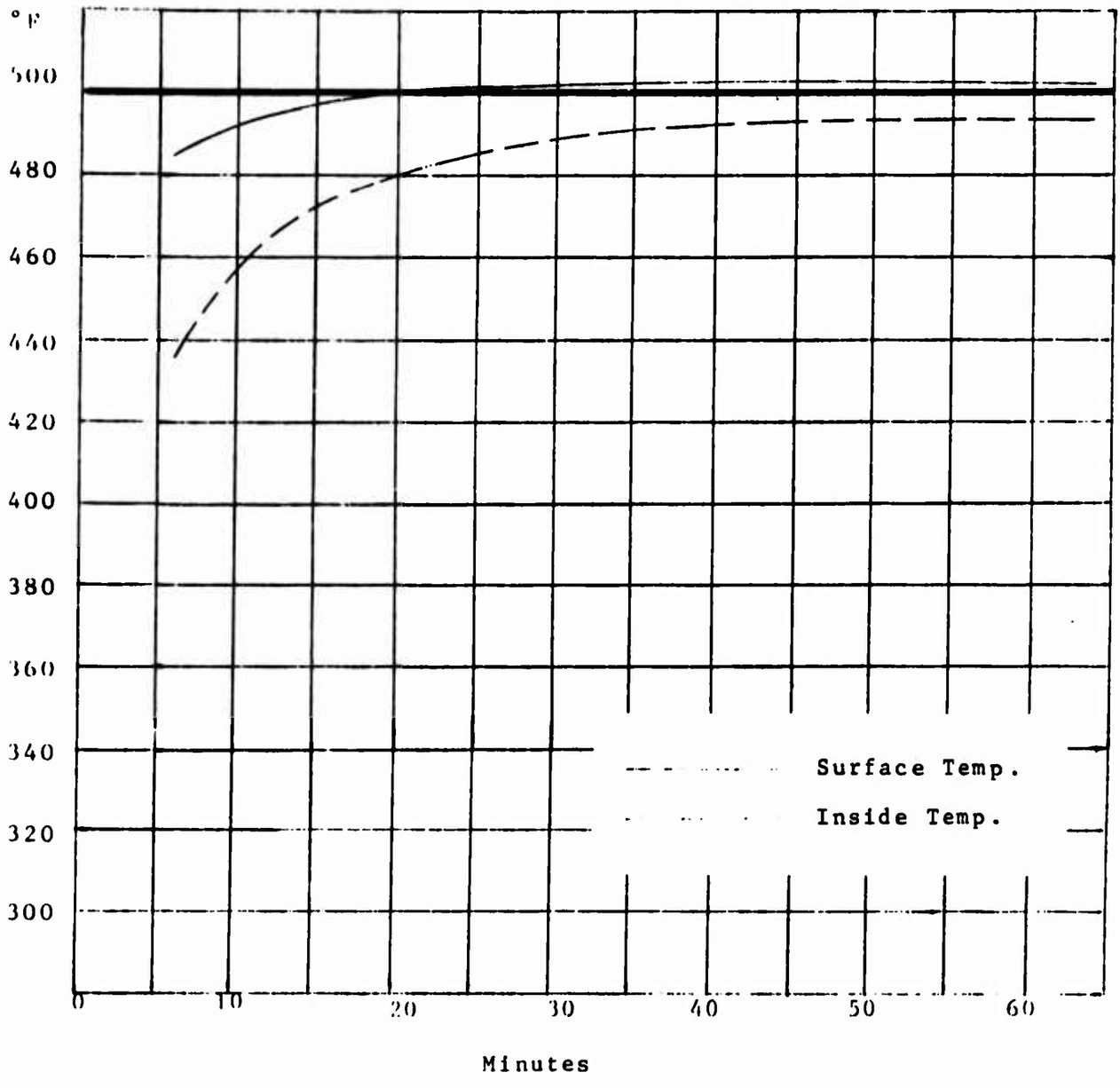

Figure 22. TIME/TEMPERATURE HISTORY 250°F TO 500°F.

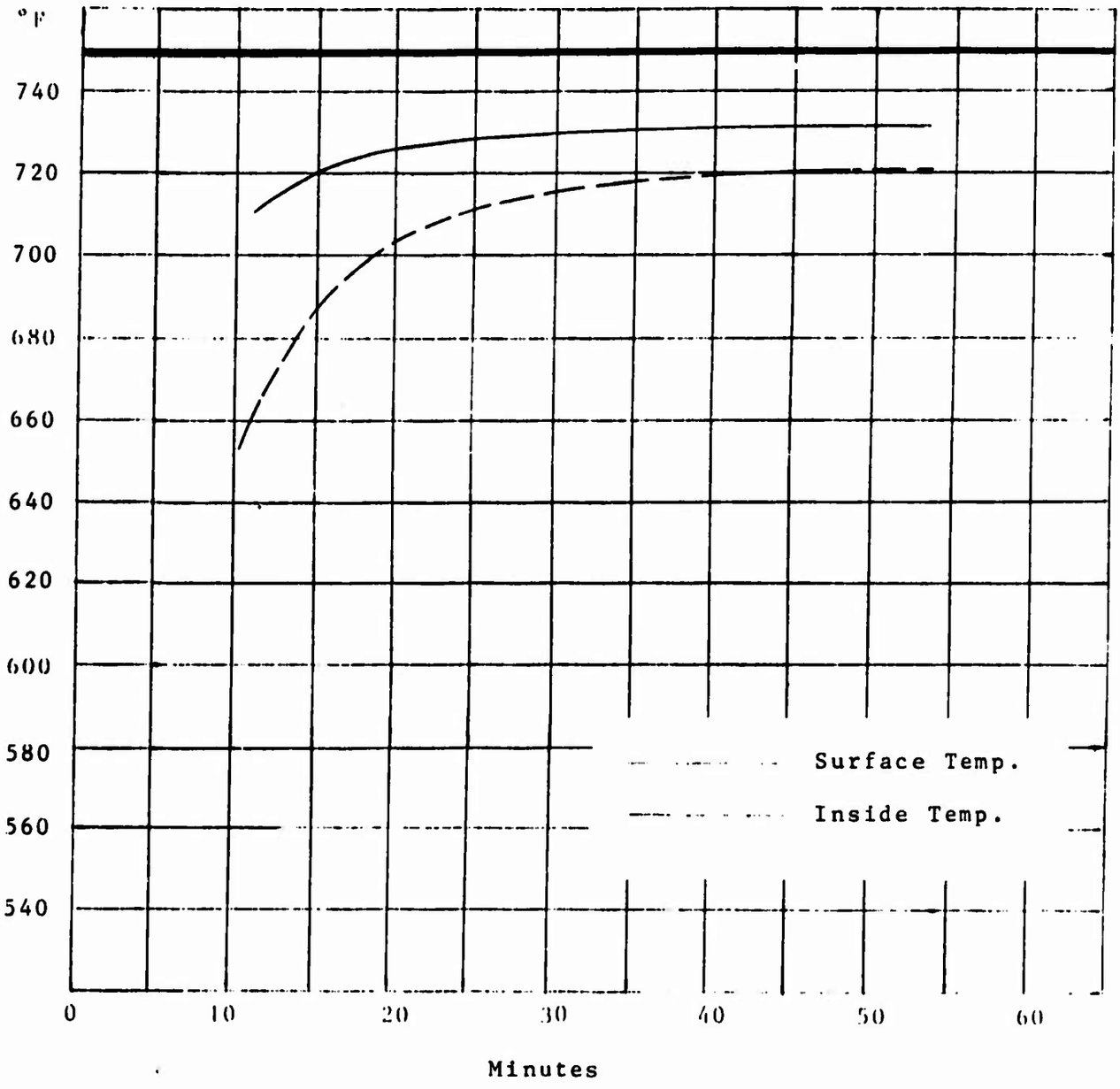

Figure 23. TIME/TEMPERATURE HISTORY 500°F TO 725°F.

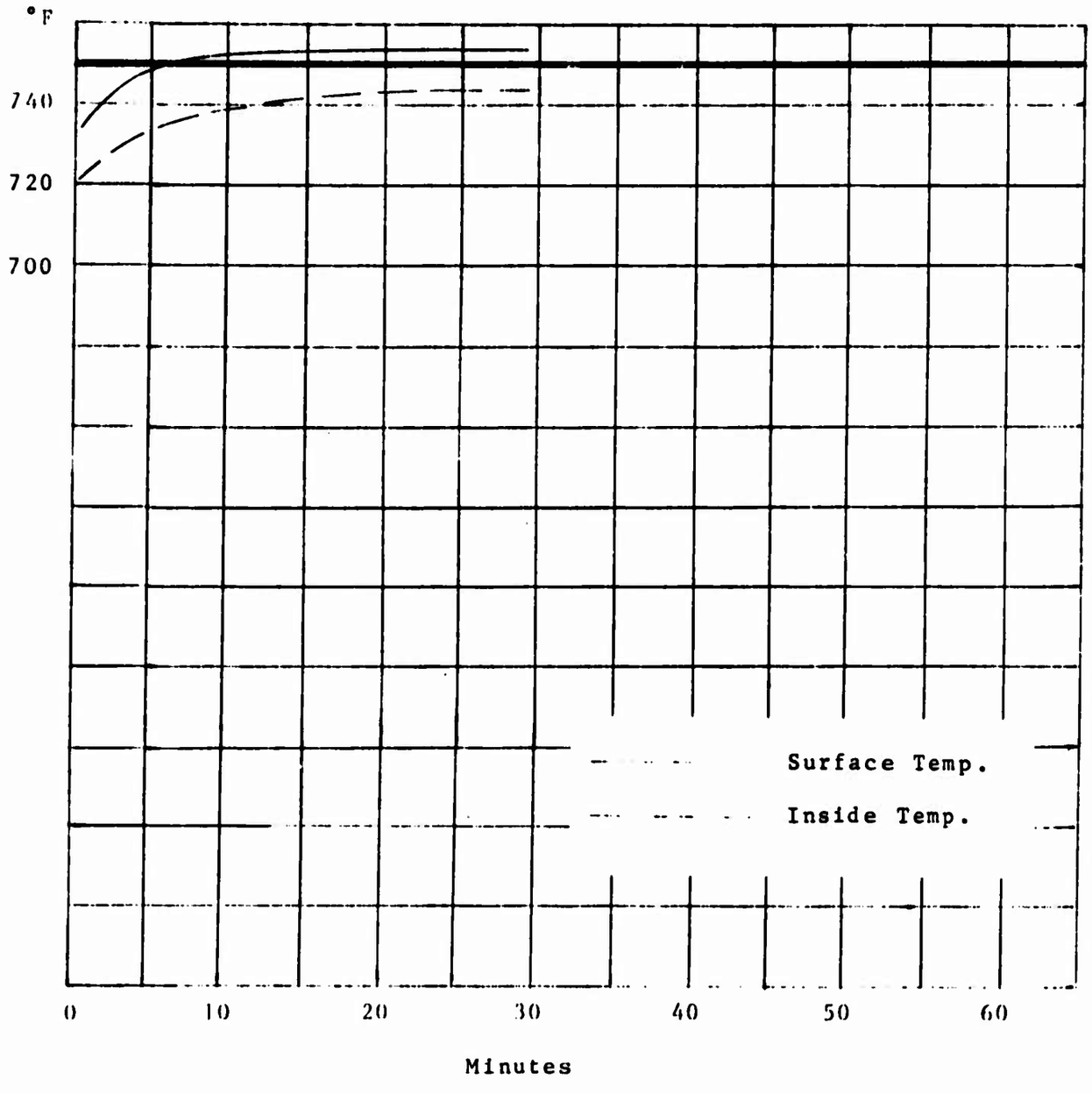

Figure 24. TIME/TEMPERATURE HISTORY 725°F TO 750°F.

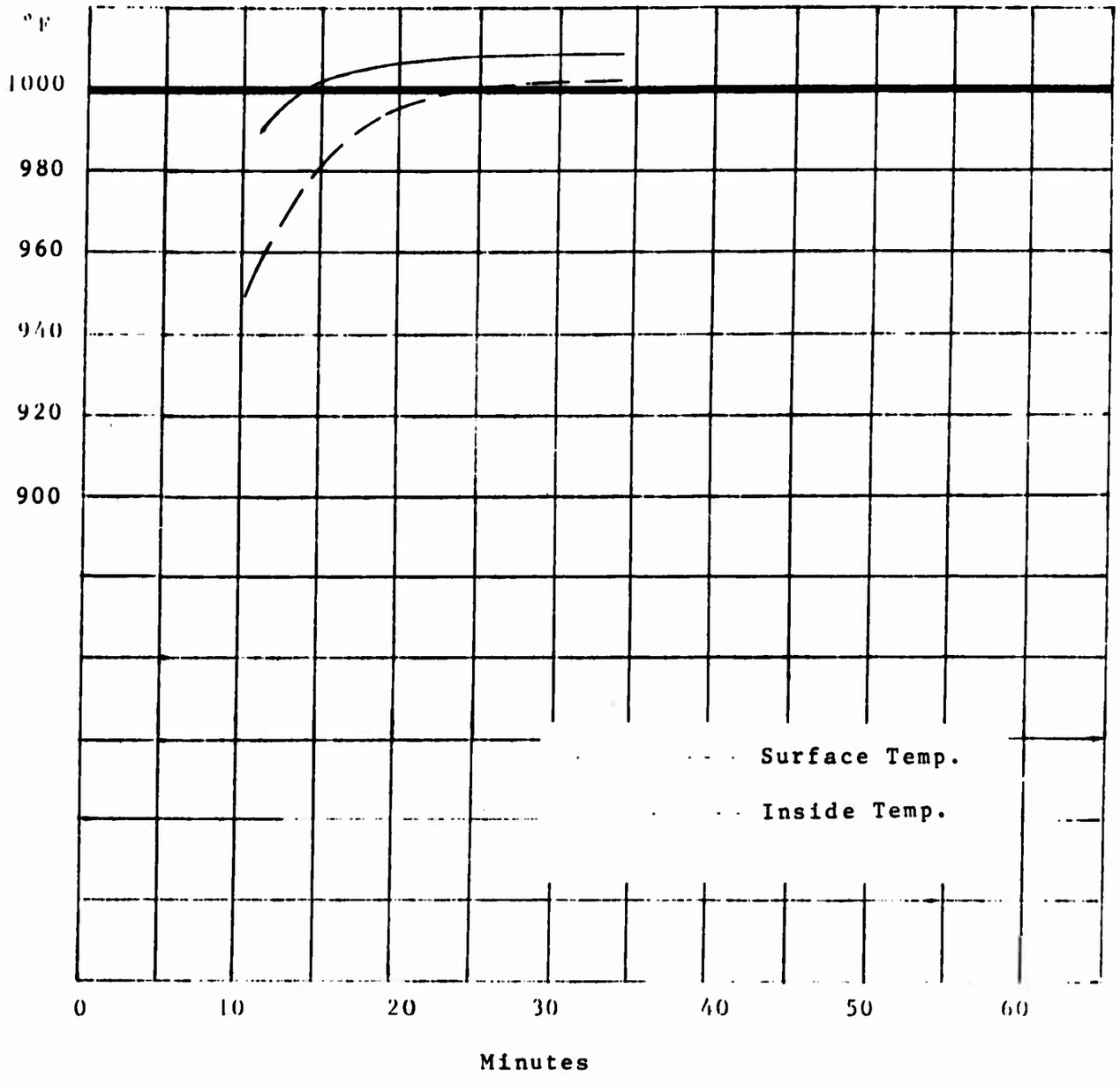

Figure 25. TIME/TEMPERATURE HISTORY 750°F TO 1000°F.

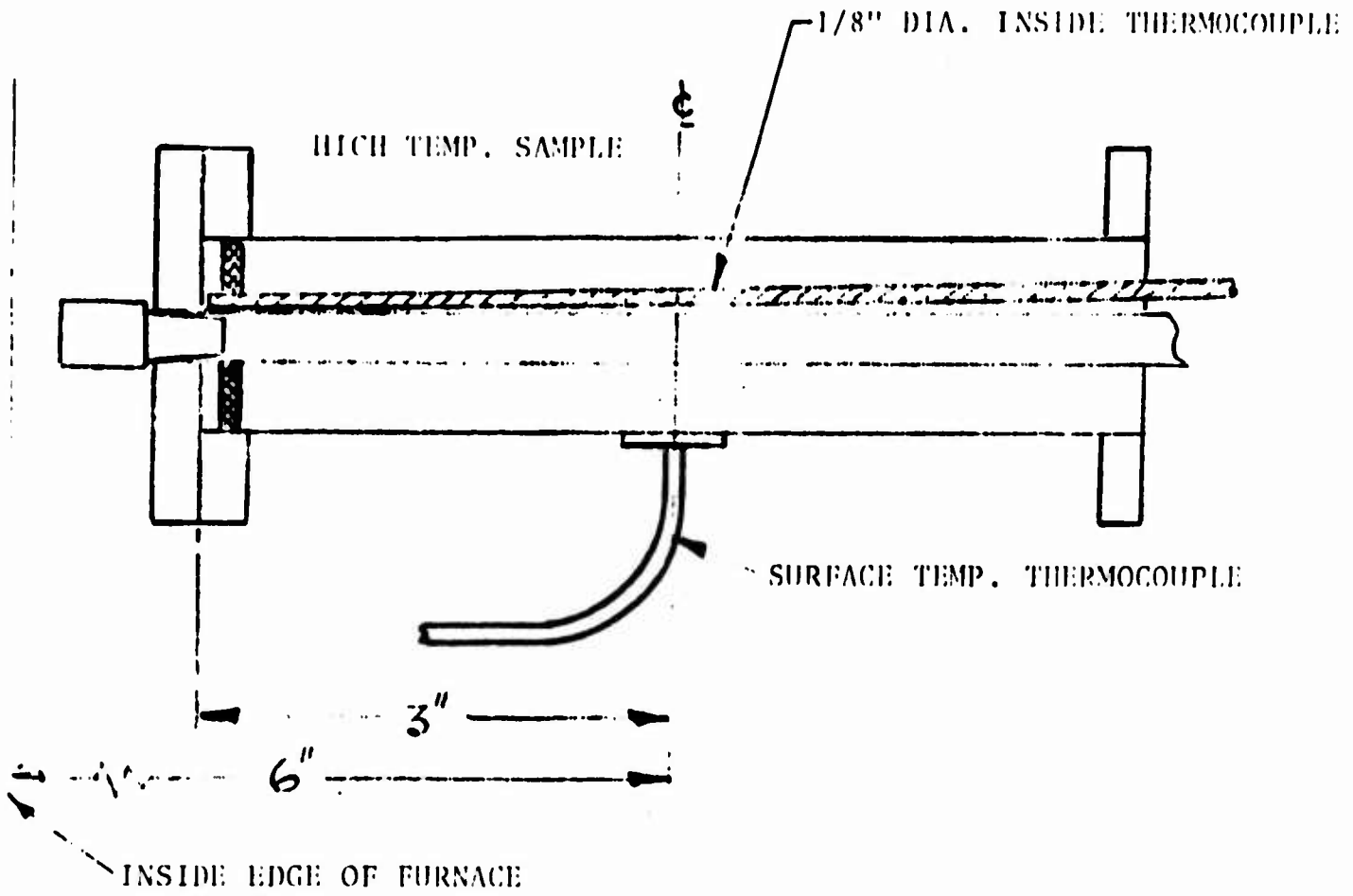

Figure 26. TEST SET-UP FOR TEMPERATURE RECOVERY TESTS.

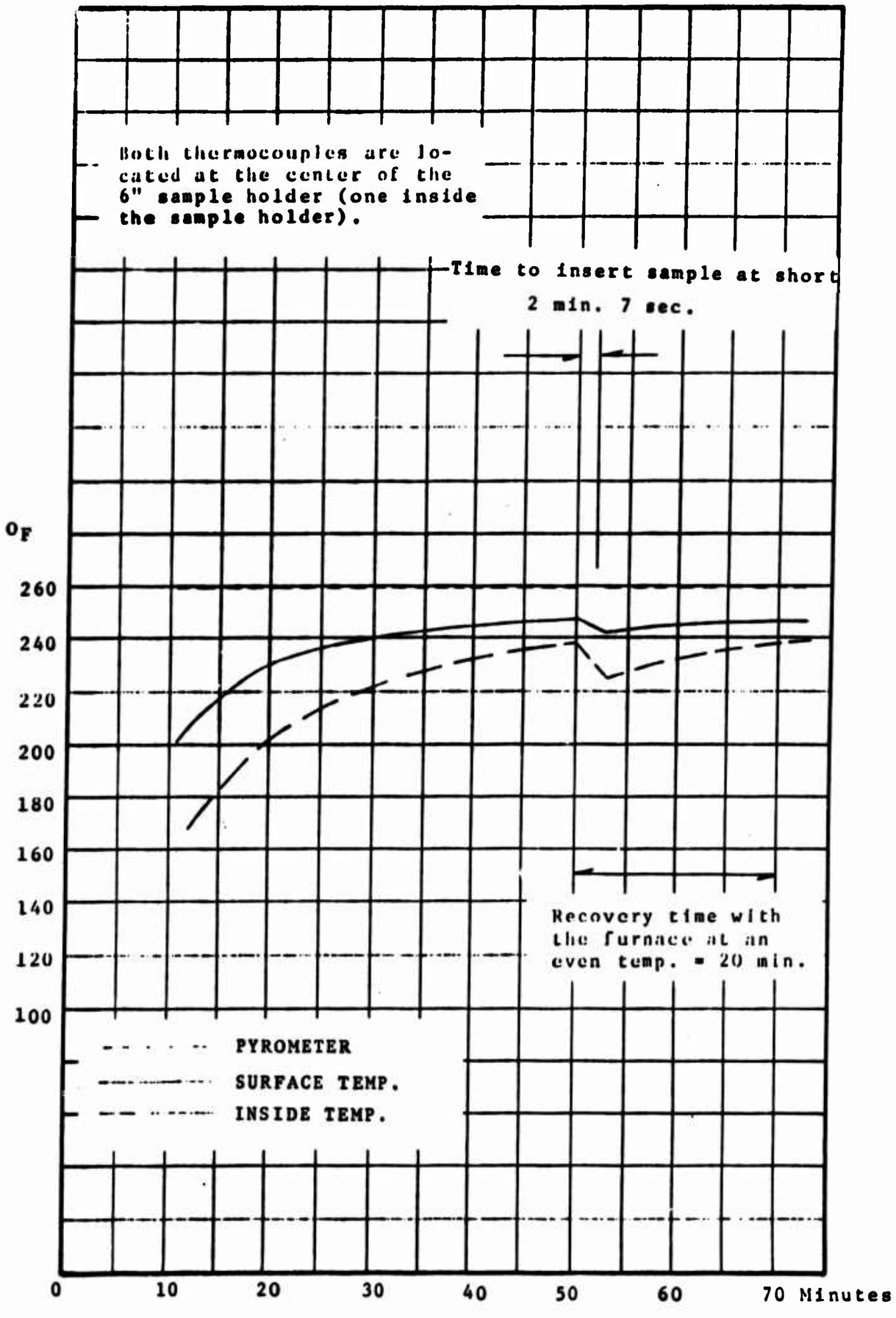

Figure 27. TEMPERATURE RECOVERY TIME 70°F to 250°F.

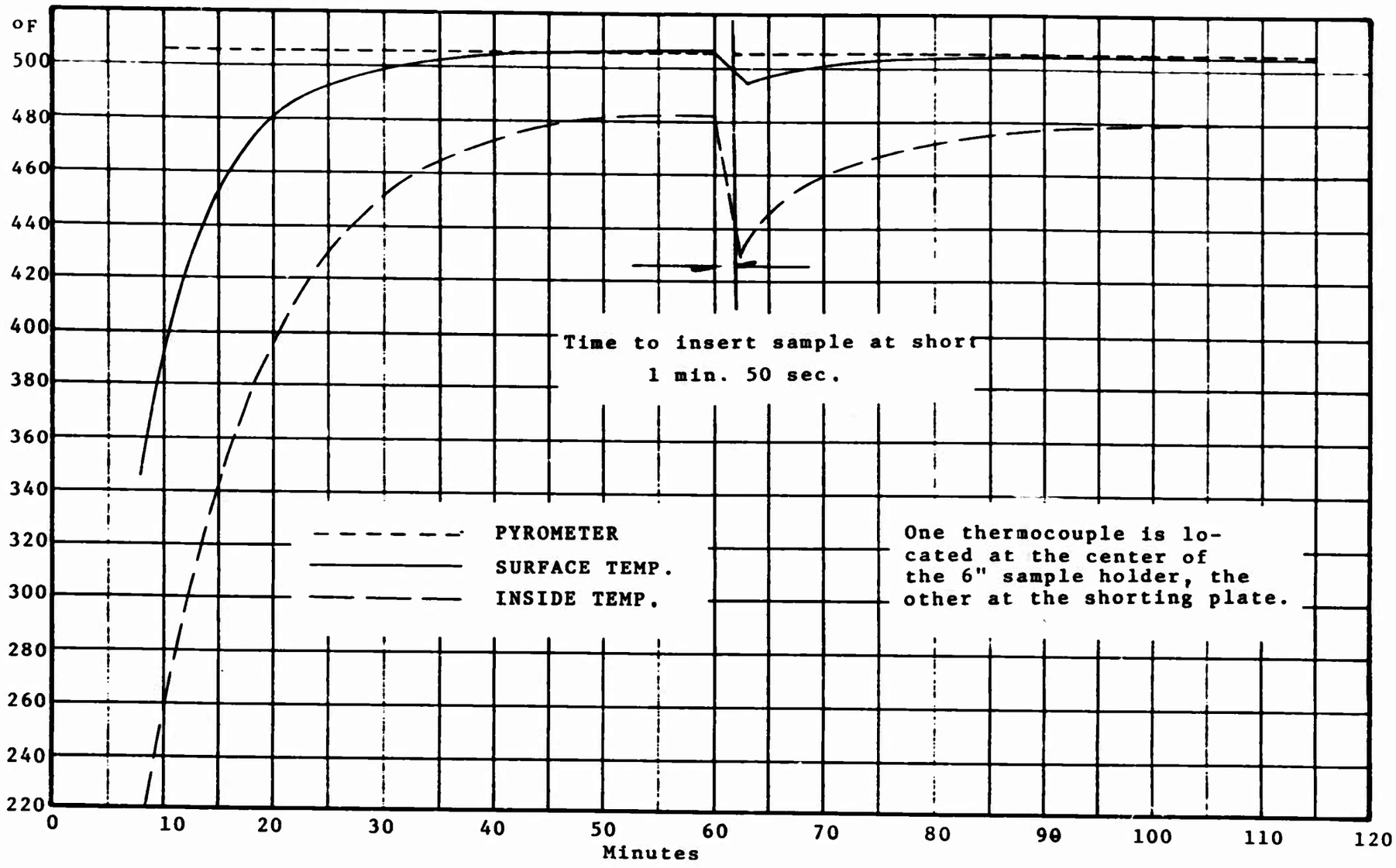

Figure 28. TEMPERATURE RECOVERY TIME 70°F to 500°F.

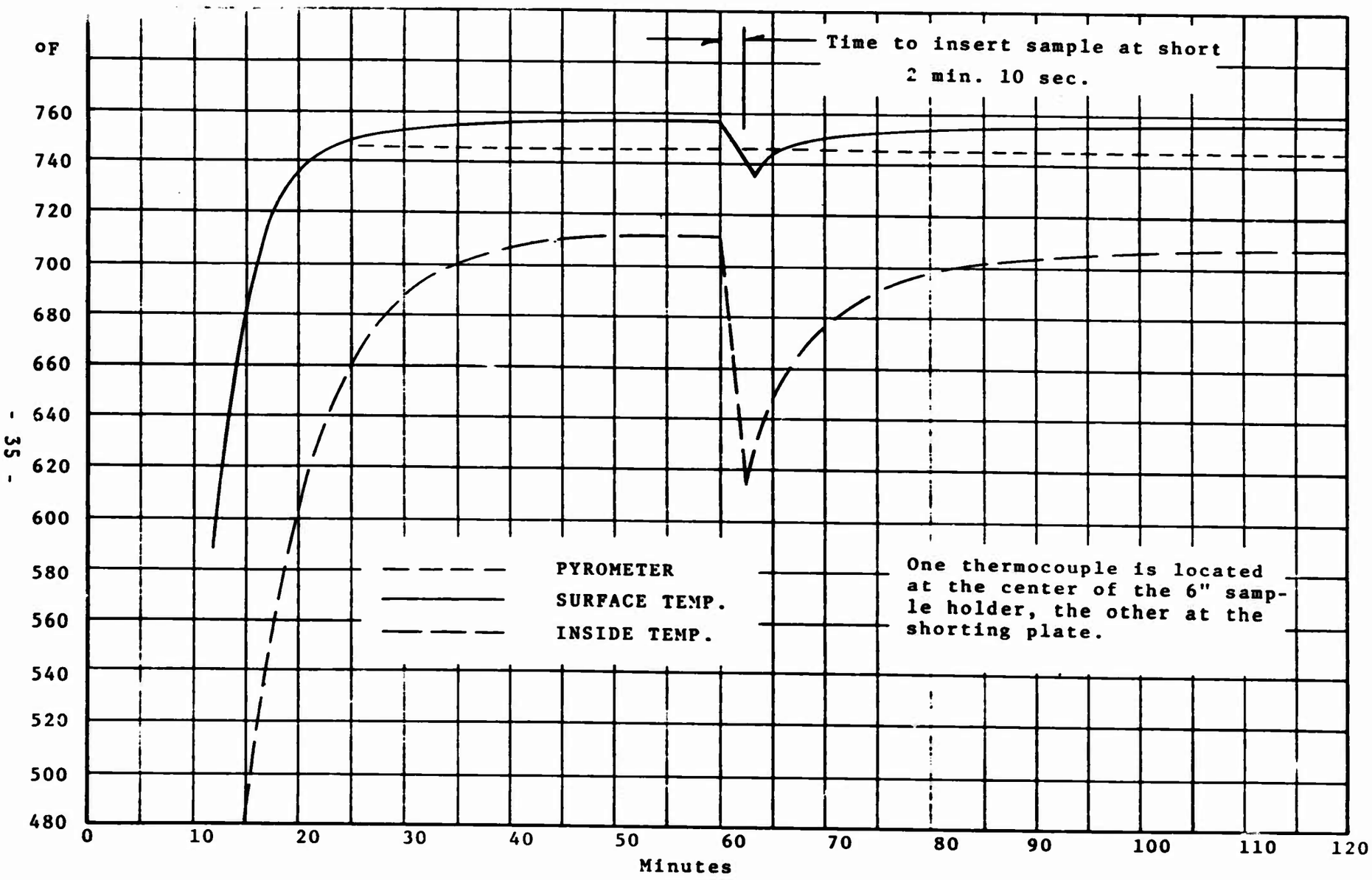

Figure 29. TEMPERATURE RECOVERY TIME 70°F to 750°F.

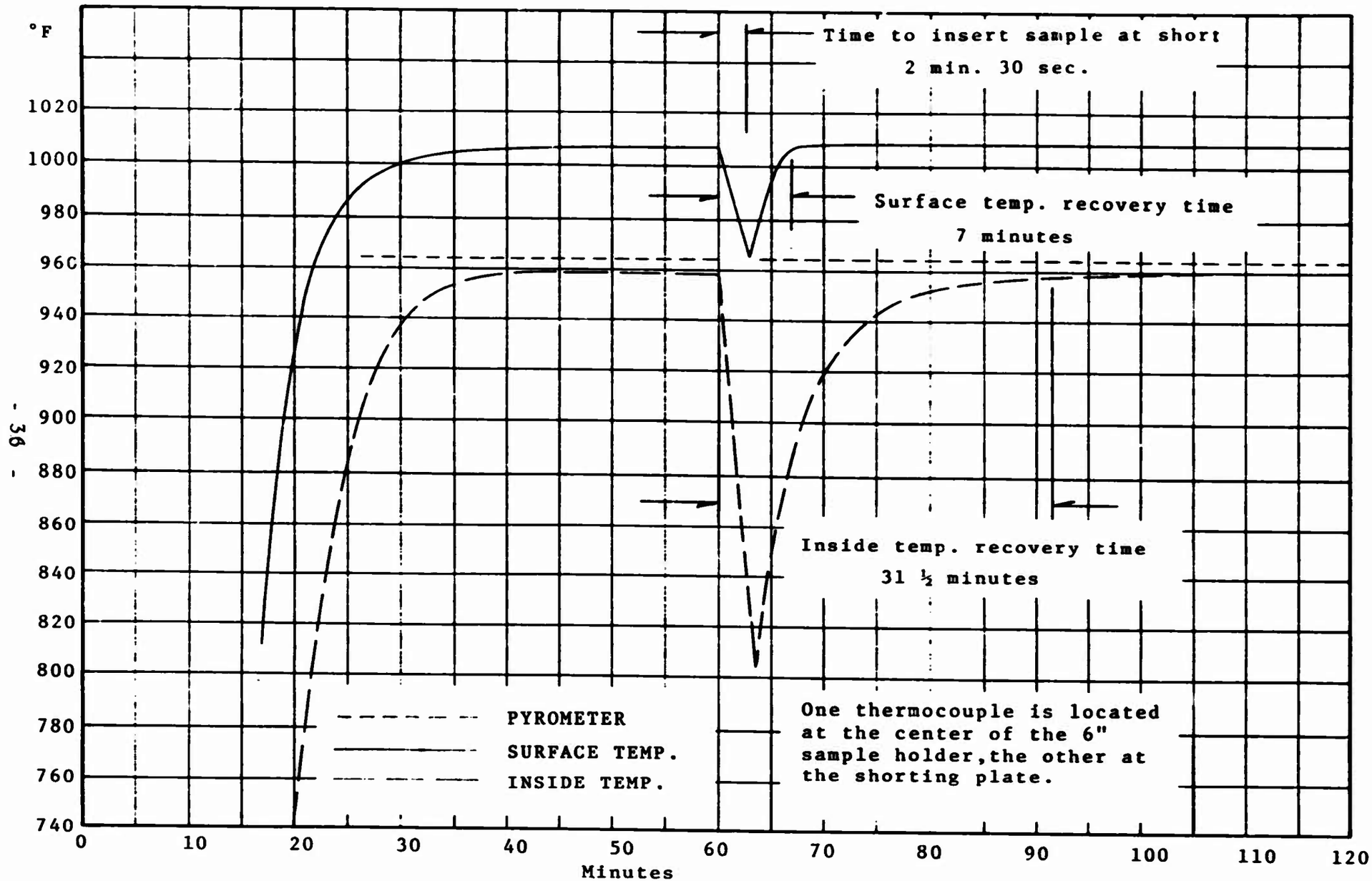

Figure 30. TEMPERATURE RECOVERY TIME 70°F TO 1000°F.

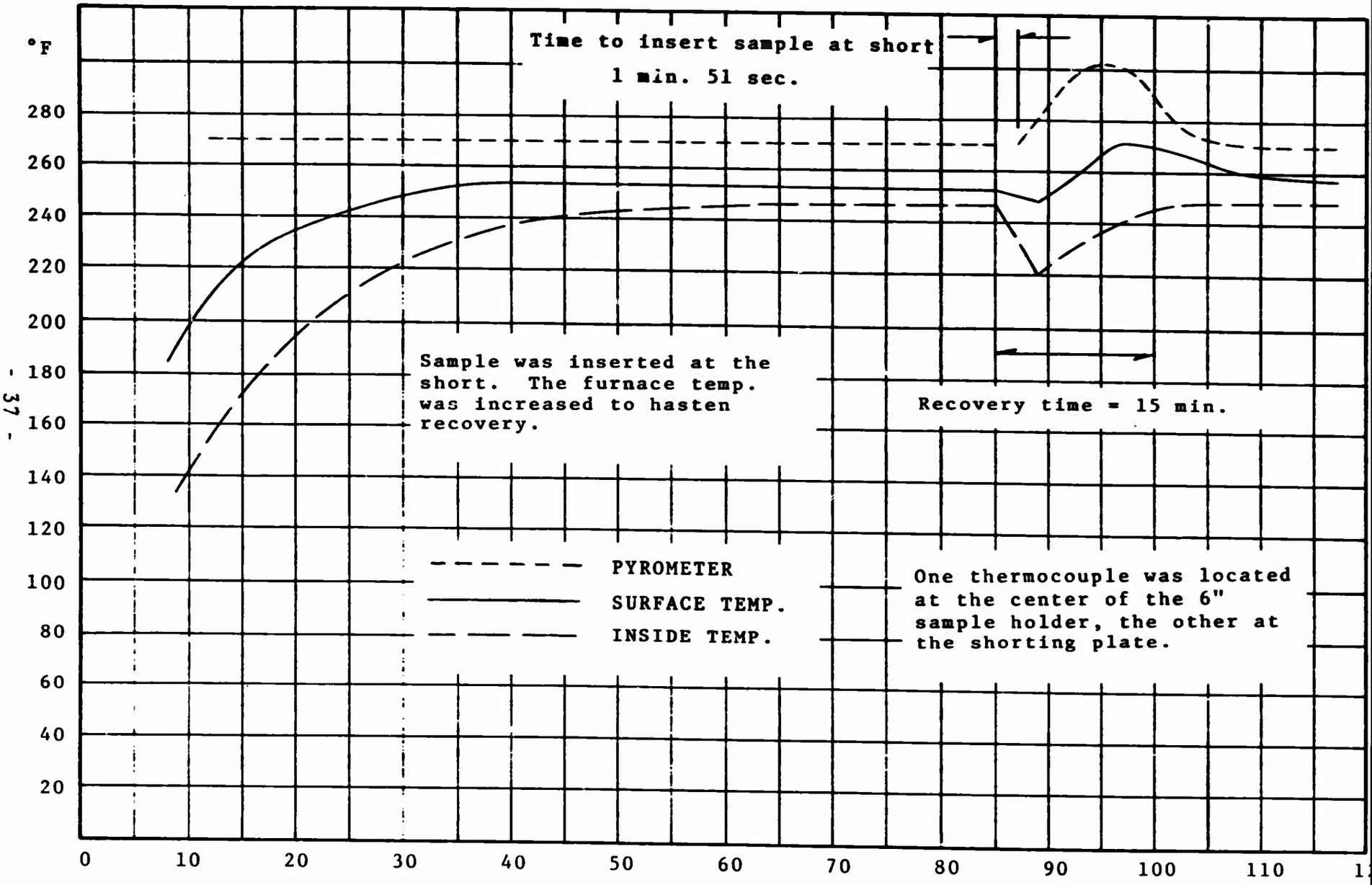

Figure 31. TEMPERATURE RECOVERY TIME 70°F TO 250°F.

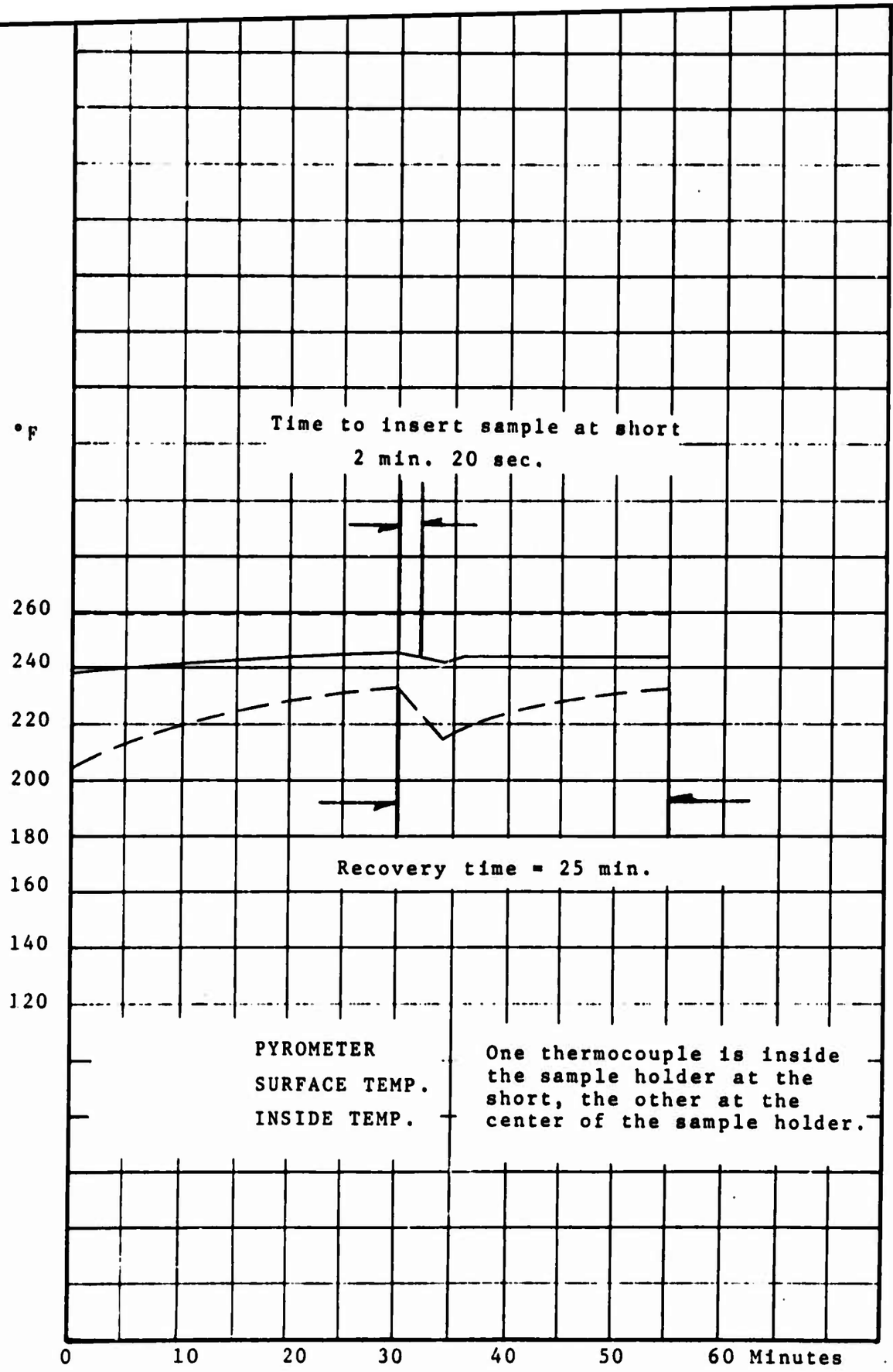

Figure 32. TEMPERATURE RECOVERY TIME 70°F to 250°F.

there are the following differences (ΔF) between the temperature at short circuits of the sample holder and the center of the furnace, three inches away:

a) $\Delta F \sim 33°$ at 1000°F
b) $\Delta F \sim 26°$ at 750°F
c) $\Delta F \sim 13°$ at 500°F
d) $\Delta F \sim 6°$ at 250°F

Hence when the sample is moved in $\lambda/4$, the furnace temperature is to be adjusted accordingly for a thermocouple at a fixed position, i.e., at the short circuit or at the center of the furnace.

2. The measurements show that for moving the sample in $\lambda/4$, requiring the opening of the furnace, 15 to 20 minutes are needed for the temperature to return to the desired temperature.

3. The temperature at the center of the sample is always lower than the temperature at the outer surface of the sample holder. From the curves given, it is possible to set the furnace temperature so that any desired temperature may be obtained at the sample by observing the temperature at the outer surface of the sample holder. The temperature difference at the inner conductor is of course due to convection currents.

4. Starting from room temperature, for the temperature at the sample to stabilize to a given temperature requires between 38 and 50 minutes, as follows:

a) 55 minutes from 70° to 250°F
b) 50 minutes from 70° to 500°F
c) 45 minutes from 70° to 750°F
d) 38 minutes from 70° to 1000°F

5. For the sample to stabilize at a temperature when the temperature is raised requires from 45 to 30 minutes for 250°F increments as follows:

a) 45 minutes from 250° to 500°F
b) 40 minutes from 500° to 750°F
c) 30 minutes from 750° to 1000°F

These results present no major obstacle other than that time and patience are required in the measurements.

Text resumes on next page

The previous discussions dealt primarily with the coaxial sample holder, since the waveguide sample holder has much thicker walls, the time lapses for temperature stabilization are much longer.

Figures 33 through 37 give the temperature rise at the sample inside the waveguide for a fixed pyrometer temperature. It is seen from Figure 33 that with the pyrometer maintained at 250°F it required approximately one hour for the temperature inside the waveguide to reach 210°F. In Figure 34 the temperature rise inside the waveguide to 510°F from room temperature required approximately one and a half hour with a fixed pyrometer temperature of 570°F. In Figure 35 it is seen that the temperature inside the waveguide required seventy-five minutes to rise from 250°F to 500°F, with the pyrometer set at 550°F. In Figure 36 it is seen that the temperature inside the waveguide required seventy-five minutes to rise from 500°F to 750°F, with the pyrometer set at 820°F. Again, in Figure 37 it is seen that the temperature inside the waveguide required seventy minutes to rise from 750°F to 1000°F with the pyrometer temperature set at 1050°F. Clearly, the time required for the temperature rise in the waveguide is more than twice that for the thinner walled coaxial sample holder.

Text resumes on page 46

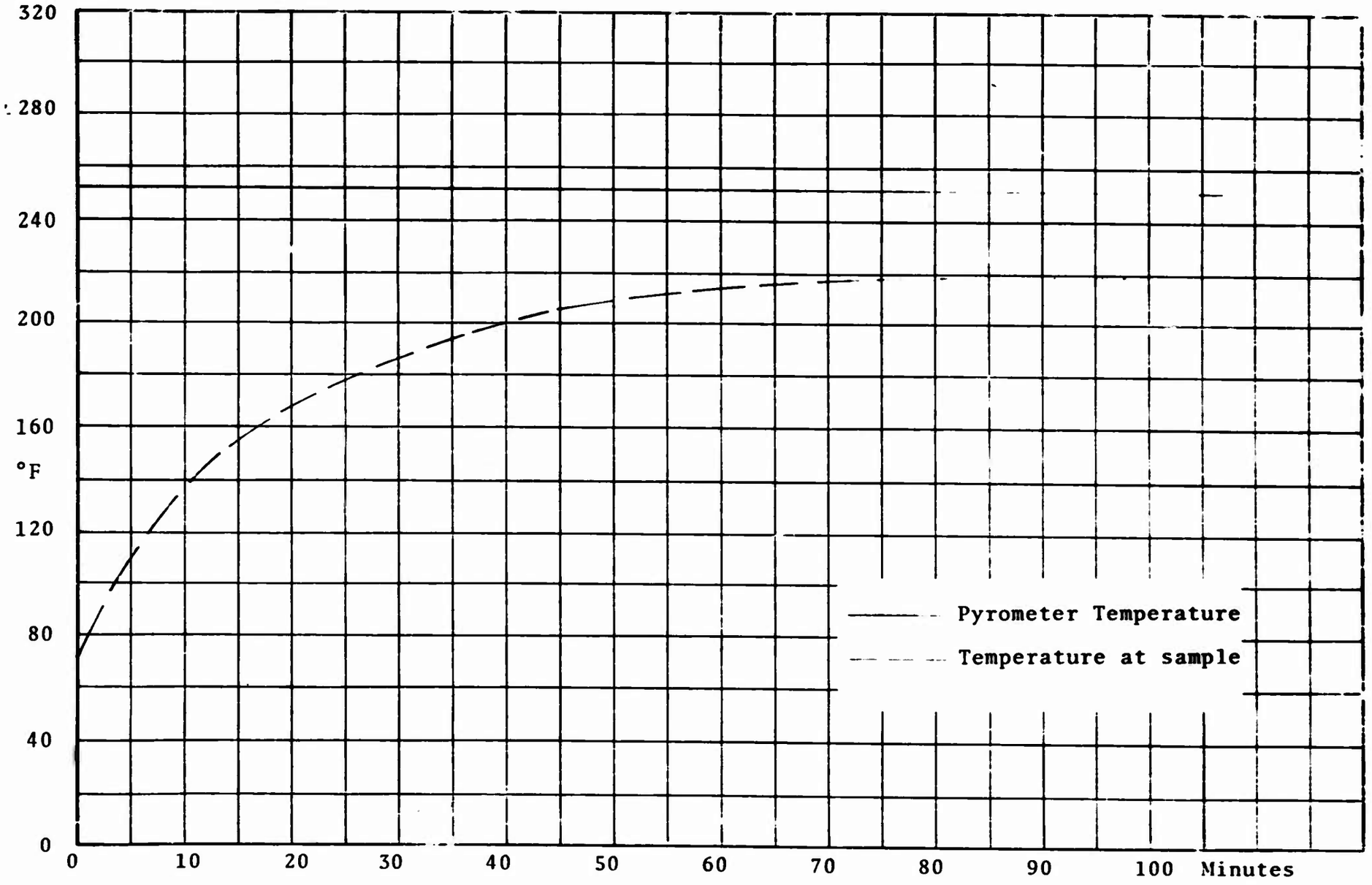

Figure 33. Time/Temperature History in Waveguide 75° to 218°F.

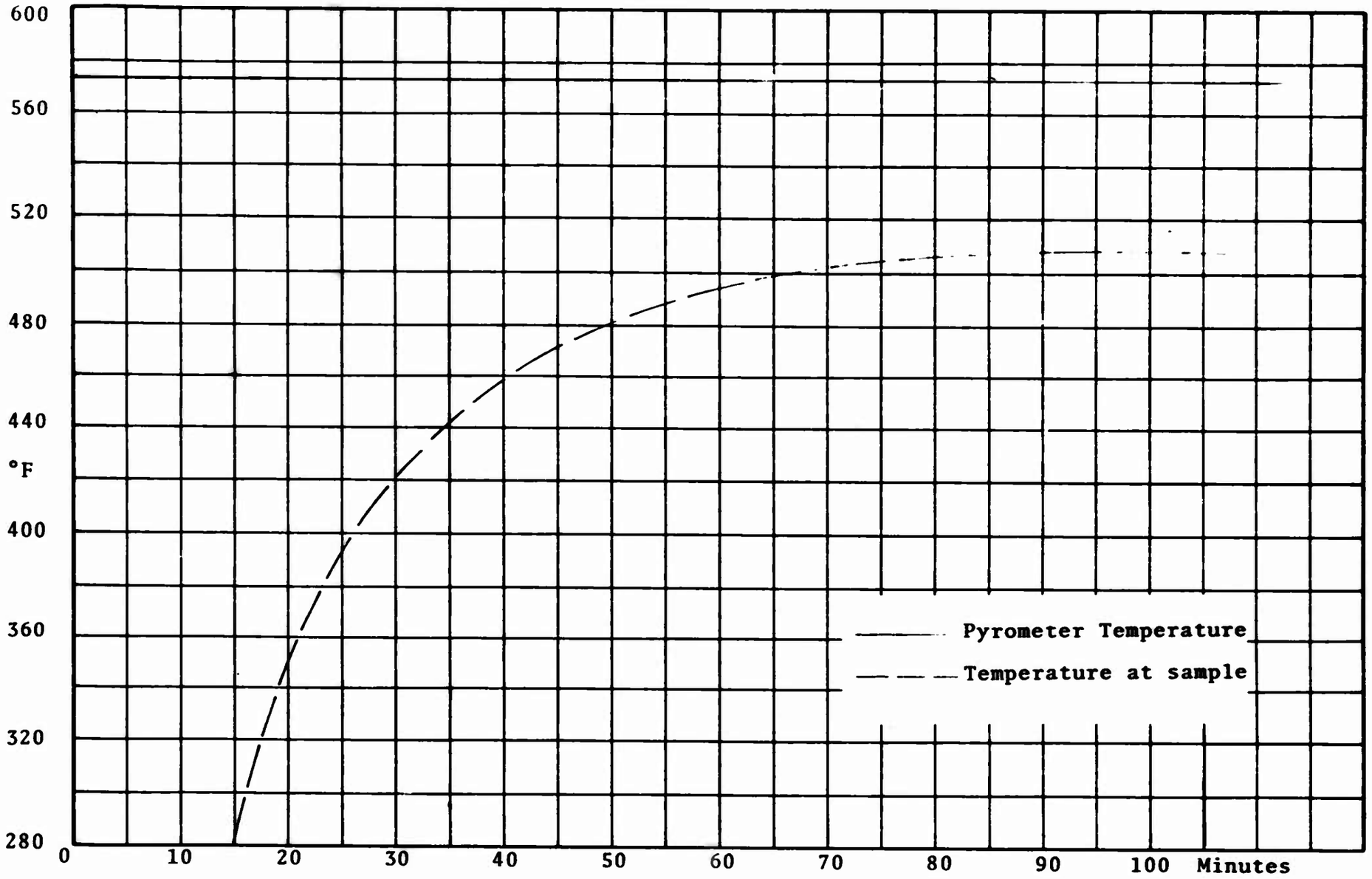

Figure 34. Time/Temperature History in Waveguide, 75° to 510°F.

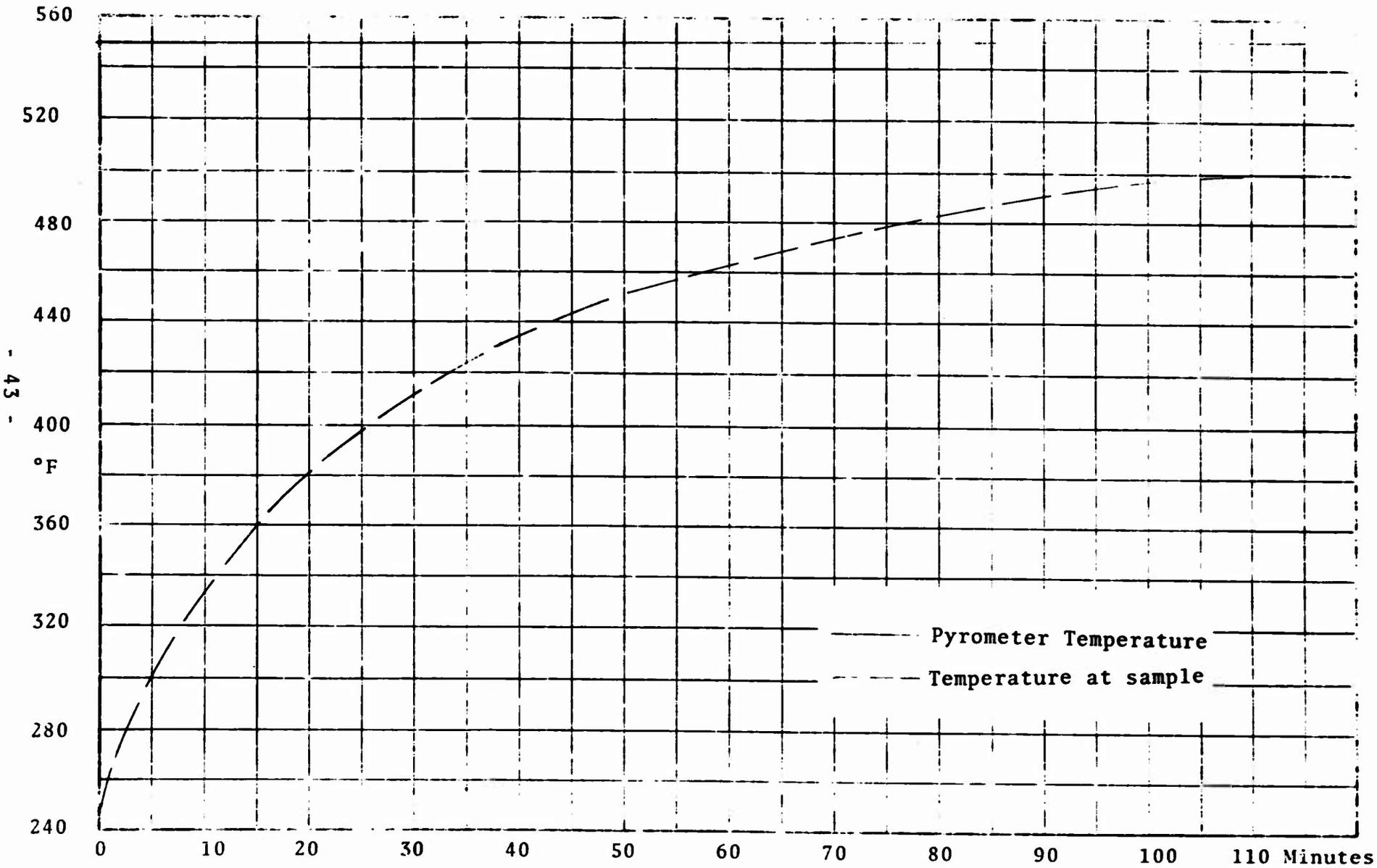

Figure 35. Time/Temperature History in Waveguide, 250° to 500°F.

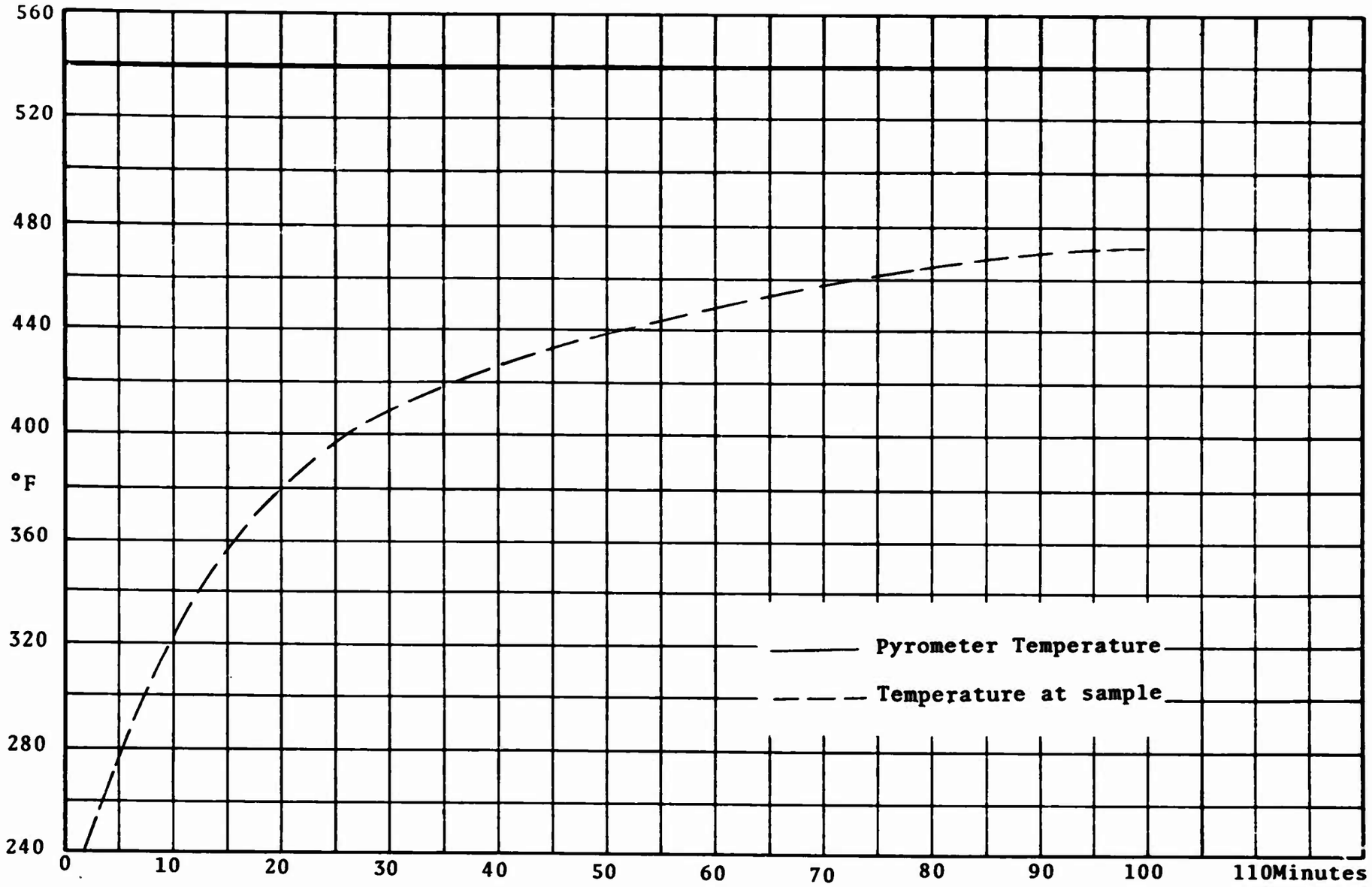

Figure 36. Time/Temperature History in Waveguide, 250° to 500°F.

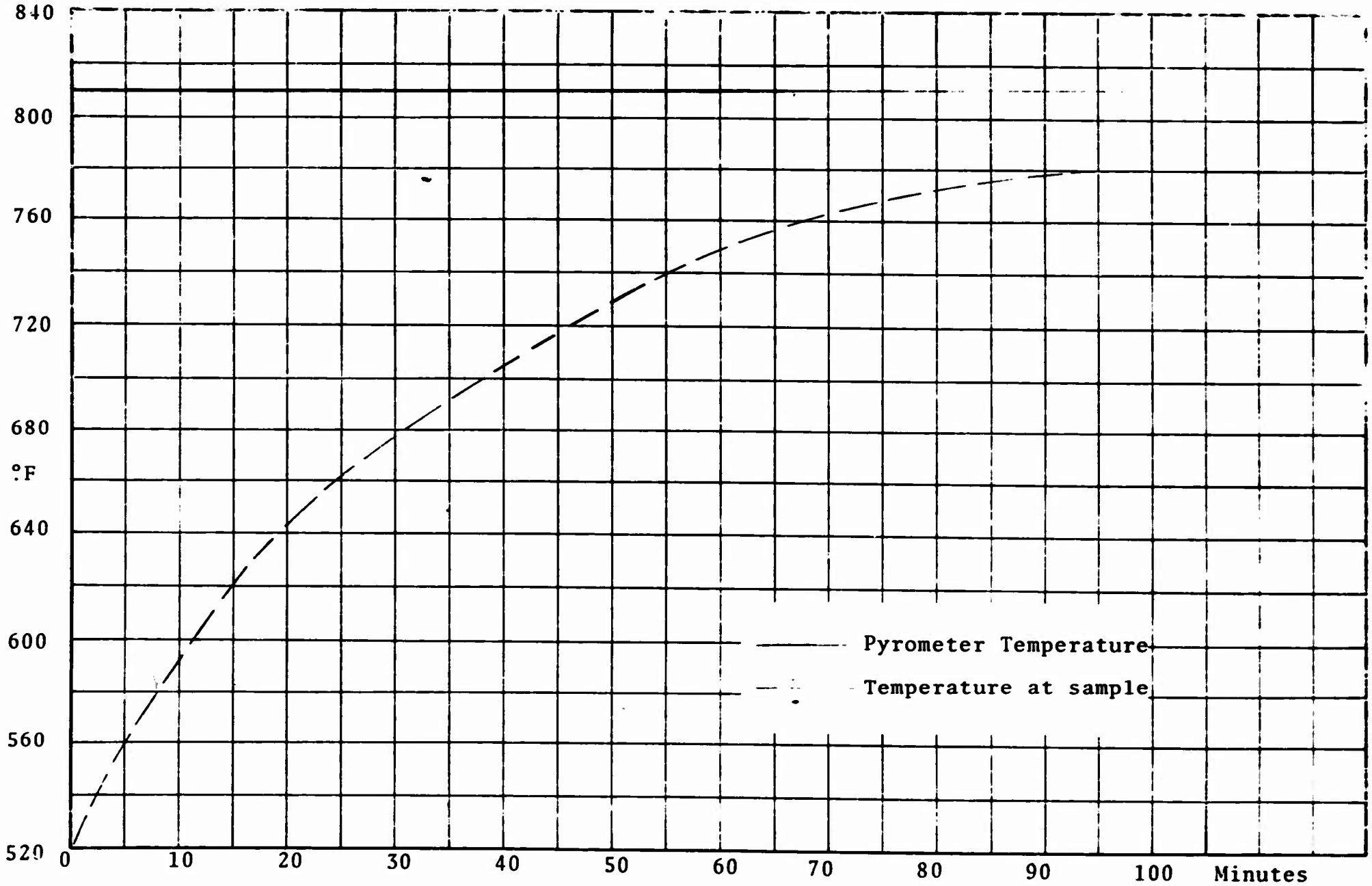

Figure 37. Time/Temperature History in Waveguide, 520° to 750°F.

IV. MEASUREMENT TECHNIQUE

The measurement technique consists of determining, as accurately as possible, the position of the minimum and the VSWR (or the distance between twice minimum points of the Voltage Standing Wave) with the sample placed at the short circuit and $\lambda/4$ away from it. The procedure is as follows:

1. The appropriate Hewlett-Packard signal generator is tuned to the desired frequency and is stabilized with the Dymec 2650A Oscillator Synchronizer. The Oscillator Synchronizer stabilizes the signal generator at discrete frequencies, at intervals of 200 $\pm$ 30 MHz.

2. The RF probe and RF tuners to the receiver are tuned with empty coaxial line to obtain the maximum VSWR. The VSWR should be greater than 48 or 50 db. The probe depth is to be adjusted until the signal on the oscilloscope is clearly visible, that is, a clear pip is to be seen on the receiver oscilloscope.

3. The position of the null nearest the sample holder is to be recorded. This is the reference for the measurement.

4. Although the synchronizer locks reliably to a frequency, nevertheless, the wave length in either the coaxial line or the waveguide should be measured by finding the distance between two successive minima ($\lambda/2$). Check that $\lambda/2$ is then equal to the length of the plunger to be used later to move the sample in for the open circuit measurement.

5. The sample is then inserted at the end of the sample holder, however, not pushed in by hand but rather have the sample pushed in by carefully tightening the bolts that hold the shorting plate to the flange of the sample holder, thus uniformly moving the sample in with the shorting plate.

Text resumes on next page

6. With the sample at the short circuit determine the position of the null nearest the sample holder. This should be in the neighborhood of the null obtained in 3 of the preceding page. Whenever possible, the position of the minimum is to be obtained by determining the positions of twice minimum power on either side of minimum. The position of the minimum is then the midpoint between these two measurements with the ΔX the distance between the two measurements. In the case of very low VSWR the position of the minimum is obtained by determining the position of the probe at a convenient power level on either side of the minimum with the minimum falling midpoint between the two measurements. Record ΔX or VSWR and the position of the minimum.

7. Move sample in $\lambda/4$. This is accomplished with a pre-cut plunger $\lambda/4$ long or by means of a plunger that can be precision set to $\lambda/4$.

8. Replace the shorting plate and measure the ΔXo and null position as in 6 above.

As is seen from the above, the procedure is rather straightforward, however, for reasonably good results considerable care in RF tuning to the receiver, adjustment of probe depth and in the measurement of the null positions and three db points is required. Ames gauges mounted on the slotted lines are used to obtain readings to approximately 0.0005 inches. Needless to say, the sample thickness is to be carefully measured.

The identical procedure as given in steps 1 to 8 above, is used for measurements at elevated temperatures for both coaxial line and waveguide. The only difference is that the gold plated Kovar sample holder is to be used and the furnace raised to the desired temperature. The temperature is to be determined from readings on a Leeds & Northrop millivolt potentiometer connected to the leads of a thermocouple mounted on the outer skin of the sample holder. Since there is a time lapse between the time the skin temperature has reached the desired temperature and the sample has reached the desired temperature, there is a minimum waiting period for each temperature before the measurements are taken.

Text resumes on next page

The test setup is given in Figure 38 which is identical for both waveguide and coaxial line except that the appropriate slotted line and sample holder are to be used.

The position of the reference null is either to be determined with empty sample holder or a correction made for the expansion of the coaxial line or waveguide for each temperature. In the measurements under this contract the null position with empty guide was determined for each temperature.

Text resumes on page 50

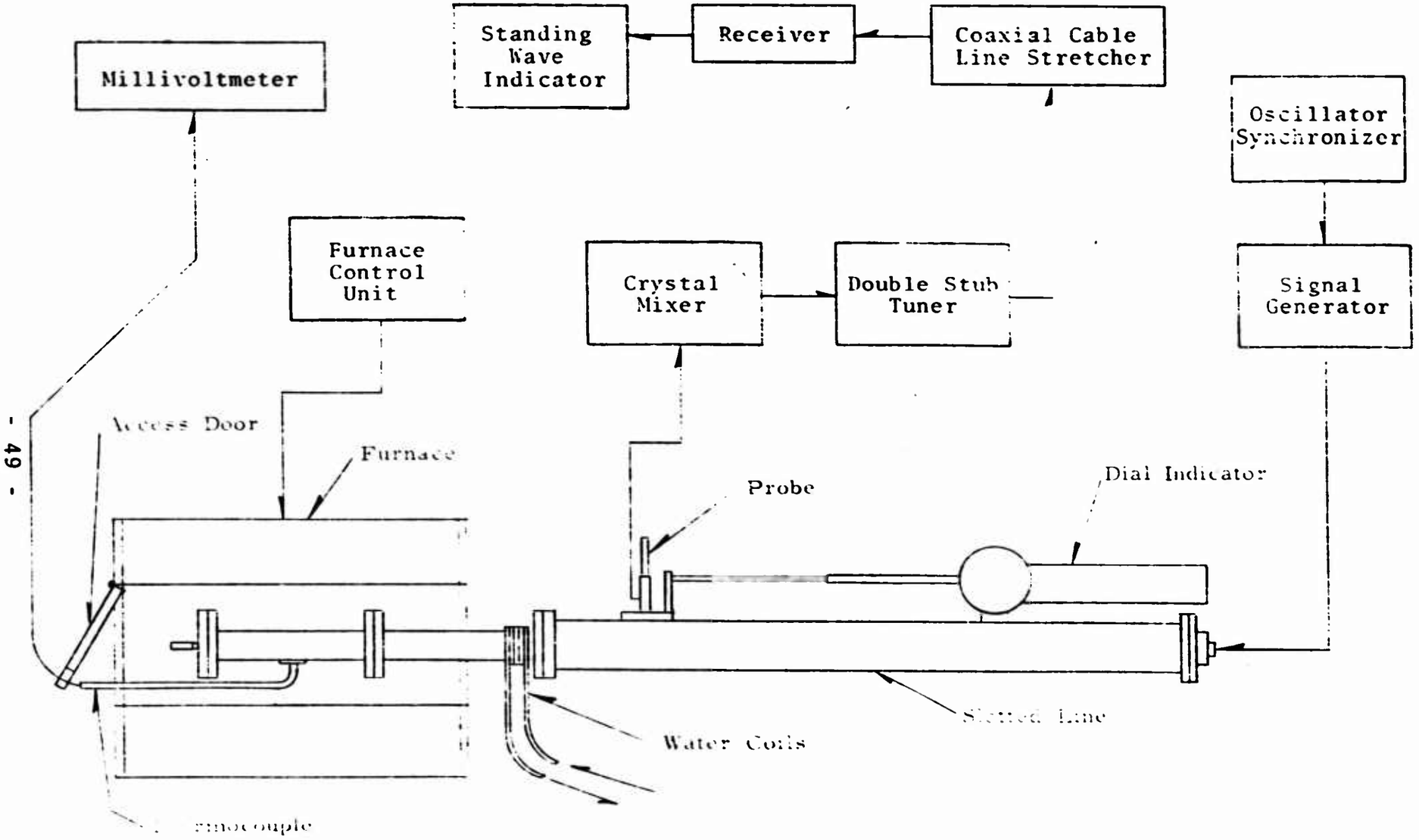

Figure 38. COMPLETE TEST SET-UP AND INSTRUMENTATION.

V. MEASUREMENT OF PURE DIELECTRIC MATERIALS AT HIGH TEMPERATURES

High and medium loss dielectric materials ($\mu=1-j0$) that do not disintegrate at high temperatures are quite rare. A useable sample was furnished by North American Aviation, Inc. Space and Information Systems Division capable of standing temperatures to 1000°F. As per instructions received with the material, after the samples were machined, they were sealed with a sealant furnished by North American Aviation. The machined surfaces were coated with the sealant and permitted to air dry for three hours at each of the following temperatures 200, 250, 300, and 350 degrees Fahrenheit and then left over night at a temperature of 400 degrees Fahrenheit. This proved to be an effective sealing of the material with no observable change in ε' and ε'' after heat cycling to 1000°F.

The ε' and ε'' for this material are given in Figures 39 through 43 for the following frequencies: 0.830, 1.230, 1.970, 2.430 and 3.170 GHz from 71°F to 1000°F. The results were checked for consistency and reliability and in every case the high temperature measurements showed no effect of sample fit or multimoding. The major problem encountered was excessive chipping of the sample at the higher temperatures. The characteristic effect of ε' and ε'' increasing with temperature was observed at all frequencies. In Figures 44 through 46 ε' and ε'' are plotted versus frequency at 250°, 500° and 1000°F showing that the distribution of ε' and ε'' with frequency has the same form as at room temperature with ε' and ε'' in this frequency range decreasing monotonically with frequency.

The ε' and ε'' wave guide measurement of this material is given in Figure 47 as a function of temperature.

In Figure 48 it is seen that with the coaxial and wave guide measurements fall in smooth Debye-type curves.

The difficulty with sample chipping and breakage is primarily due to moving the samples $\lambda/4$ away from the short circuit and then extracting them back to the short circuit. The first remedy that comes casually to the mind of the reader is why not use an adjustable short circuit? Careful deliberation will show that this is not feasible at high temperatures as the temperature gradient in the oven presents serious problems in shifting the short circuit $\lambda/4$. To do this reliably requires

Text resumes on page 61

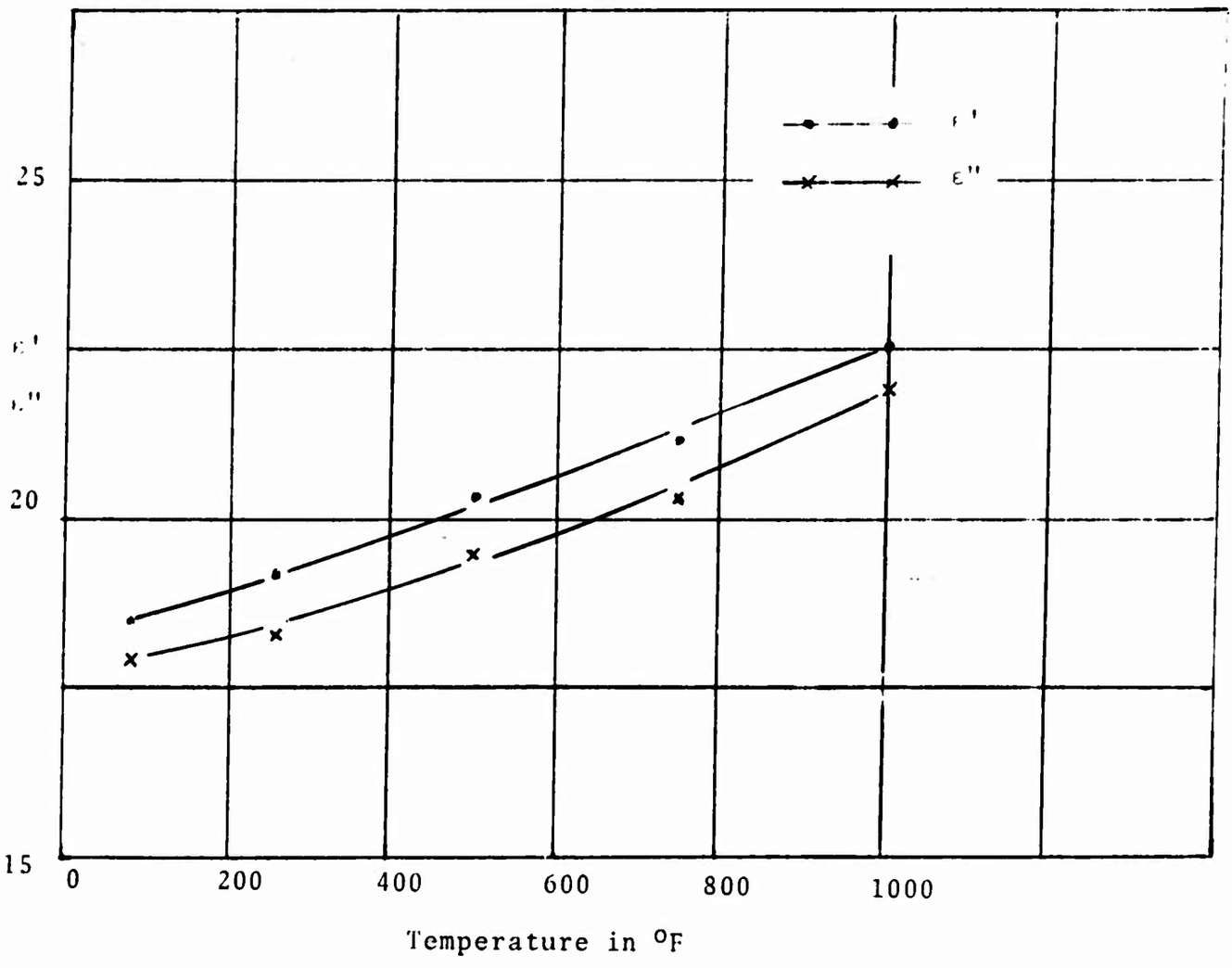

Figure 39. ε' and ε" Vs TEMPERATURE FOR HI-TEMP DIELECTRIC AT 0.830GHz.

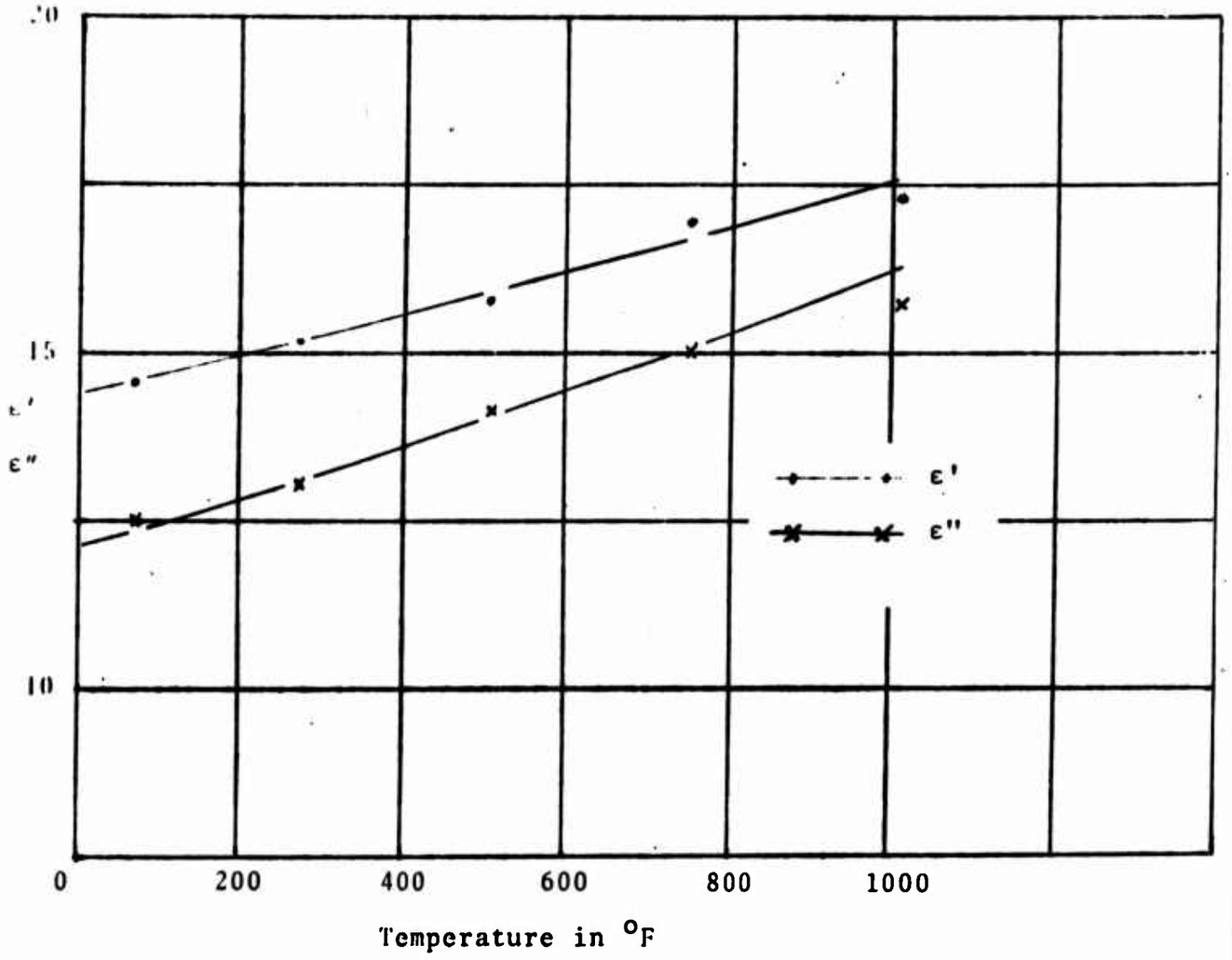

Figure 40. ε' and ε" Vs TEMPERATURE FOR HI-TEMP DIELECTRIC AT 1,230 GHz.

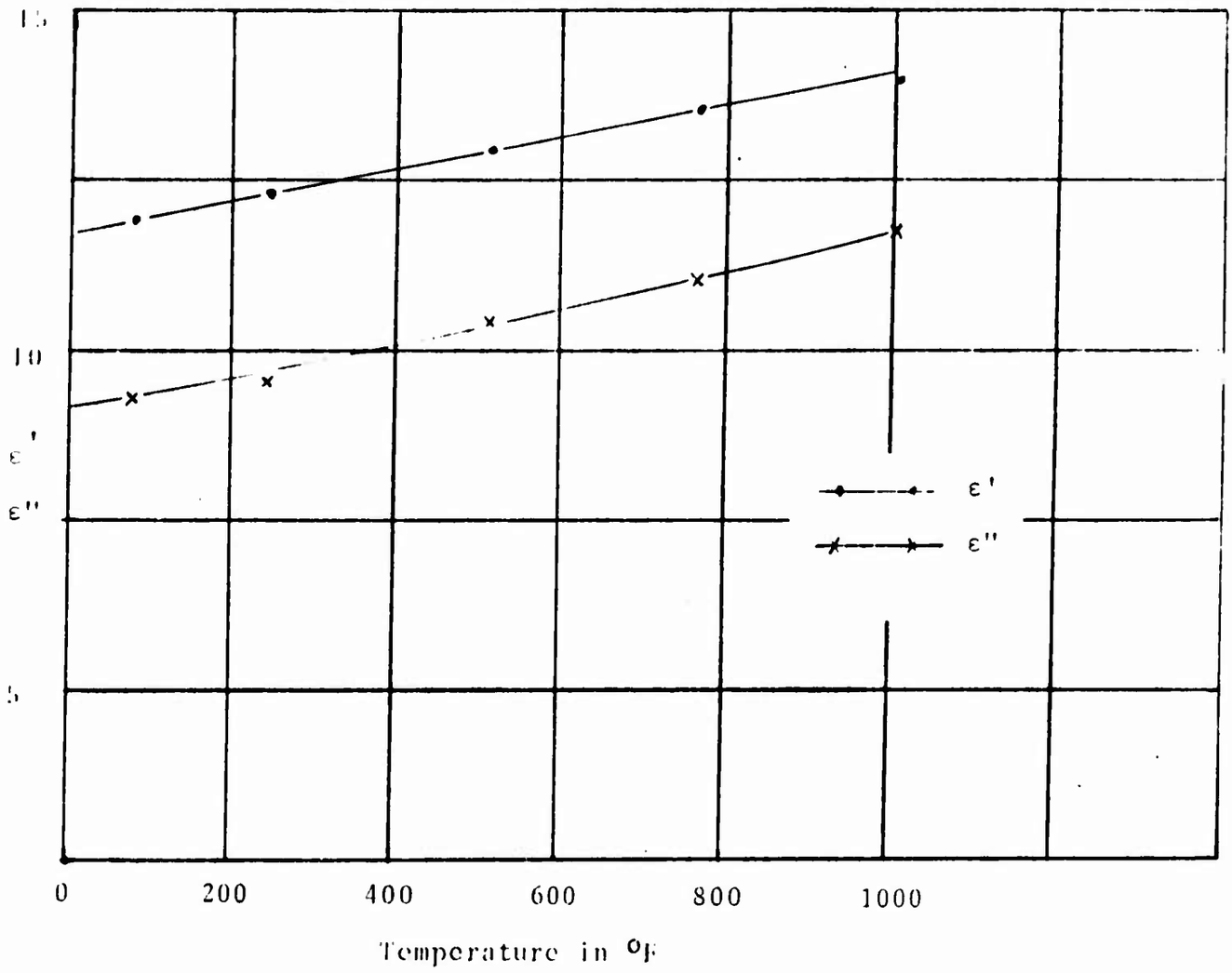

Figure 41. ε' and ε'' Vs TEMPERATURE FOR HI-TEMP DIELECTRIC AT 1.970 GHz.

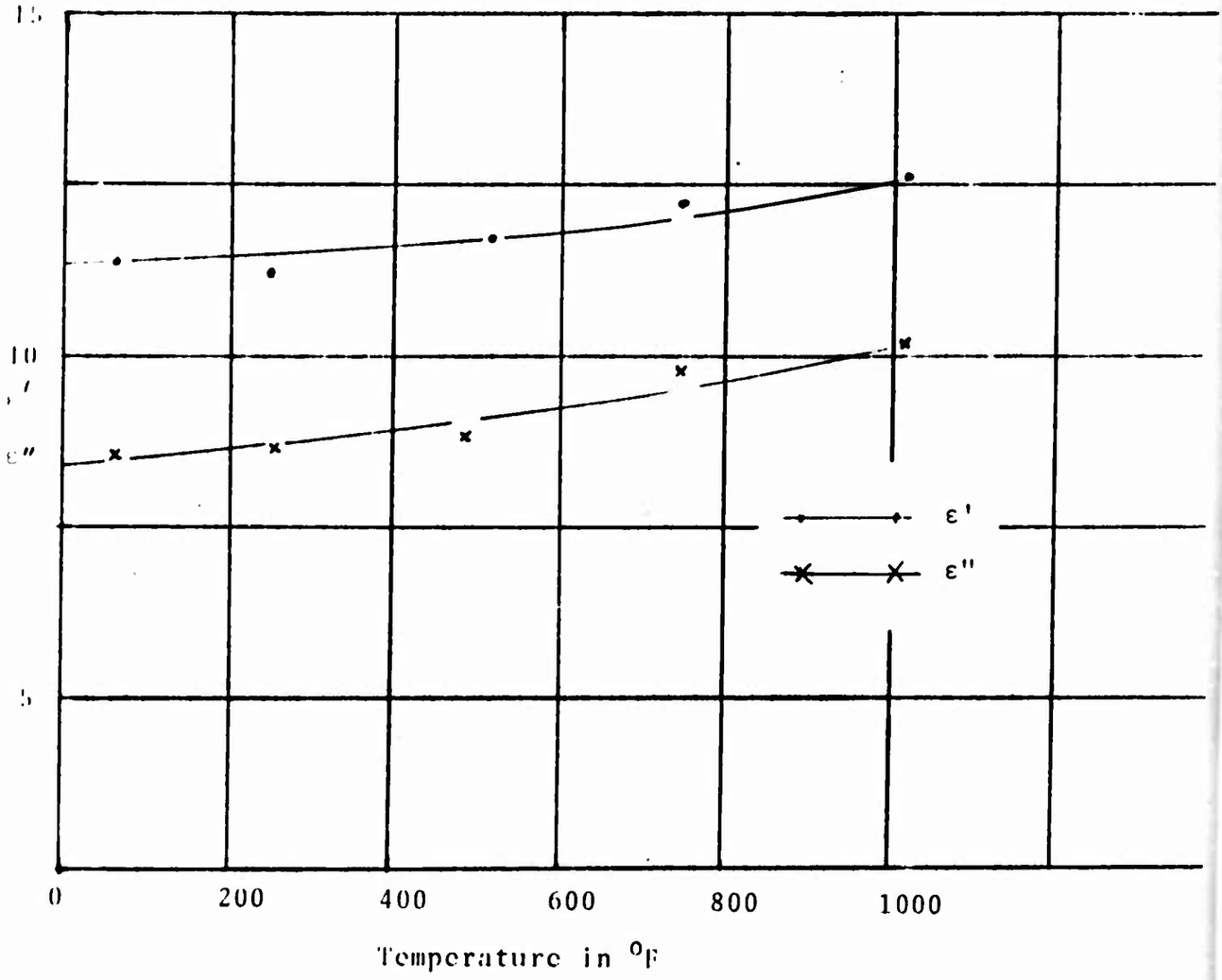

Figure 42. ε' and ε" Vs TEMPERATURE FOR HITEMP DIELECTRIC AT 2430 GHz.

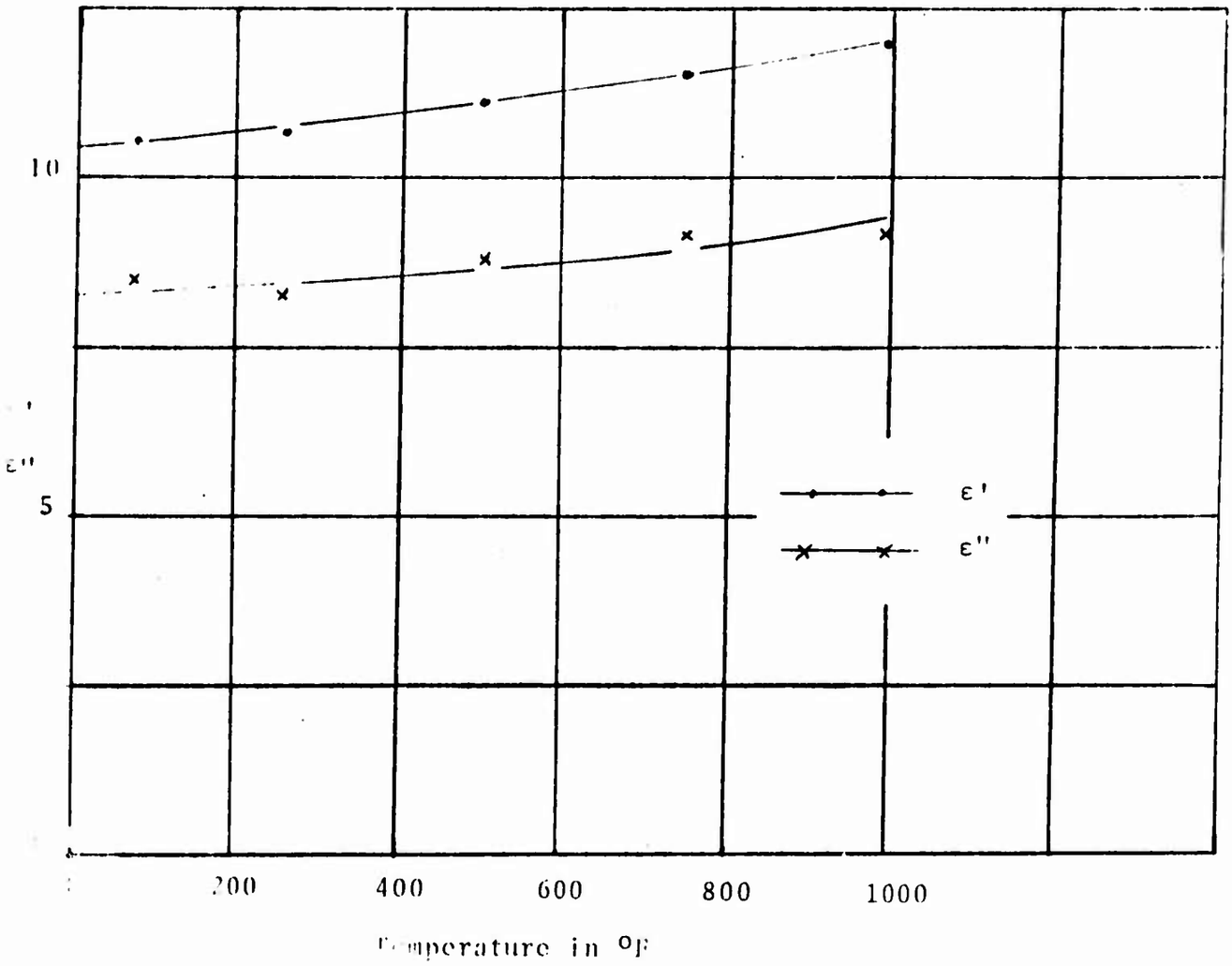

Figure 43. ε' and ε'' Vs TEMPERATURE FOR HI-TEMP DIELECTRIC AT 3.170 GHz.

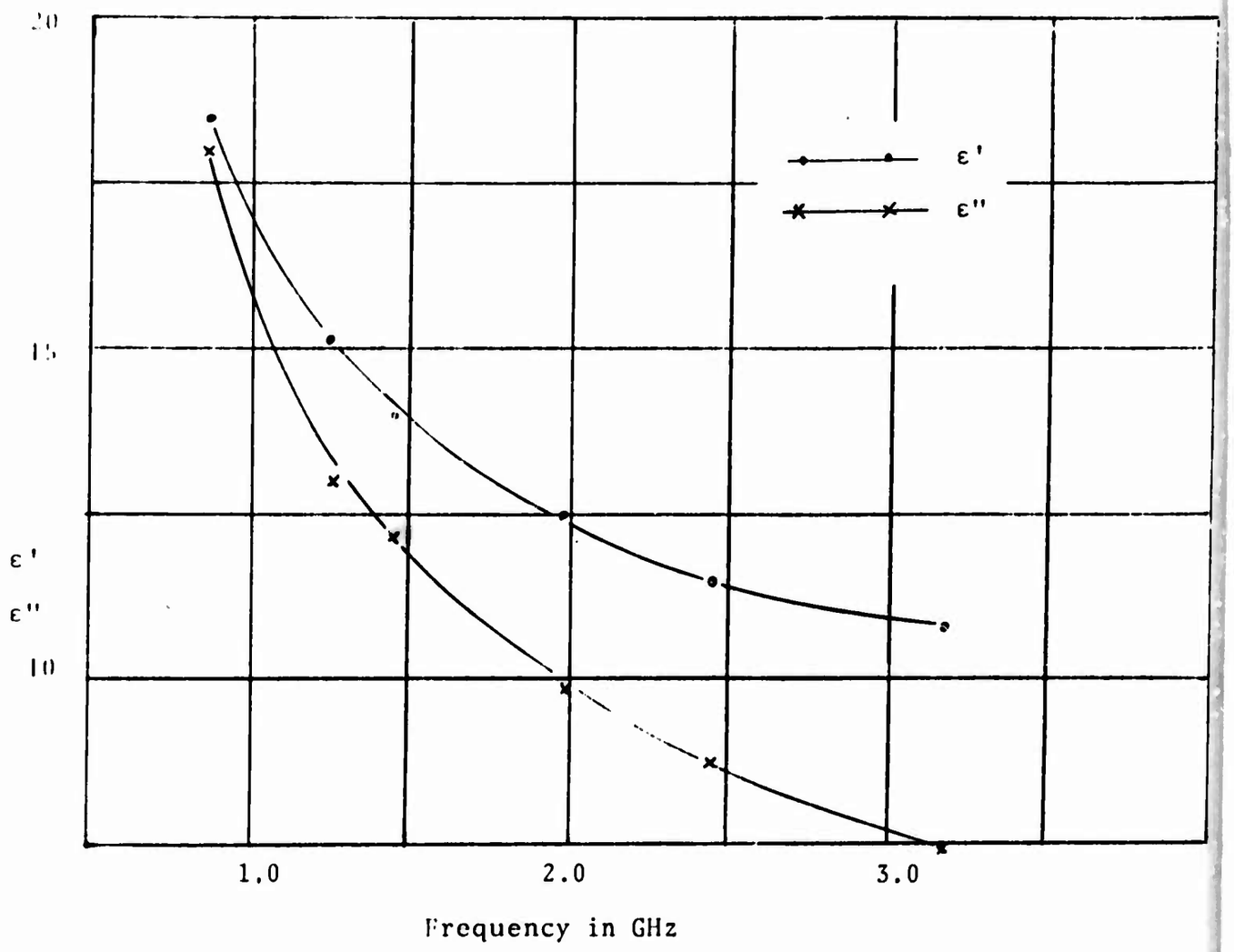

Figure 44. ε' and ε" Vs FREQUENCY FOR HI-TEMP DIELECTRIC AT 250°F.

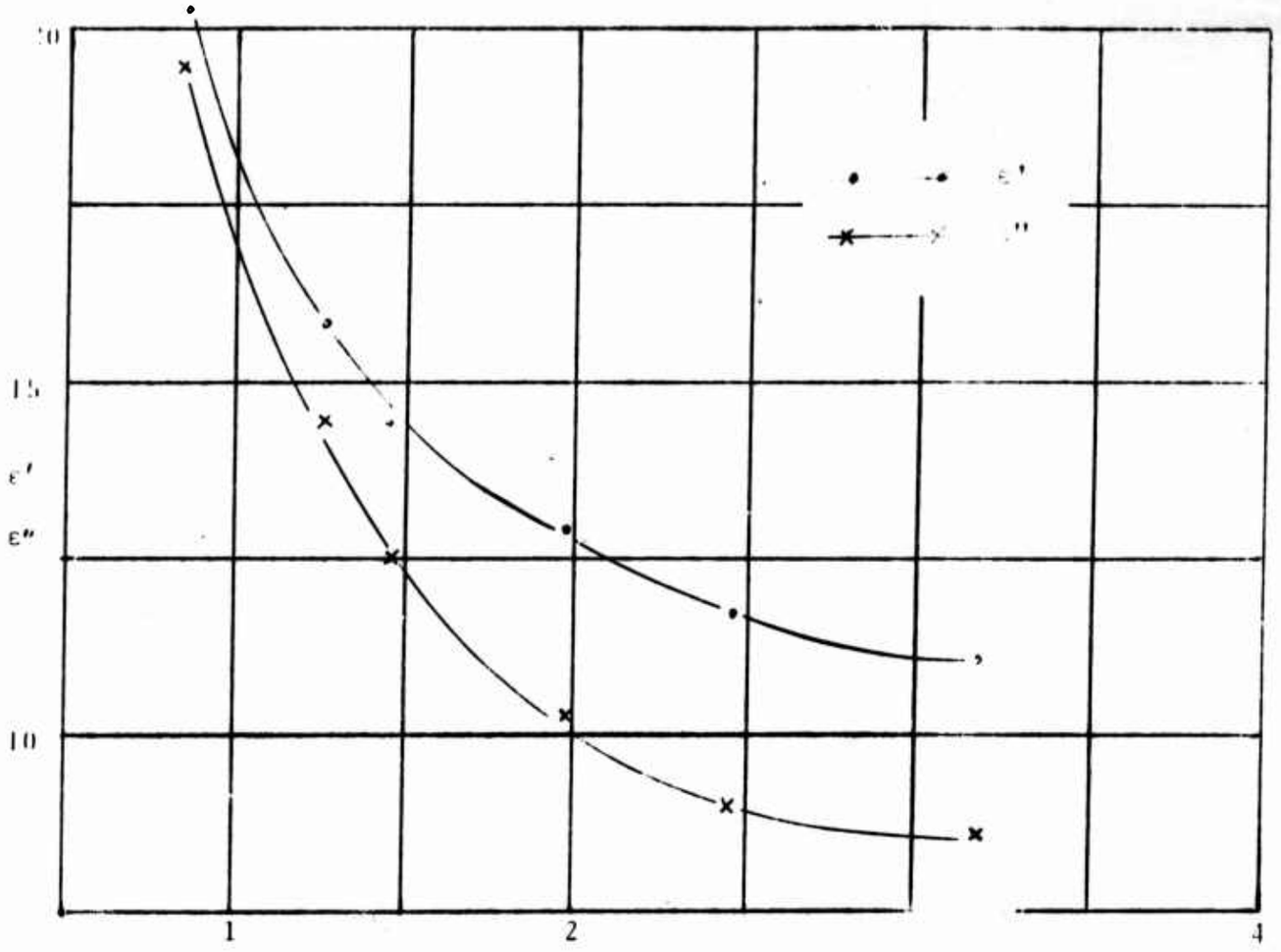

Figure 45. ε' and ε" Vs FREQUENCY FOR HI-TEMP DIELECTRIC AT 500°F.

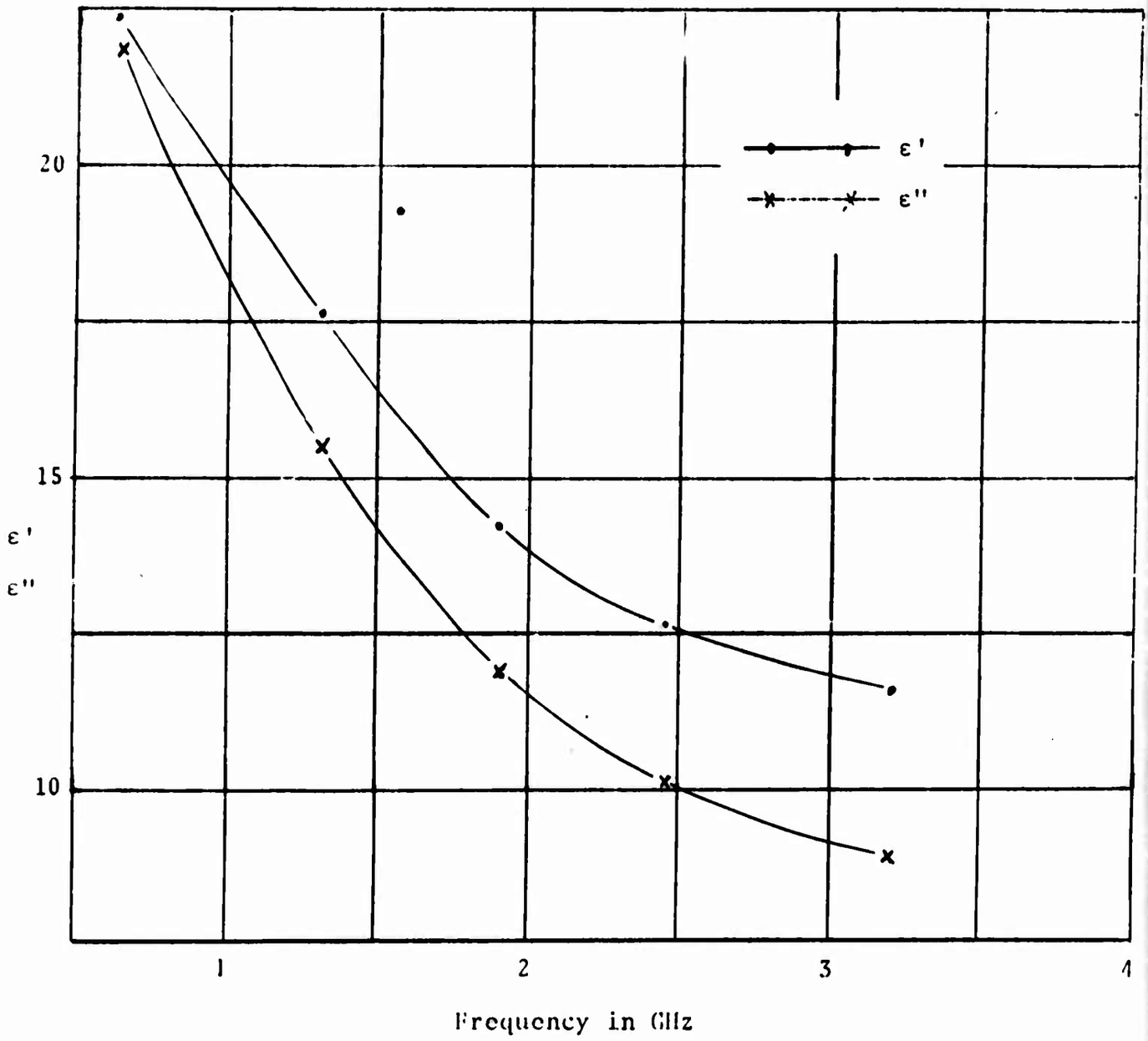

Figure 46. ε' and ε'' Vs FREQUENCY FOR HI-TEMP DIELECTRIC AT 1000°F.

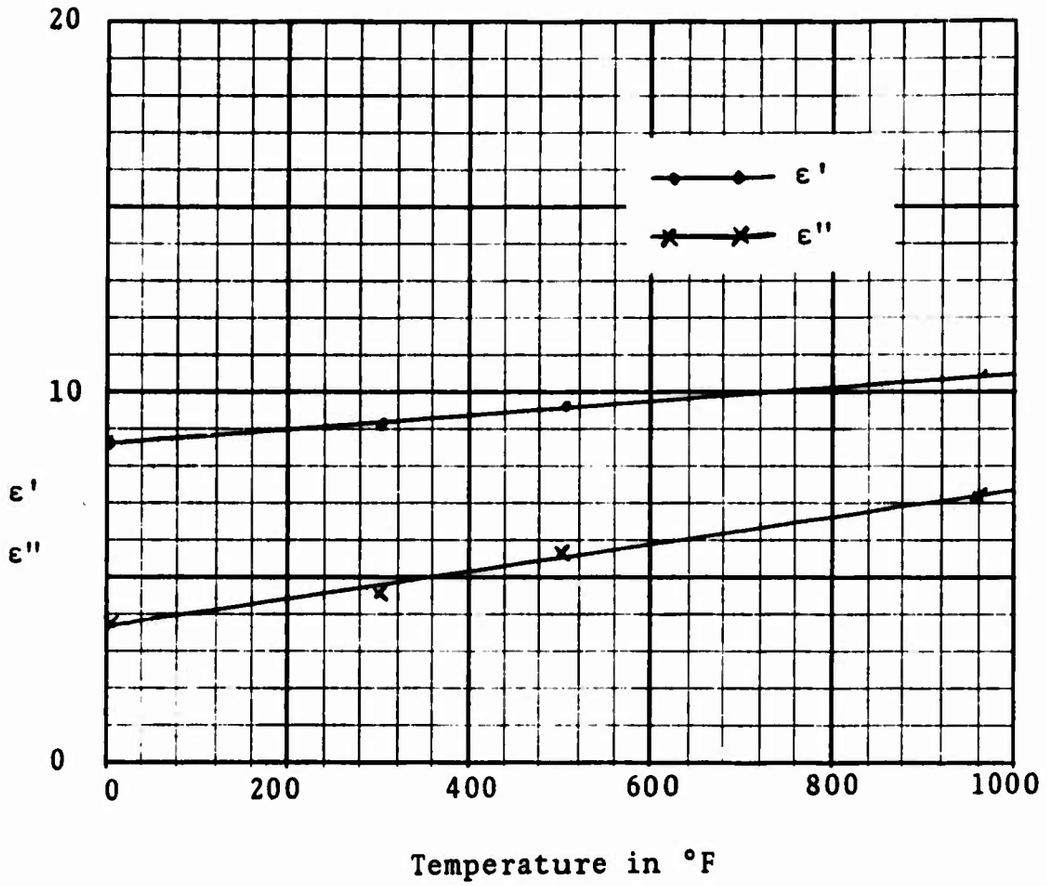

Figure 47. ε' and ε'' Versus Temperature for Hi-Temp Dielectric in Waveguide at 6.778 GHz.

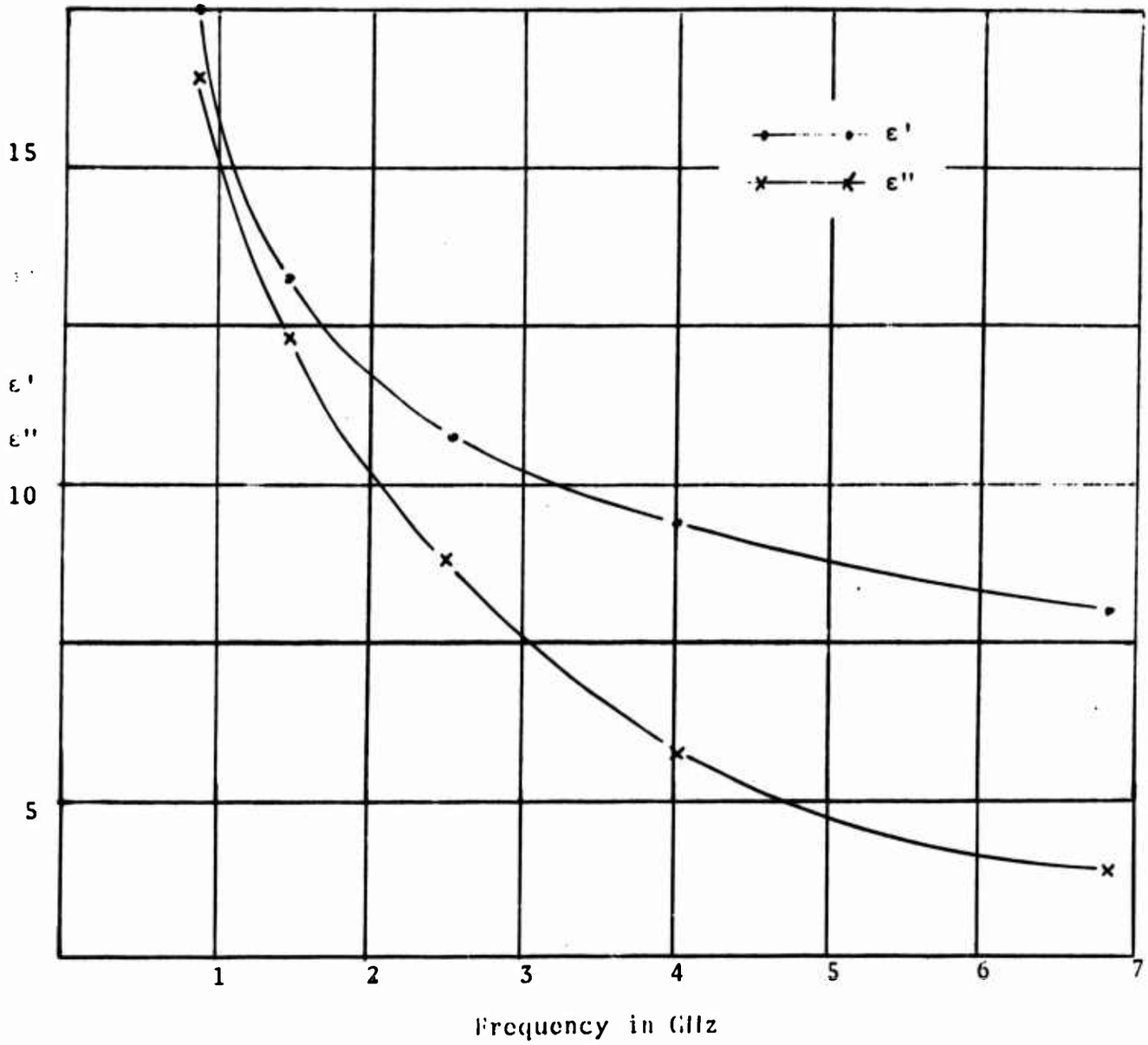

Figure 48. ε' and ε'' Vs FREQUENCY FOR HI-TEMP DIELECTRIC AT ROOM TEMPERATURE - MEASUREMENTS TAKEN IN COAXIAL LINE AND WAVEGUIDE.

the total removal of the sample from the sample holder, adjusting the moveable short and then reinserting the sample. This is a far more tedious task than that of moving the sample in $\lambda/4$.

The results reported above are based on measurements with the sample at the short circuit and $\lambda/4$ away from the short circuit. It was clearly demonstrated and given in detail in Technical Report AFML-TR-69- 18, March 1969 that by decrementing ΔXs and ΔXo the reliability and consistency of the measurements is established. This approach was verified experimentally by comparing measured and computed reflection coefficients from 830 MHz to 4,000 MHz of a 13 layer system consisting of five different materials. The agreement throughout was within 0.5 db which is well within the expected error of the reflectivity measurements.

In order to avoid the breakage of brittle, ceramic pure dielectric materials due to moving the sample away from the short circuit by $\lambda/4$, the use of a sample thickness d and 2d at the short circuit was studied. This requires the use of two samples of thickness d as follows:

1. A sample of thickness d is placed the at the short circuit and ΔXs and null position are determined and

2. The second sample of thickness d is inserted by placing it at the end of the sample holder and carefully tightening the bolts that hold the shorting plate to the flange of the sample holder, and uniformly moving the sample in with the shorting plate, thus placing a sample of thickness 2d at the shorting plate and NPS and ΔXs are then determined.

These two measurements will permit the unique determination of ε and μ. For a material with $\mu=1$ the technique of decrementing the ΔX's similar to that used with the sample at the short and open circuit position may be used. This approach will provide the same reliability as the sample at the open and short circuit provides, once the fully automatic computer program is completed.

Text resumes on next page

For samples of thickness d and 2d at the short circuit and $\mu \equiv 1$ the following expressions hold:

$$\frac{\tanh \gamma d}{\gamma d} = A_1 + jB_1 \qquad (1)$$

$$\frac{\tanh 2\gamma d}{2\gamma d} = A_2 + jB_2 \qquad (2)$$

where the subscripts 1 and 2 refer to thicknesses d and 2d respectively.

$$\gamma = j \frac{2\pi}{\lambda_o} \sqrt{\varepsilon - \left(\frac{\lambda_o}{\lambda_c}\right)^2} \qquad (3)$$

λ_o = The free space wave length

ε = The complex permittivity normalized to free space

λ_c = cut-off wave length of the wave guide

$$A_1 \text{ and } A_2 = \frac{P \tan \theta (R^2 - 1)}{1 + R^2 \tan^2 \theta} \qquad (4)$$

$$B_1 \text{ and } B_2 = \frac{PR (1 + \tan^2 \theta)}{1 + R^2 \tan^2 \theta} \qquad (5)$$

$$P = \frac{\lambda_g}{2\pi t} \qquad (6)$$

$$t = d \text{ or } 2d \qquad (7)$$

$$\theta = \frac{2\pi X_o}{\lambda_g} \qquad (8)$$

λ_g = guide wave length

Text resumes on next page

X_o = distance of the first minimum outside the sample from the face of the sample so that

$$X_o = NPS - NPA + \frac{\lambda g}{2} - t \qquad (9)$$

NPA = position of the minimum in the air filled line

NPS = position of the minimum with the sample at the short circuit

$$R = \frac{1}{VSWR} = \frac{\sin \theta}{1 + \sin^2 \phi} \qquad (10)$$

$$\phi = \frac{\pi \Delta X}{\lambda g} \qquad (11)$$

ΔX = distance between the points of twice minimum power

Equations (1) and (2) are readily solved as follows:

$$\text{Since } \tanh^2 \gamma d = \frac{2 \tanh \gamma d}{1 + \tanh^2 \gamma d} \qquad (12)$$

equation (2) becomes

$$\frac{\tanh \gamma d}{\gamma d \,(1 + \tanh^2 \gamma d)} = A_2 + jB_2 \qquad (13)$$

substituting from equation (1) for $\tanh \gamma d$ gives

$$\frac{A_1 + jB_1}{1 + (A_1 + jB_1)^2 \,(\gamma d)^2} = A_2 + jB_2 \qquad (14)$$

Text resumes on next page

solving equation (14) for γd gives:

$$(\gamma d)^2 = \frac{(A_1 + jB_1) - (A_2 + jB_2)}{(A_1 + jB_1)^2 (A_2 + jB_2)} \qquad (15)$$

and from equations (15) and (3), for:

1. Waveguide

$$\varepsilon = -\left\{\frac{\lambda_0}{2\pi d}\right\}^2 \cdot \frac{(A_1 + jB_1) - (A_2 + jB_2)}{(A_1 + jB_1)^2 (A_2 + jB_2)} + \left\{\frac{\lambda_0}{\lambda_c}\right\}^2$$

2. Coaxial line measurements

$$\frac{\lambda_0}{\lambda_c} = 0, \text{ so that}$$

$$\varepsilon = \left(\frac{\lambda_0}{2\pi d}\right) \frac{(A_1 + jB_1) - (A_2 + jB_2)}{(A_1 + jB_1)\ (A_2 + jB_2)} \qquad (17)$$

Since u is set as identically equal to 1.0-j0.0 the computed ε will not uniquely satisfy equations (1) and (2) unless the measured values of ΔX or VSWR and NPS are exact.

Now let

$$\left.\begin{matrix} \frac{\tanh\gamma d}{\gamma d} \\ \frac{\tanh 2\gamma d}{2\gamma d} \end{matrix}\right\} = \frac{\tanh u + jv}{u + jv} = \begin{cases} A_{1_C} + jB_{1_C} \\ A_{2_C} + jB_{2_C} \end{cases} \qquad (18)$$

where for thickness d

Text resumes on next page

$$u + jv = \gamma d$$

and for thickness 2d

$$u + jv = 2\gamma d$$

where

$$A_{1_C} \text{ or } A_{2_C} = \frac{u \sinh 2u + v \sin 2v}{(u^2 + v^2)(\cosh 2u + \cos 2v)} \tag{19}$$

and

$$B_{1_C} \text{ or } B_{2_C} = \frac{u \sin 2v - v \sin 2u}{(u^2 + v^2)(\cosh 2u + \cos 2v)} \tag{20}$$

A_{1C}, A_{2C}, B_{1C} and B_{2C} are the values computed from the γd obtained from the A_1, A_2, B_1 and B_2 computed from the measured ΔX and NPS for the single and double thickness. Ideally, then, the computed A_{1C}, B_{1C}, A_{2C}, B_{2C} should agree identically with the value of A_1, B_1, A_2, and B_2 used to compute γd in equation (15).

This is the same approach as was reported in detail in Technical Report AFML-TR-69-18 for the measurements of a single thickness of the short circuit and at the open circuit. In that case decrementing ΔXs equally, resulted in close agreement and it was clearly demonstrated that the results were indeed valid. However, in this case it was found that unequal decrementing of ΔXs, due to the fact the samples were of thickness d and 2d, was required.

The approach is clearly illustrated in Table I for two samples of the same material, with one sample

Text resumes on page 67

TABLE I

DIELECTRICS AT SHORT ONLY

Measured $\varepsilon^* = 17.3969 - j16.0685$	$d_1 = 0.0995"$	$NPS_1 = 2.1125$	$\Delta X_1 = 0.0140$	decr $\Delta X_1 = 0.0$
	$d_2 = 0.1990"$	$NPS_2 = 2.0944$	$\Delta X_2 = 0.0848$	decr $\Delta X_2 = 0.0$
	A1 = 1.038309	B1 = -0.070787	$A_2 = 1.118452$	$B_2 = -0.219065$
	$A1_c = 1.033539$	$B1_c = -0.033468$	$A2_c = 1.129169$	$B2_c = -0.170045$
	%A1 = 0.459	%B1 =-52.719	%A2 = 0.958	%B2 =-22.377
'Decremented' $\varepsilon^* = 17.25 - j20.10$	$d_1 = 0.0995"$	$NPS_1 = 2.1125$	$\Delta X_{1c} = .00830$	decr $\Delta X_1 = -0.0057$
	$d_2 = 0.1990"$	$NPS_2 = 2.0944$	$\Delta X_{2c} = .08195$	decr $\Delta X_2 = -0.00285$
	A1 = 1.038328	B1 = -0.041967	A2 = 1.118531	B2 = -0.211712
	$A1_c = 1.032506$	$B1_c = -0.041800$	$A2_c = 1.111556$	$B2_c = -0.208423$
	%A1 = 0.560	%B1 = -0.397	%A2 = 0.623	%B2 = -1.553

having a thickness d = 0.0995" and the second sample of twice the thickness 2d = 0.1990". The computed ε from the measured data is 17.3969- j16.0685. However, it is seen that there is very poor agreement between B_1 and B_{1C} and B_2 and B_{2C}. However, by decreasing ΔX_1, from 0.0140" to .0083" and ΔX_2 from 0.0848" to .08195" where the subscripts 1 and 2 refer to the sample of thickness d and 2d respectively, it is seen that the largest per cent deviation is 1.553% indicating that the corrected ΔXs were the more consistent values for the material measured. Here the computed is 17.25-j20.10 giving significant change in ε".

Although this approach has the disadvantage of requiring two samples of equal thickness, it is believed that it will significantly simplify the measurements at high temperature and minimize chipping and breakage of brittle material. The computer program as yet is not completely automated.

Text resumes on next page

VI. FERRITE MEASUREMENTS

The ferrites were measured at room and elevated temperatures using two thicknesses of material, a single and a double thickness. Two types of materials were used, sample designated 101 has a Curie point below 1000°F and the sample designated 102 has a Curie point above 1000°F. Both of these ceramic materials are fragile and resulted in a high incidence of breakage. The lower limit in thickness of the material was approximately 0.05", hence samples of 0.05" and 0.10" were used in the measurements. The reason for using as thin a sample as possible is due to the fact that for these materials at the short circuit the VSWR is rather low hence having a very shallow wave form which presents a problem in the accurate determination of the position of the minimum. Ideally as sharp a minimum as possible is desired.

Theoretically, the determination of ΔX and null position with the sample at the short circuit and the sample at the open circuit ($\lambda/4$ away from the short circuit) should, from the solution of the following well-known transcendental equations

$$\frac{\mu \tanh \gamma d}{\gamma d} = A + jB \qquad (21)$$

$$\frac{\mu \coth \gamma d}{\gamma d} = C + jD \qquad (22)$$

give the exact value of ε and μ of the material, provided that there are no errors in the four measured parameters. It was clearly demonstrated with dielectric materials that a correction for ΔX measured with the sample at the short circuit and at the open circuit was essential. Unfortunately,

Text resumes on next page

when equations (21) and (22) are solved, giving ε and μ, unlike the dielectric case where μ was assumed to be identically one (1.000), no check is possible on either the consistency or reliability of the measurement. Here the solution is unique, but resultant value of ε and μ may not be the true parameters.

As in the case of the dielectric materials a correction for the measured VSWR or ΔX is required and a means of establishing the consistency and validity of the result is needed.

Hence, single and double thicknesses were used throughout this study. With the measurements at the short and $\lambda/4$ away from the short and thicknesses of d and 2d, six determinations of ε and μ are possible as follows: solving equations (21) and 22) with thickness d and 2d gives the two standard determinations of ε and μ; the third is obtained from the simultaneous solution of

$$\frac{\mu \tanh \gamma d}{\gamma d} = A_1 + jB_1 \qquad (23)$$

$$\frac{\mu \tanh 2\gamma d}{2\gamma d} = A_2 + jB_2 \qquad (24)$$

where subscripts 1 and 2 relate to single and double thickness repsectively giving ε and μ from the measurements with the samples at the short circuit; the fourth determination, by the simultaneous solution of

Text resumes on next page

$$\frac{\mu \coth \gamma d}{\gamma d} = C_1 + jD_1 \qquad (25)$$

$$\frac{\mu \coth 2\gamma d}{2\gamma d} = C_2 + jD_2 \qquad (26)$$

giving ε and μ from the measurements with the samples at the open circuit.

Two other determinations of ε and μ are possible from the solutions of (23) and (26) and (24) and (25). These determinations seem not to give very meaningful information and were abandoned.

The method used has been to compute

(1) ε and μ from the measurement of the single thickness at the short and open circuit (SOS)

(2) ε and μ from the measurement at the short and open circuit of the sample of double thickness (SOD)

(3) from the measurements of the sample of single thickness at the short circuit and double thickness at the short circuit (S)

(4) from the measurements of the sample of single and double thickness at $\lambda/4$ away from the short circuit (0).

These will be referred to henceforth as SOS (short and open single), SOD (short and open double), S (single and double at the short circuit) and 0 (single and double at the open circuit).

Text resumes on next page

To illustrate this approach Table II gives the computed values of ε and μ for SOS, SOD, S and O. It is seen that the values of ε'' in the single and double thickness measured at the open and short circuit differ significantly. Again the values of ε'' computed from the measurements of the short circuit (S) and from the measurements at the open circuit (O) differ significantly. This certainly implies errors in the measurements of ΔX or the VSWR.

Now from the values of ε and ε'', μ' and μ'' computed from the measurements of the sample of single thickness, (.05 inches) at the short and open circuit (SOS) the expected value of NPS, NOP, ΔXs and ΔXo are obtained for the sample of double thickness, (0.10 inches) at short and open circuit.

Note that the ΔXo obtained from the measurements for the sample that is 0.10 inches thick is 0.1362 inches greater than that computed from the ε and μ obtained from the measurements of the sample of thickness 0.05 inches. Conversely, from the ε and μ obtained from the SOD measurements it is seen that the measured ΔXo in the thickness of 0.05 inches is 0.1362 inches less than that computed for this thickness from the 0.10 inch thickness. Hence it is clear that the differences in ε'' are due to inconsistencies in the measured ΔXo for the single and double thickness, Again the ΔXs values are also inconsistent.

Now by correcting the ΔX's to the values given in Table III and recomputing the parameters NPS, NPO, ΔXs and ΔXo from the ε and μ obtained from the single thickness for the expected values for the double thickness and conversely from the double thickness to the single thickness, it is seen that with the exception of the NPO's the differences are very small and the values of ε', ε'', μ' and μ'' are in very close agreement for SOS, SOD and S. The computation of ε and μ from S could be considered to be the most reliable since the minimum difference in the parameters NPS and ΔXs for the single and double thickness are 0.00353 inches.

Text resumes on page 74

TABLE II

COMPUTED ε AND μ FROM MEASURED DATA.

Frequency GHz	Thickness Inches		Measured	Comp. From SOS or SOD	Diff.
1.230	0.050	NPS	5.7525	5.7523	+0.0002
		NPO	5.2881	5.2582	+0.0299
		ΛX_s	0.2731	0.2538	-0.0193
		ΔX_o	0.2517	0.3879	-0.1362
	0.100	NPS	5.4850	5.4820	+0.0030
		NPO	4.7023	4.7512	-0.0489
		ΛX_s	0.6002	0.6246	-0.0244
		ΔX_o	0.5781	0.4329	+0.1362
		ε'	-ε"	μ'	-μ"
	SOS	15.9144	-2.7921	5.7309	-2.5904
	SOD	16.5159	-4.4871	5.7455	-2.4025
	S	13.3956	-1.7244	5.7427	-2.6234
	O	15.6535	-2.3599	9.9114	-5.5872

TABLE III

RECOMPUTED ϵ AND μ WITH CORRECTED ΔX_s AND ΔX_o.

Frequ. GHz	Thick. inch		Measured	Corrected	Comp. from SOS or SOD	Diff.
1.230	0.050	NPS	5,7525		5.7535	- .0020
		NPO	5.2881		5.2543	+ .0339
		ΔX_s	0.2538	0.25919	0.25752	+ .00257
		ΔX_o	0.3879	0.3333	0.3384	+ .0051
	0.100	NPS	5.4850		5.4851	-0.0001
		NPO	4.7023		4.7460	-0.04370
		ΔX_ϵ	0.6246	0.60578	0.60225	-0.00353
		ΔX_o	0.4329	0.51416	0.51946	+0.00530
			ϵ'	$-\epsilon''$	μ'	$-\mu''$
		SOS	15.8514	-3.7749	5.7405	-2.4679
		SOD	16.6656	-3.9004	5.7159	-2.4425
		S	16.1270	-3.9714	5.7399	-2.4632
		O	15.6116	-3.7478	8.1154	-1.5607

Tables IV and V give the same story for the same pair of samples measured at 1.430 GHz. Here SOS, SOD and O come in close agreement after corrections of ΔX and certainly the average of SOS and SOD may be accepted since ε', ε'', μ' and μ'' have differences of less than 5% and the average should certainly give the representative value of the material.

From Tables VI, III, IV and V, it is seen that S and O are far more sensitive to errors than SOS and SOD, with SOS and SOD coming in to close agreement more readily than either S or O. The negative sign for ε' and μ' in S is due to the large differences in NPS and ΔXs.

Table VI gives data for measurements of the same samples at 1.970 GHz. Here again the negative signs of ε' and μ' and the positive sign of μ'' is due to the inconsistencies in NPS or ΔXs. The measured ΔXs for the thickness of 0.1000 inches is very large, 1.4250", which readily leads to the assumption that such a large ΔX is difficult to accurately determine and can lead to an error in NPS. As seen from Table VII, after correcting for ΔXs and ΔXo, SOS, SOD and O are reasonably close with O filling in between SOS and SOD, hence O should be accepted. S for ε and ε'' is still out of line, primarily due to inconsistencies in NPS, although corrections for ΔXs changed the algebraic signs of ε' and μ' from negative to positive and " from positive to negative.

Table VIII and IX give data for measurements at 3.170 GHz. Note in Table VIII that the maximum deviation is **for** ΔXs of thickness 0.1000", a deviation of +0.0086" and after correction of ΔX the maximum deviation is 0.0048 in NPO of the sample with a thickness of 0.0500. Here ε and μ computed from either SOS and SOD may be considered as the values for the material at this frequency with the average from the two thicknesses being the most realistic.

Text resumes on page 81

TABLE IV

COMPUTED ϵ AND μ FROM MEASURED DATA.

Frequency GHz	Thickness Inches		Measured	Comp. From SOS or SOD	Diff.
1.434	0.050	NPS	3.7394	3.7196	+0.0193
		NPO	3.2962	3.3081	-0.0119
		ΔX_s	0.5516	0.51703	+0.04457
		ΔX_o	0.2508	0.2909	-0.0401
	0.100	NPS	3.4145	3.4572	-0.0427
		NPO	2.8251	2.8204	+0.0047
		ΔX_s	1.3033	1.4112	-0.1079
		ΔX_o	0.5442	0.5002	+0.0440
			ϵ'	$-\epsilon''$	μ'	$-\mu''$
	SOS		15.8412	-2.5654	5.7502	-5.1427
	SOD		15.4661	-3.0773	6.1363	-4.8384
	S		-12.5996	-1.1501	-5.6491	5.2459
	O		15.8640	-2.4185	5.9573	-6.2953

TABLE V

RECOMPUTED ε AND μ WITH CORRECTED ΔX_s AND ΔX_o.

Frequ. GHz	Thick. inch		Measured	Corrected	Comp. from SOS or SOD	Diff.
1.430	0.050	NPS	3.7394		3.7200	+0.0194
		NPO	3.2962		3.3076	-0.0114
		ΔX_s	0.5516	0.5454	0.5205	+0.0249
		ΔX_o	0.2508	0.2580	0.2868	-0.0388
	0.100	NPS	3.4145		3.4594	-0.0449
		NPO	2.8251		2.8193	+0.0059
		ΔX_s	1.3033	1.3141	1.3747	-0.0606
		ΔX_o	0.5442	0.5400	0.5146	+0.0354
			ε'	$-\varepsilon''$	μ'	$-\mu''$
		SOS	15.8292	-2.7970	5.7560	-5.008
		SOD	15.5330	-2.8172	6.0992	-4.9859
		S	-15.5591	- .7873	-5.6554	5.0275
		O	15.8677	-2.7675	5.5574	-5.3324

TABLE VI

COMPUTED ϵ AND μ FROM MEASURED DATA.

Frequency GHz	Thickness Inches		Measured	Comp. From SOS or SOD	Diff.
1.970	0.050	NPS	3.5207	3.5150	+0.0057
		NPO	3.0050	3.0055	-0.0005
		ΔX_s	0.4867	0.5044	-0.0177
		ΔX_o	0.1173	0.1150	+0.0023
	0.100	NPS	3.5175	3.5274	-0.0099
		NPO	2.7024	2.7033	-0.0011
		ΔX_s	1.4250	1.3418	+0.0832
		ΔX_o	0.2984	0.2942	+0.0042
			ϵ'	$-\epsilon''$	μ'	$-\mu''$
	SOS		14.3462	-0.9084	2.3203	-4.4904
	SOD		14.3121	-0.8511	2.4318	-4.6176
	S		-14.5849	-1.3133	-2.2819	4.4546
	O		14.3347	0.8902	2.3935	-4.5756

TABLE VII

RECOMPUTED ε AND μ FROM CORRECTED ΔX_s AND ΔX_o.

Frequ. GHz	Thick. inch		Measured	Corrected	Comp. from SOS or SOD	Diff.
1.970	0.050	NPS	3.5207		3.5174	+0.0023
		NPO	3.0050		3.0053	-0.0003
		ΔX_s	0.4867	0.48808	0.4871	-0.0023
		ΔX_o	0.1173	0.1166	0.1167	-0.0001
	0.100	NPS	3.5175		3.5272	-0.0097
		NPO	2.7024		2.7033	-0.0009
		ΔX_s	1.4250	1.3451	1.3405	+0.0046
		ΔX_o	0.2984	0.2939	0.2936	+0.0003
			ε'	$-\varepsilon''$	μ'	$-\mu''$
		SOS	14.3459	-0.9019	2.3199	-4.4871
		SOD	14.3237	-0.9038	2.3795	-4.4751
		S	13.6756	-0.4114	2.3012	-4.4928
		O	14.3376	-0.9017	2.3630	-4.4813

TABLE VIII

COMPUTED ϵ AND μ FROM MEASURED DATA.

Frequency GHz	Thickness Inches		Measured	Comp. From SOS or SOD	Diff.
3.170	0.050	NPS	2.7845	2.7824	+ .0021
		NPO	2.3157	2.3213	- .0056
		ΔX_s	0.3671	0.3651	+ .0020
		ΔX_o	0.0950	0.1017	- .0067
	0.100	NPS	2.9320	2.9401	- .0081
		NPO	2.1801	2.1766	+ .0035
		ΔX_s	0.8725	0.8639	+ .0086
		ΔX_o	0.2288	0.2244	+ 4
		ϵ'	$-\epsilon''$	μ'	$-\mu''$
	SOS	13.1947	-0.6858	0.9832	-3.3183
	SOD	12.9455	-0.8411	1.0134	-3.3035
	S	12.5109	-0.9270	0.9697	-3.3343
	O	13.2462	-0.6292	0.8811	-3.4688

TABLE IX

RECOMPUTED ϵ AND μ FROM CORRECTED ΔX_s AND ΔX_o.

Frequ. GHz	Thick. inch		Measured	Corrected	Comp. from SOS or SOD	Diff.
3.170	0.050	NPS	2.7845		2.7844	+ .0001
		NPO	2.3157		2.3205	- .0048
		ΔX_s	0.3671	0.3611	0.3603	+ .0008
		ΔX_o	0.0950	0.1009	0.1013	- .0004
	0.100	NPS	2.9320		2.9348	- .0028
		NPO	2.1801		2.1765	+ .0036
		ΔX_s	0.8725	0.8493	0.8466	+ .0027
		ΔX_o	0.2288	0.2263	0.2263	0.0000
			ϵ'	$-\epsilon''$	μ'	$-\mu''$
		SOS	13.1985	-0.8322	0.9765	-3.2739
		SOD	12.9931	-0.8473	0.9727	-3.2707
		S	12.9566	-0.9105	0.9718	-3.2792
		O	13.2641	-0.8186	0.8283	-3.3316

Throughout this study the primary problem has been that the samples differ in properties from sample to sample, while the secondary problem is caused by the large, broad minima making the location of NPS and NPO difficult.

As seen from Tables II through IX computations of ϵ and μ from SOS and SOD generally agree fairly closely but seldom within 5% for the four parameters ϵ', ϵ'', μ' and μ'' due to either errors in NPO, NPS, ΔX_s or ΔX_o or individual differences between the samples. It has been found that generally corrections for ΔX brings SOS and SOD within acceptable agreement. However, the computations from the measurements of the samples at the short circuit only or $\lambda/4$ away from the short circuit are very sensitive to NPS and NPO. Hence, from analysis of the results, it is possible to determine which measurement or measurements are in error, or if the deviations are due to differences in the properties of the samples. The computer program is still in the developmental stage; it is expected that the completed program will give the criteria under which the measurements are accepted or rejected.

It is recognized that in all coaxial line or wave guide measurements a correction of the measured ΔX or VSWR is needed. If, by correcting ΔX or VSWR, the computed ϵ', ϵ'', μ' and μ'' agree from at least three of the four computating, SOS, SOD, S and O and the analysis of the recomputed parameters NPS, NPO, ΔX_s and ΔX_o are in close agreement for the ΔX's and one set of null positions, NPO or NPS, the result is to be excepted as valid.

Text resumes on next page

VII. EFFECT OF SAMPLE FIT ON FERRITE MEASUREMENTS

As a preliminary to the performance of high temperature measurements on ferrite samples, a study has been conducted on the effects of sample fit on ε', ε'', μ', and μ'' for type 101 samples. The choice of the sample was dictated by the availability.

Samples of exact fit with outside diameter 1.0 inch were measured for thicknesses of 0.05 and 0.10 inch. The measurements were performed in a coaxial line. The results are given in Figure 49. The two samples were ground to an outer diameter of 0.999 inches and measured. The results are given in Figure 50. In Figure 51 ε and μ are given versus frequency for the samples ground down to an outer diameter of 0.9975 inches. In Figures 52 and 53 ε and μ are given versus frequency for the samples ground down to an outer diameter of 0.9956 and 0.9936 inch, respectively. It is clear from Figures 49 through 53 that the decrease in diameter of the samples had only a minor effect. The misfit here is much greater than can be expected from the differential expansion of the sample holder and ferrite at a temperature of 1000°F, hence it is concluded that the sample fit does not present a problem.

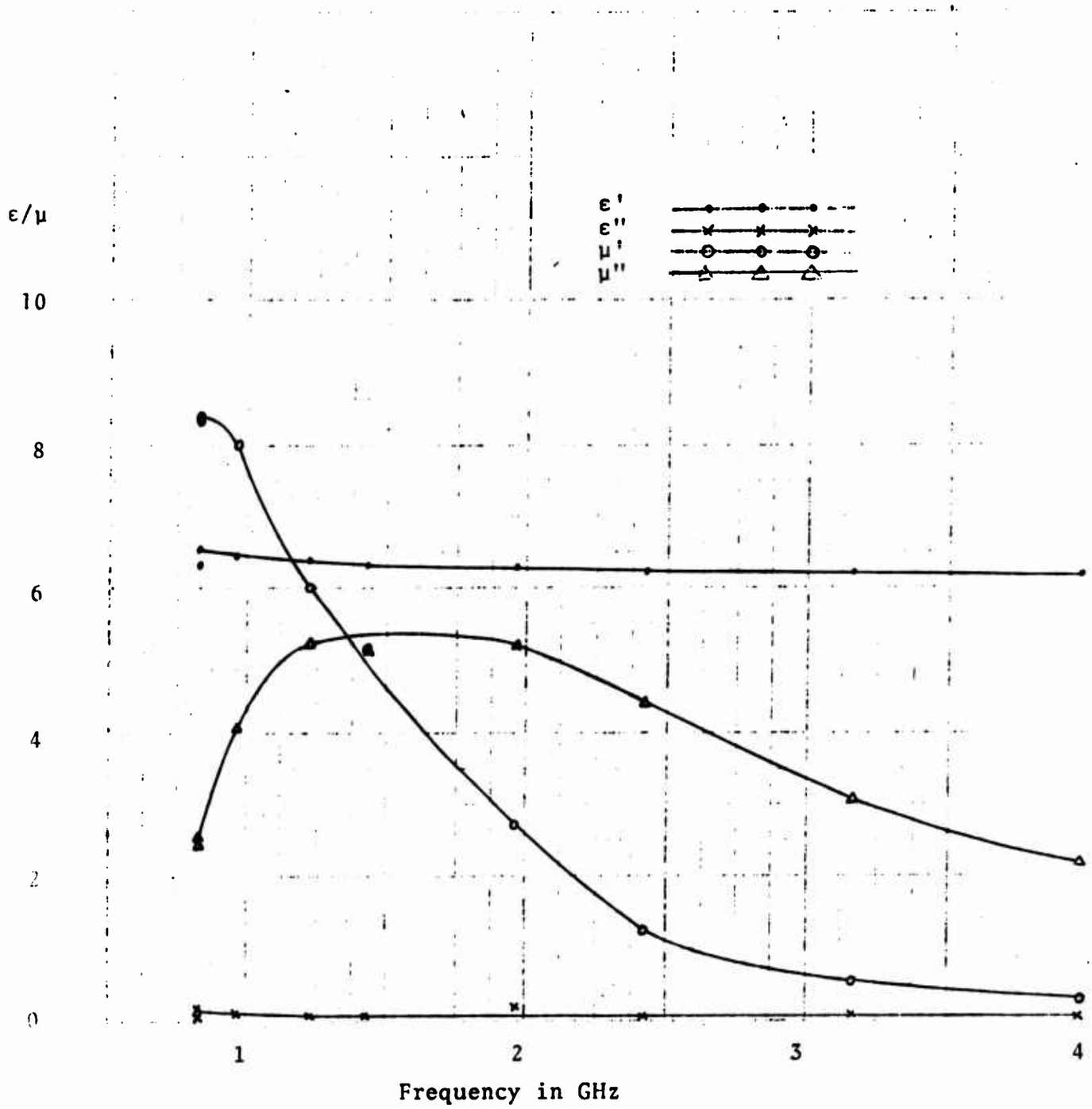

Figure 49. SAMPLE 101 EXACT FIT (1.000" Dia.)
ε AND μ Vs Frequency.

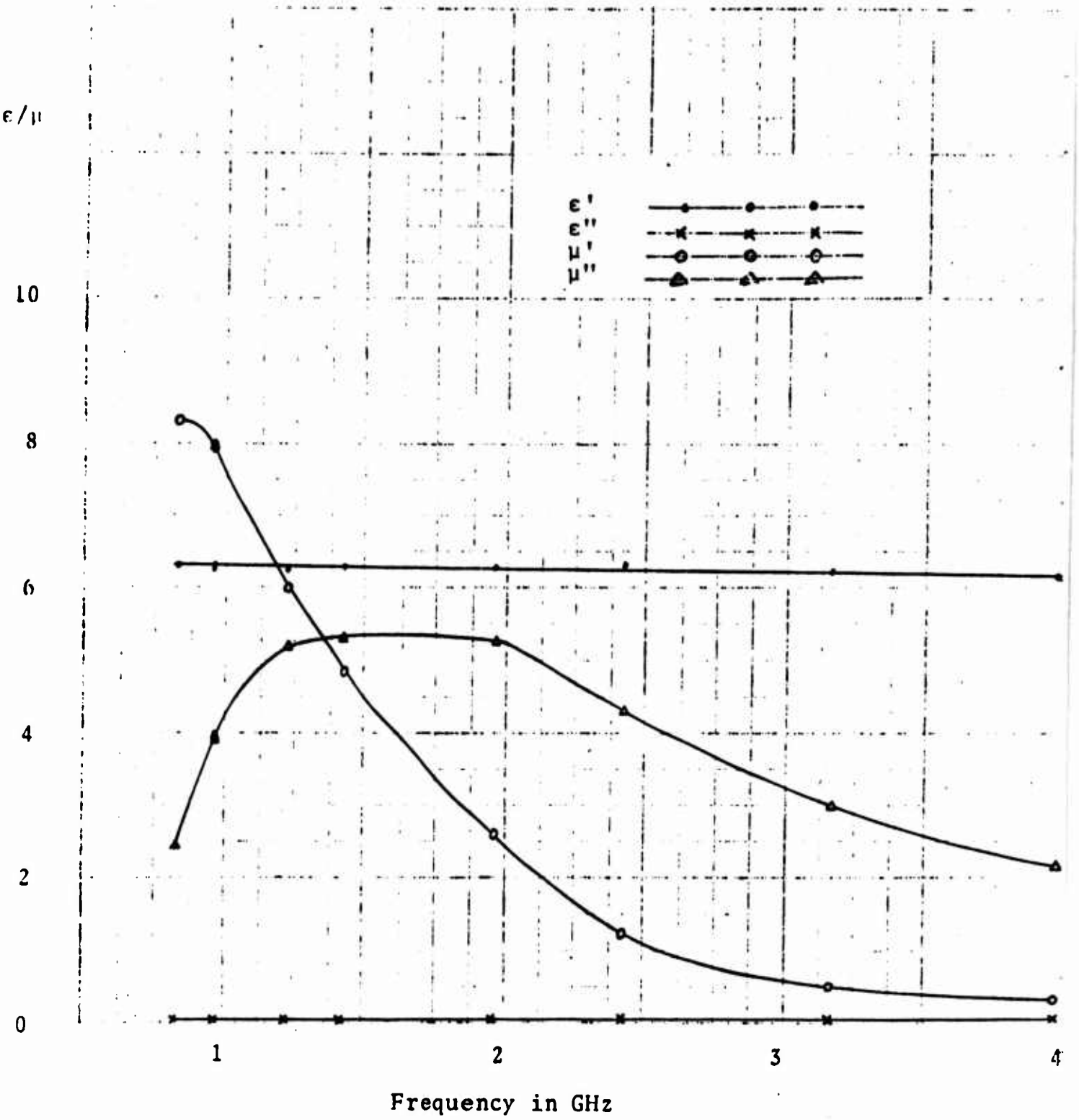

Figure 50. SAMPLE 101 0.999"Diameter, ε and μ Vs Frequency.

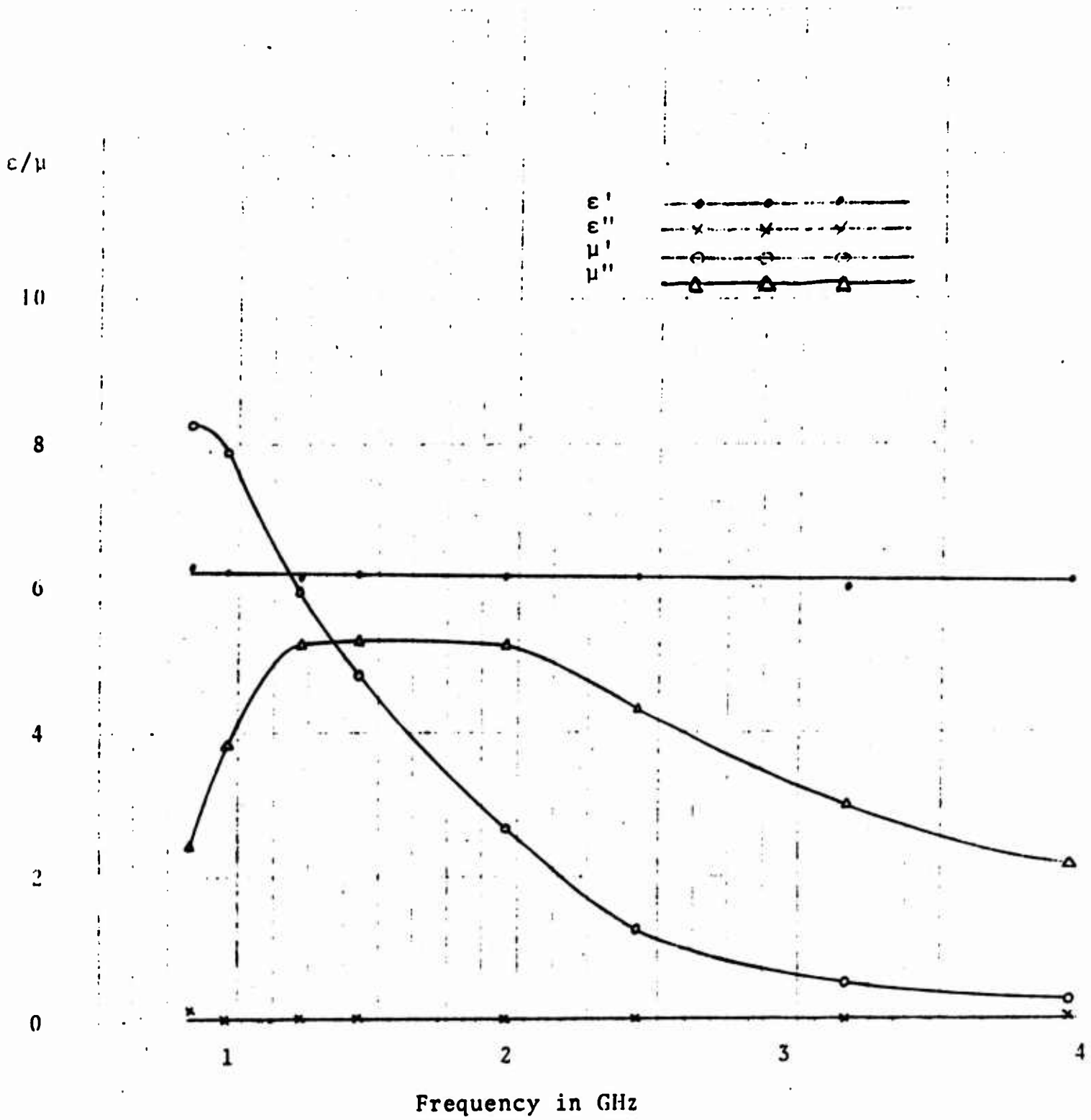

Figure 51. SAMPLE 101. 0.9975" Diameter
ε and μ Vs Frequency.

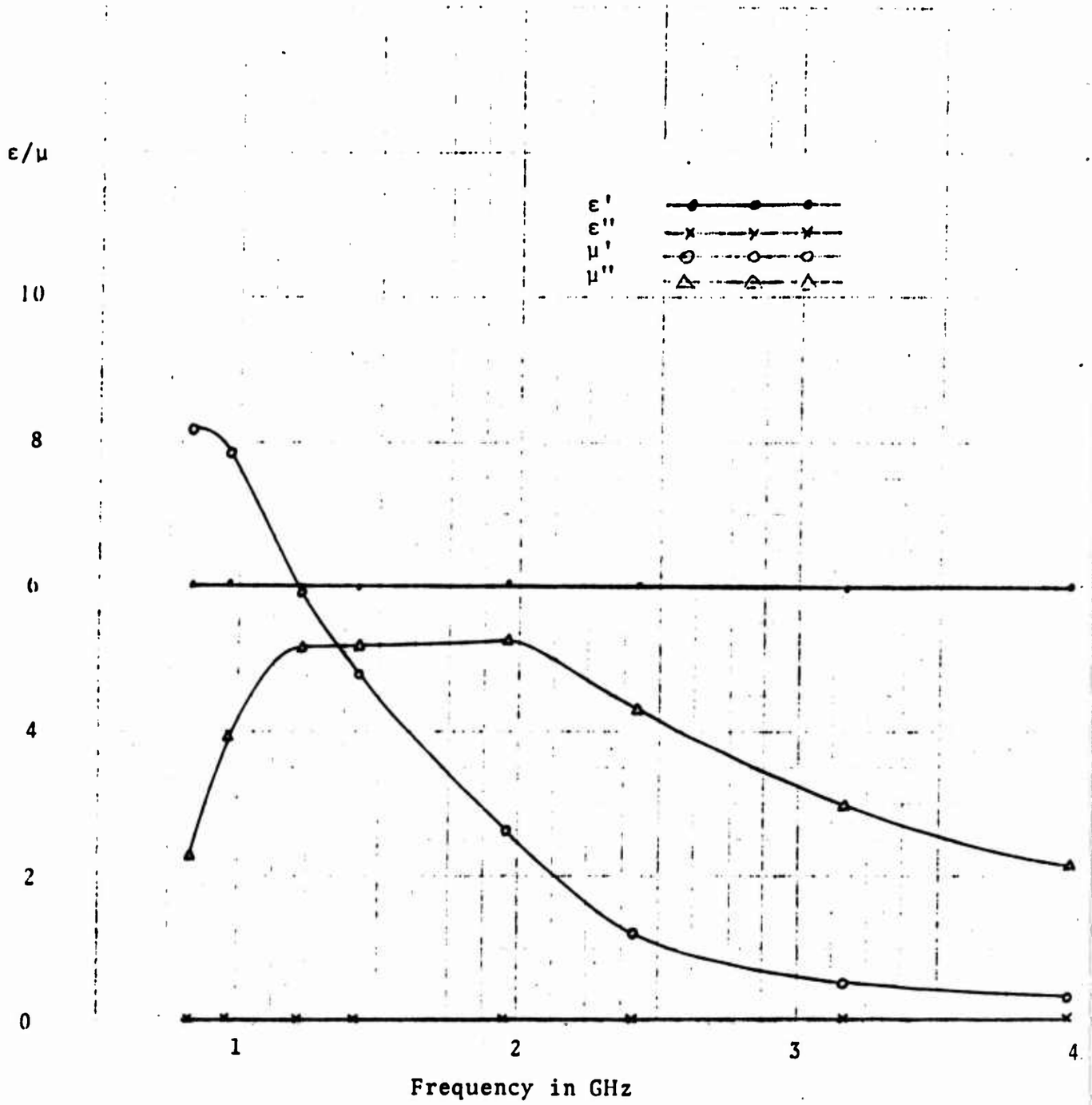

Figure 52. SAMPLE 101 0.9956" Diameter.
ε and μ Vs Frequency.

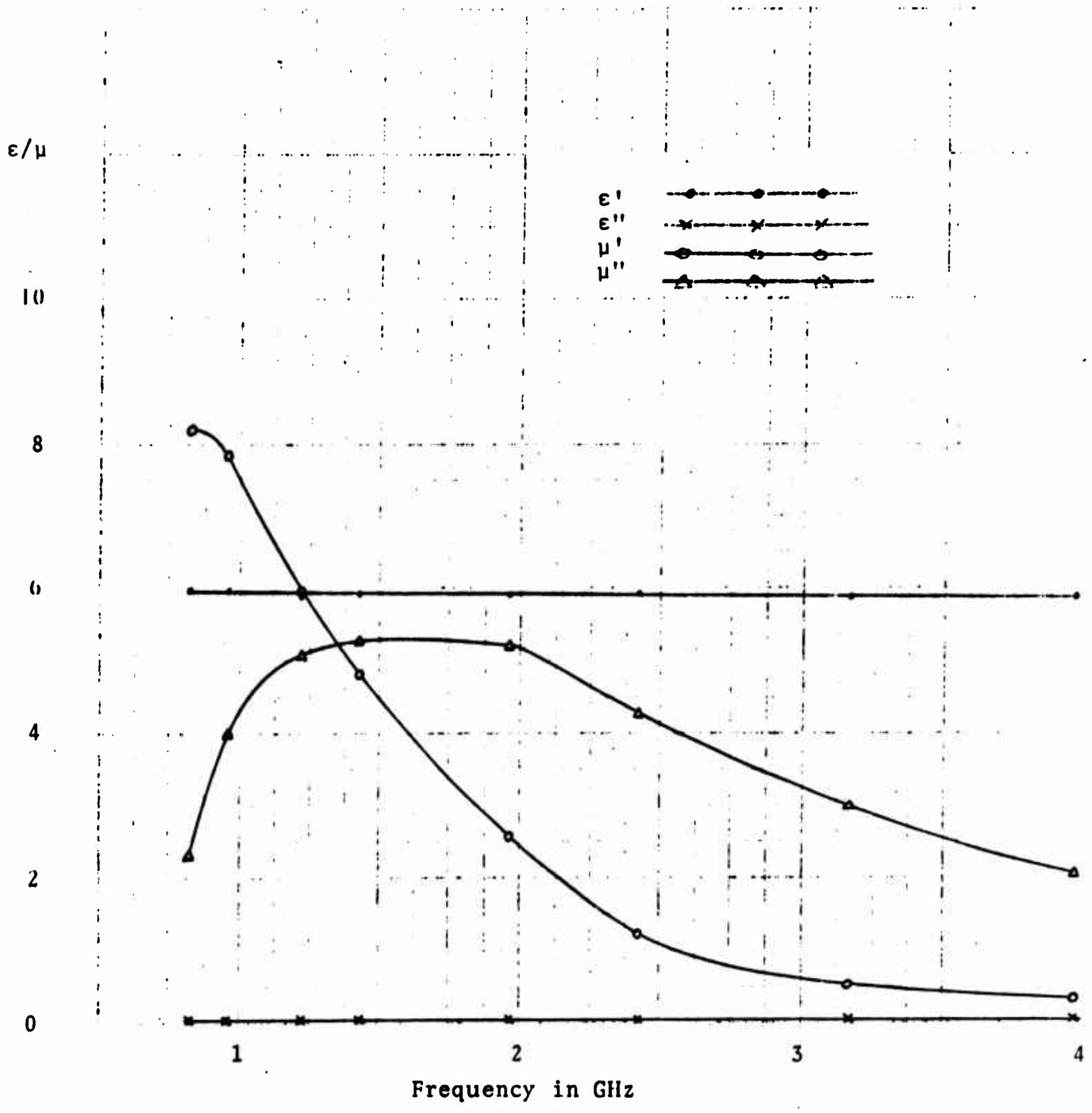

Figure 53. SAMPLE 101 0.9936" Diameter
ε and μ Vs Frequency

VIII. MEASUREMENT OF FERRITE MATERIALS AT HIGH TEMPERATURE

Other than the problems associated with insertion and moving of the samples which were discussed previously in this report, and the breakage of the samples, no additional problems were encountered at elevated temperatures.

Figures 54 and 55 give ε', ε'', μ', μ'' measured at 0.830 GHz and 3.970 GHz at elevated temperatures for sample 101. Here it is seen that μ reaches 1.0-j0.0 between 500°F and 750°F and remains 1.0-j0.0 with increased temperature.

In Figure 56 is given the waveguide measurement at 7.00 GHz of a material received at a later date and supposedly identical to sample 101; However, it turned out to be significantly different. In this material there was very significant variation from sample to sample. The waveguide sample required the cementing together of four tiles for each sample. Here again μ'' falls to 0.00 between 500°F and 750°F with μ'=1.00.

In Figures 57 and 58 the ε and μ versus temperature for sample 102 is given for measurements at 0.830 and 3.970 GHz, respectively. Since this is a lithium ferrite μ does not become 1.0 - j0.0.

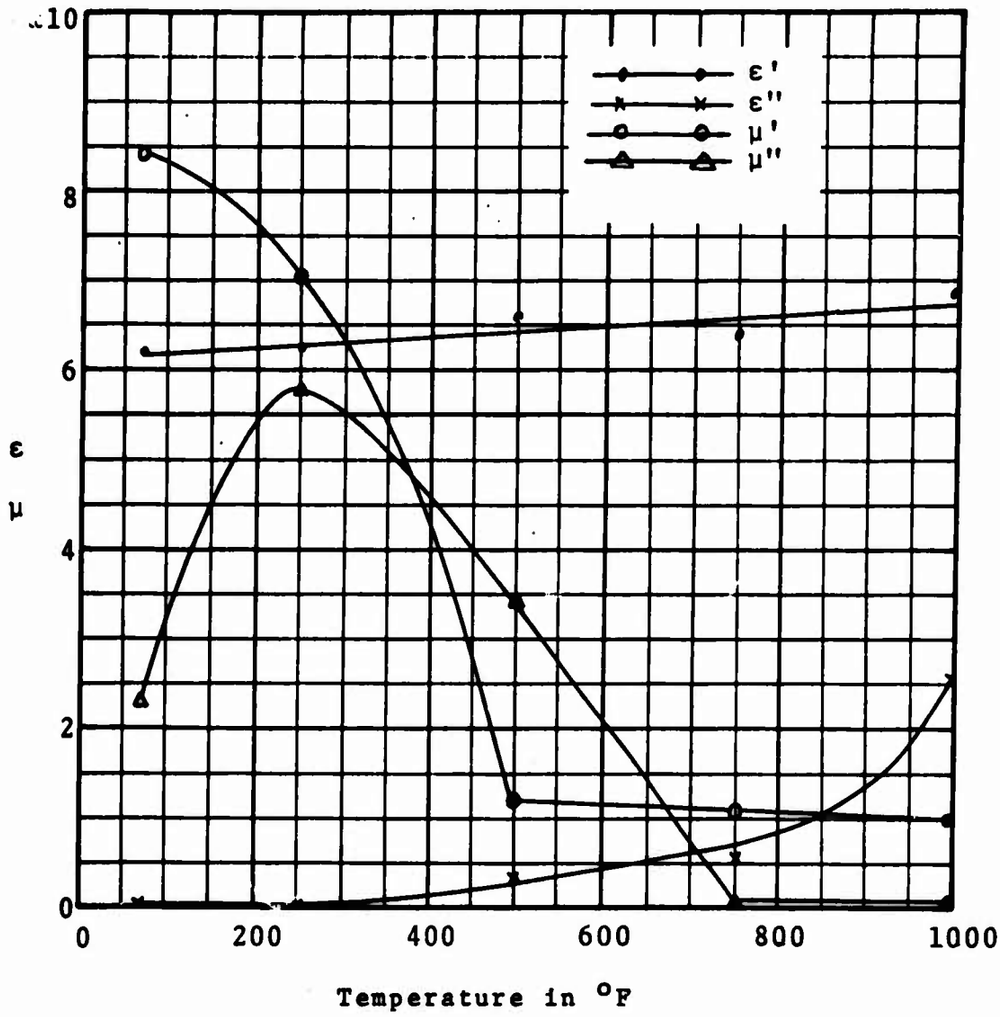

Figure 54. Sample 101; ε and μ Vs Temperature at 0.830GHz.

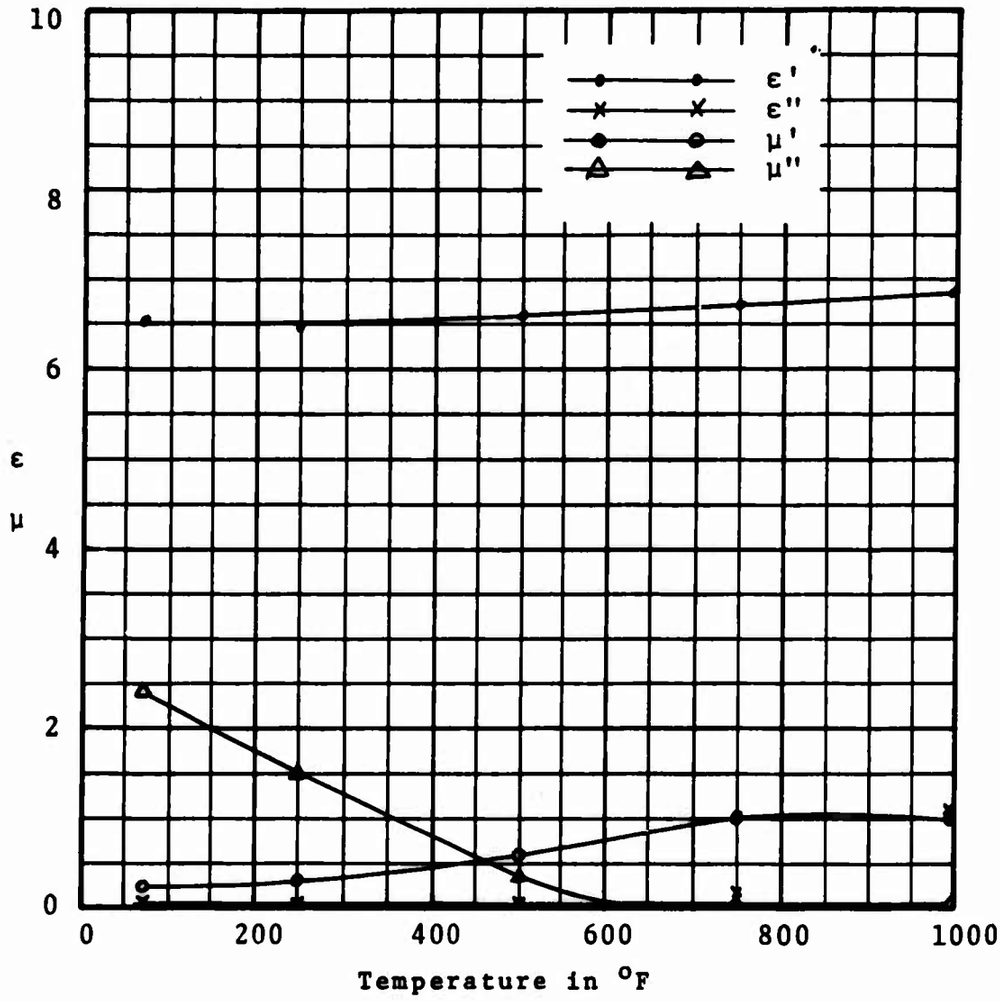

Figure 55. Sample 101; ε and μ Vs Temperature at 3.970 GHz.

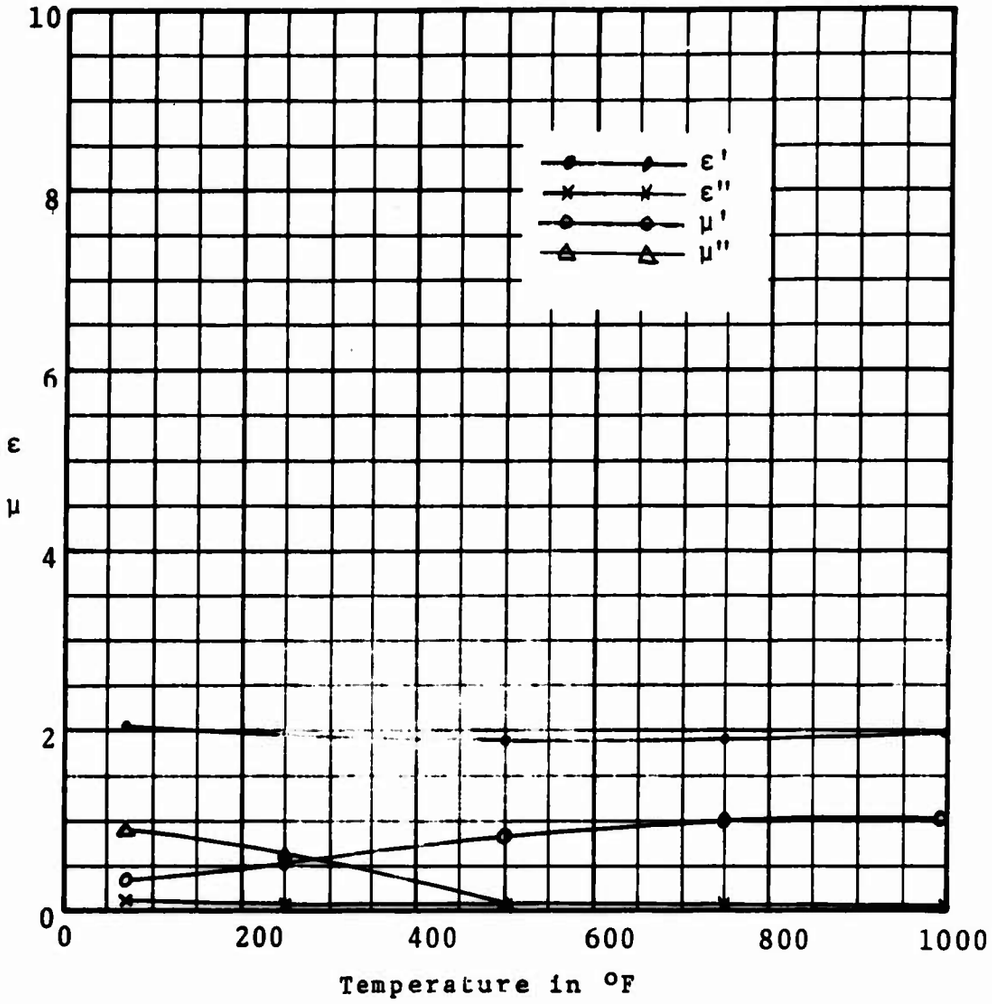

Figure 56. ε and μ Vs Temperature at 7.000 GHz (waveguide).

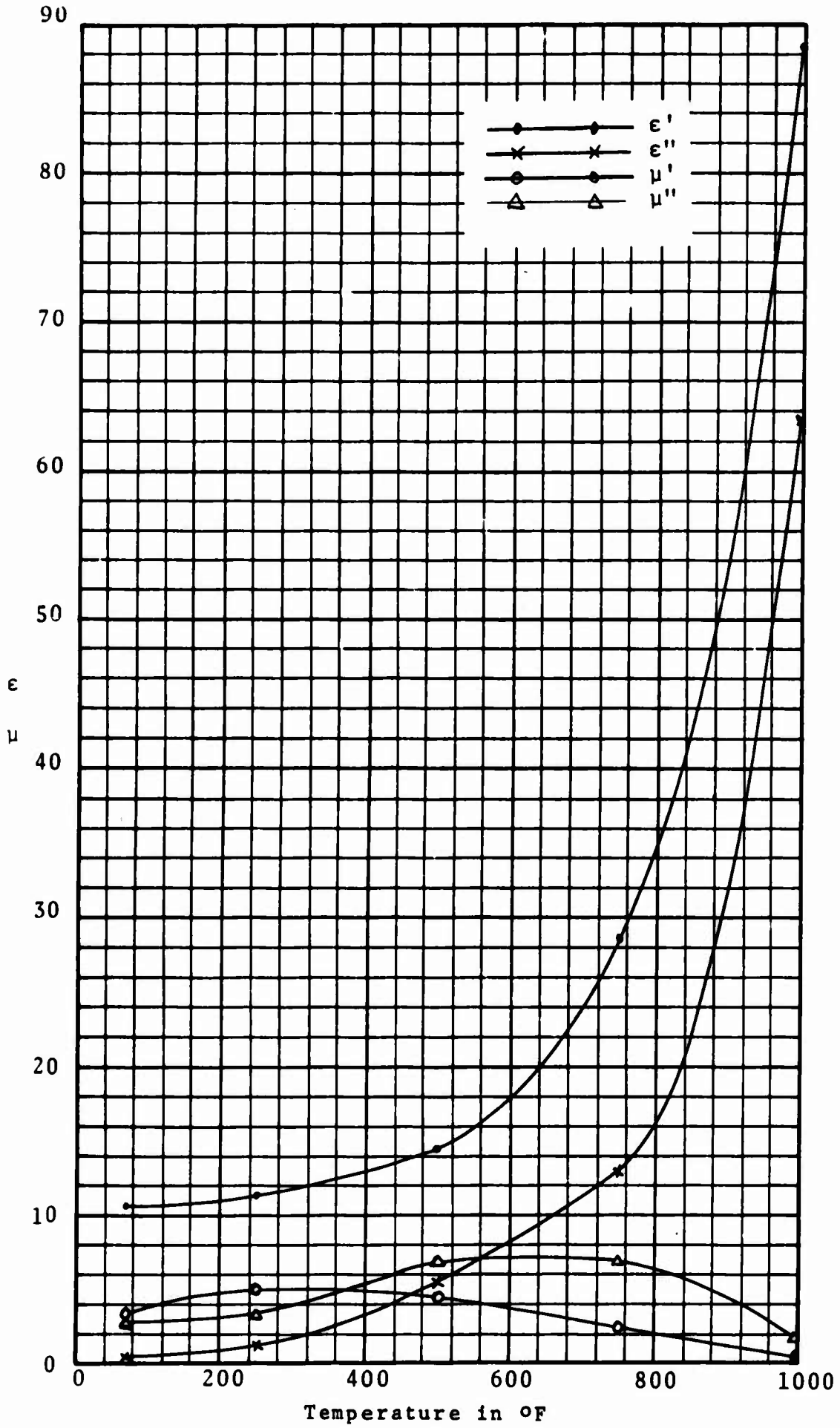

Figure 57. Sample 102; ε and μ Vs Temperature at 0.830 GHz.

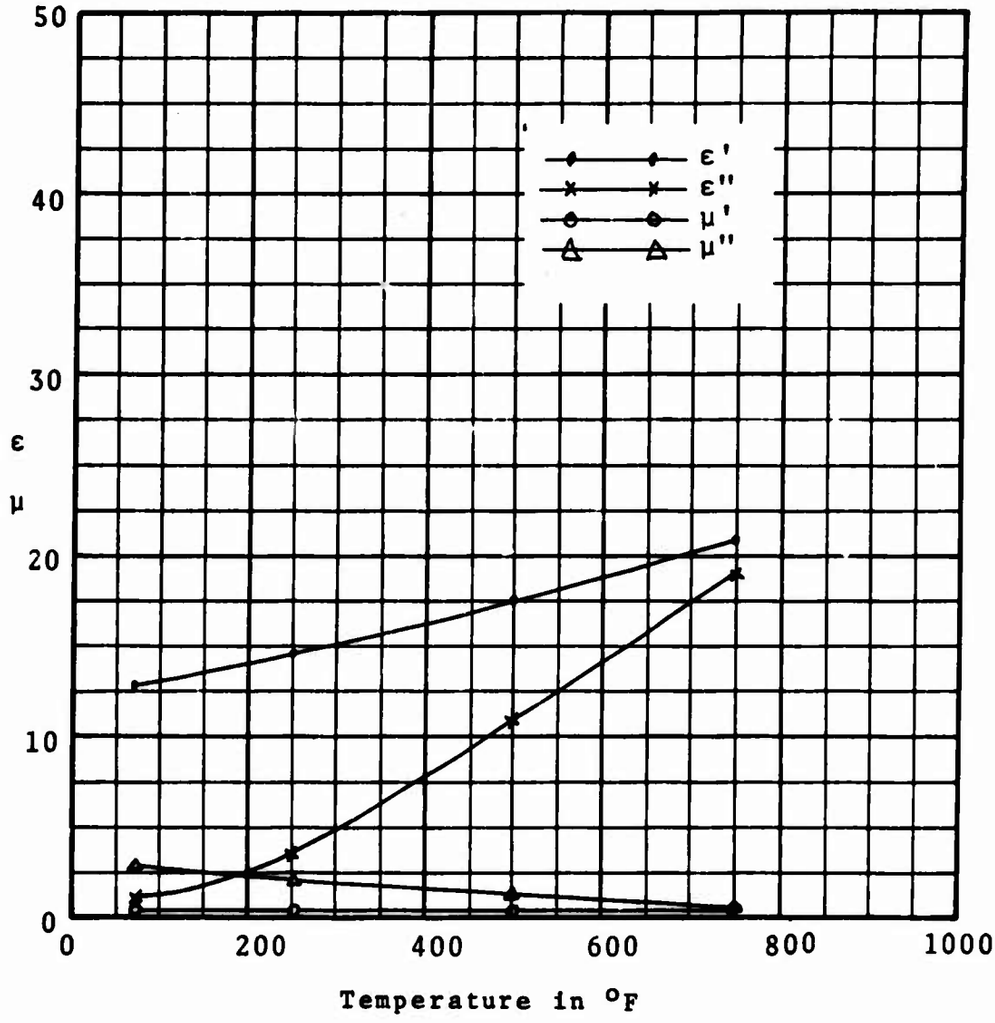

Figure 58. Sample 102; ε and μ Vs Temperature at 3.970 GHz.

IX. CONCLUSIONS AND RECOMMENDATIONS

It has been found that although the high temperature measurements are time-consuming, they are as reliable as the room temperature measurements.

No effect of sample fit on the measurements taken in the coaxial or waveguide gold plated Kovar sample holder has been observed.

Dielectric Materials. As reliable results can be obtained with samples of two equal thicknesses measured singly and together at the short circuit only, as with the samples measured at the short and a quarter wavelength away from the short circuit. This technique is particularly desirable for the high temperature measurements, eliminating the need of either moving the sample in by a quarter wavelength or adding a quarter wavelength section.

The completely automatic zeroing-in program, paraleling that for the sample at the open and short circuit requires further development.

Ferrites. Again, considerable advantage exists for the ferrite measurements if the samples can be measured merely at the short circuit. However, here three samples of identical thickness are needed to uniquely determine the ε^* and μ^*. By placing first one sample at the shorting plate and measuring the null position and VSWR, then pushing the second sample in behind the first with the shorting plate and measuring the null position and VSWR, one unique determination of ε^* and μ^* can be made. Repeating with the third sample added to the first two, will give a second determination of ε^* and μ^*. From a practical point of view for high temperature measurements, this technique warrants serious consideration.

The presently used, open and short circuit technique with single and double thickness requires four different ΔX decrements to obtain consistency in the four results. Thus the automating of the computational technique requires further study.

At least six different materials (two each of low, medium, and high loss) should be studied to obtain sufficient experience to write an automatic ferrite program.

A major underlying problem is the variability of the ferrite materials from sample to sample. This should be studied in detail with many samples of the same material. Another problem is the unavailability of samples larger than one square inch.

DOCUMENT CONTROL DATA - R&D

(Security classification of title, body of abstract and indexing annotation must be entered when the overall report is classified)

1 ORIGINATING ACTIVITY (Corporate author)

A. S. THOMAS, INC.
355 Providence Highway
Westwood, Massachusetts 02090

2a. REPORT SECURITY CLASSIFICATION
UNCLASSIFIED

2b GROUP

3 REPORT TITLE

MEASUREMENTS OF COMPLEX PERMITTIVITY AND PERMEABILITY

4 DESCRIPTIVE NOTES (Type of report and inclusive dates)
Final Report - March 1969 - March 1970

5 AUTHOR(S) (Last name, first name, initial)

THOMAS, Abdelnour S.
THOMAS, Eva M.

6 REPORT DATE	7a TOTAL NO OF PAGES	7b NO. OF REFS
September 1970	96	

8a CONTRACT OR GRANT NO.	9a. ORIGINATOR'S REPORT NUMBER(S)
F33615-69-C-1065	M68-1
b. PROJECT NO. 5546	
c Task 554603	9b. OTHER REPORT NO(S) (Any other numbers that may be assigned this report) AFML-TR-70-87
d	

10 AVAILABILITY/LIMITATION NOTICES

This document is subject to special export controls and each transmittal to foreign government or foreign nationals may be made only with prior approval of AFML(MAYE),WPAFB,Ohio 45433.

11 SUPPLEMENTARY NOTES	12 SPONSORING MILITARY ACTIVITY
	Air Force Materials Laboratory Wright-Patterson AFB, Ohio 45433

13 ABSTRACT

This program was conducted to derive a better technique for the measurement of the permeability and permittivity of lossy ferrites at microwave frequencies at temperatures up to 1000°F. Although the classical method of waveguide measurement techniques was used, a careful analysis of the sources of errors was undertaken and a computer aided analysis technique developed to establish the validity of the measurements.

The design of the sample holders and special tools for insertion of material is detailed.

The problem areas inherent in this type of measurement are not compounded by high temperatures, and good results can be obtained, provided great care is taken and sufficient homogeneous ferrite samples are available.

Three different ferrites were measured at microwave frequencies and temperatures up to 1000°F.

DD FORM 1 JAN 64 1473

Unclassified
Security Classification

14. KEY WORDS	LINK A		LINK B		LINK C	
	ROLE	WT	ROLE	WT	ROLE	WT
High Temperature Measurements						
Complex Permittivity						
Complex Permeability						

INSTRUCTIONS

1. ORIGINATING ACTIVITY: Enter the name and address of the contractor, subcontractor, grantee, Department of Defense activity or other organization *(corporate author)* issuing the report.

2a. REPORT SECURITY CLASSIFICATION: Enter the overall security classification of the report. Indicate whether "Restricted Data" is included. Marking is to be in accordance with appropriate security regulations.

2b. GROUP: Automatic downgrading is specified in DoD Directive 5200.10 and Armed Forces Industrial Manual. Enter the group number. Also, when applicable, show that optional markings have been used for Group 3 and Group 4 as authorized.

3. REPORT TITLE: Enter the complete report title in all capital letters. Titles in all cases should be unclassified. If a meaningful title cannot be selected without classification, show title classification in all capitals in parenthesis immediately following the title.

4. DESCRIPTIVE NOTES: If appropriate, enter the type of report, e.g., interim, progress, summary, annual, or final. Give the inclusive dates when a specific reporting period is covered.

5. AUTHOR(S): Enter the name(s) of author(s) as shown on or in the report. Enter last name, first name, middle initial. If military, show rank and branch of service. The name of the principal author is an absolute minimum requirement.

6. REPORT DATE: Enter the date of the report as day, month, year; or month, year. If more than one date appears on the report, use date of publication.

7a. TOTAL NUMBER OF PAGES: The total page count should follow normal pagination procedures, i.e., enter the number of pages containing information.

7b. NUMBER OF REFERENCES: Enter the total number of references cited in the report.

8a. CONTRACT OR GRANT NUMBER: If appropriate, enter the applicable number of the contract or grant under which the report was written.

8b, 8c, & 8d. PROJECT NUMBER: Enter the appropriate military department identification, such as project number, subproject number, system numbers, task number, etc.

9a. ORIGINATOR'S REPORT NUMBER(S): Enter the official report number by which the document will be identified and controlled by the originating activity. This number must be unique to this report.

9b. OTHER REPORT NUMBER(S): If the report has been assigned any other report numbers *(either by the originator or by the sponsor)*, also enter this number(s).

10. AVAILABILITY/LIMITATION NOTICES: Enter any limitations on further dissemination of the report, other than those imposed by security classification, using standard statements such as:

(1) "Qualified requesters may obtain copies of this report from DDC."

(2) "Foreign announcement and dissemination of this report by DDC is not authorized."

(3) "U. S. Government agencies may obtain copies of this report directly from DDC. Other qualified DDC users shall request through _____."

(4) "U. S. military agencies may obtain copies of this report directly from DDC. Other qualified users shall request through _____."

(5) "All distribution of this report is controlled. Qualified DDC users shall request through _____."

If the report has been furnished to the Office of Technical Services, Department of Commerce, for sale to the public, indicate this fact and enter the price, if known.

11. SUPPLEMENTARY NOTES: Use for additional explanatory notes.

12. SPONSORING MILITARY ACTIVITY: Enter the name of the departmental project office or laboratory sponsoring *(paying for)* the research and development. Include address.

13. ABSTRACT: Enter an abstract giving a brief and factual summary of the document indicative of the report, even though it may also appear elsewhere in the body of the technical report. If additional space is required, a continuation sheet shall be attached.

It is highly desirable that the abstract of classified reports be unclassified. Each paragraph of the abstract shall end with an indication of the military security classification of the information in the paragraph, represented as *(TS), (S), (C), or (U).*

There is no limitation on the length of the abstract. However, the suggested length is from 150 to 225 words.

14. KEY WORDS: Key words are technically meaningful terms or short phrases that characterize a report and may be used as index entries for cataloging the report. Key words must be selected so that no security classification is required. Idenfiers, such as equipment model designation, trade name, military project code name, geographic location, may be used as key words but will be followed by an indication of technical context. The assignment of links, rules, and weights is optional.

Unclassified
Security Classification